



University of Kentucky  
UKnowledge

---

Theses and Dissertations--Toxicology and  
Cancer Biology

Toxicology and Cancer Biology

---

2016

## EXPLORATION OF THE SRX-PRX AXIS AS A SMALL-MOLECULE TARGET

Murli Mishra

University of Kentucky, mm.murli@gmail.com

Digital Object Identifier: <http://dx.doi.org/10.13023/ETD.2016.177>

[Right click to open a feedback form in a new tab to let us know how this document benefits you.](#)

---

### Recommended Citation

Mishra, Murli, "EXPLORATION OF THE SRX-PRX AXIS AS A SMALL-MOLECULE TARGET" (2016). *Theses and Dissertations--Toxicology and Cancer Biology*. 14.

[https://uknowledge.uky.edu/toxicology\\_etds/14](https://uknowledge.uky.edu/toxicology_etds/14)

This Doctoral Dissertation is brought to you for free and open access by the Toxicology and Cancer Biology at UKnowledge. It has been accepted for inclusion in Theses and Dissertations--Toxicology and Cancer Biology by an authorized administrator of UKnowledge. For more information, please contact [UKnowledge@lsv.uky.edu](mailto:UKnowledge@lsv.uky.edu).

## **STUDENT AGREEMENT:**

I represent that my thesis or dissertation and abstract are my original work. Proper attribution has been given to all outside sources. I understand that I am solely responsible for obtaining any needed copyright permissions. I have obtained needed written permission statement(s) from the owner(s) of each third-party copyrighted matter to be included in my work, allowing electronic distribution (if such use is not permitted by the fair use doctrine) which will be submitted to UKnowledge as Additional File.

I hereby grant to The University of Kentucky and its agents the irrevocable, non-exclusive, and royalty-free license to archive and make accessible my work in whole or in part in all forms of media, now or hereafter known. I agree that the document mentioned above may be made available immediately for worldwide access unless an embargo applies.

I retain all other ownership rights to the copyright of my work. I also retain the right to use in future works (such as articles or books) all or part of my work. I understand that I am free to register the copyright to my work.

## **REVIEW, APPROVAL AND ACCEPTANCE**

The document mentioned above has been reviewed and accepted by the student's advisor, on behalf of the advisory committee, and by the Director of Graduate Studies (DGS), on behalf of the program; we verify that this is the final, approved version of the student's thesis including all changes required by the advisory committee. The undersigned agree to abide by the statements above.

Murli Mishra, Student

Dr. Qiou Wei, Major Professor

Dr. Isabel Mellon, Director of Graduate Studies

EXPLORATION OF THE SRX-PRX AXIS  
AS A SMALL-MOLECULE TARGET

---

DISSERTATION

---

A dissertation submitted in partial fulfillment of the  
requirements for the degree of Doctor of Philosophy in the  
College of Medicine at the University of Kentucky

By  
Murli Mishra  
Lexington, Kentucky

Co-Director: Dr. Qiou Wei, Assistant Professor,  
And Dr. Xianglin Shi, Professor  
Department of Toxicology and Cancer Biology  
Lexington, Kentucky

2016

Copyright © Murli Mishra 2016

## ABSTRACT OF DISSERTATION

Lung cancer is a leading cause of cancer-related mortality irrespective of gender. The Sulfiredoxin (Srx) and Peroxiredoxin (Prx) are a group of thiol-based antioxidant proteins that plays an essential role in non-small cell lung cancer. Understanding the molecular characteristics of the Srx-Prx interaction may help design the strategies for future development of therapeutic tools. Based on existing literature and preliminary data from our lab, we hypothesized that the *Srx plays a critical role in lung carcinogenesis and targeting the Srx-Prx axis or Srx alone may facilitate future development of targeted therapeutics for prevention and treatment of lung cancer*. First, we demonstrated the oncogenic role of Srx in urethane-induced lung carcinogenesis in genetically modified FVB mice. The Srx-null mice showed resistance to urethane-induced lung cancer. Second, we demonstrated the Srx and Prx sites important for *Srx-Prx interaction*. The orientation of this arm is demonstrated to cause some steric hindrance for the *Srx-Prx interaction* as it substantially reduces the rate of association between Srx and Prx. Finally, we carried out virtual screening to identify molecules that can successfully target *Srx-Prx interaction*. Multiple in-silico filters were used to minimize the number of chemicals to be tested. We identified ISO1 as an inhibitor of the *Srx-Prx interaction*.  $K_D$  value for Srx-ISO1 interaction is calculated to be 42 nM. Together, these data helps to identify an inhibitor (ISO1) of the *Srx-Prx interaction* that can be further pursued to be developed as a chemotherapeutic tool.

KEYWORDS: *Srx-Prx interaction*; lung cancer; urethane; Srx inhibitor; drug-discovery

Student: Murli Mishra

---

Date: 27 April , 2016

EXPLORATION OF THE SRX-PRX AXIS  
AS A SMALL-MOLECULE TARGET

By  
Murli Mishra

Dr. Qiou Wei

---

Director of Dissertation

Dr. Xianglin Shi

---

Co-Director of Dissertation

Dr. Isabel Mellon

---

Director of Graduate Studies

27 April , 2016

---

Dedicated to Almighty God;

My Parents; Siblings; Shohana Tawrin and Rakesh Nankar

*(For all their support in my journey)*

## ACKNOWLEDGMENTS

The following dissertation could not have been completed without the continuous support of many individuals. I would like to express my sincere appreciation to the individuals who played key roles in my journey. First, I want to thank my doctoral mentor and dissertation chair, Dr. Qiou Wei, for his invaluable guidance and unending support. He has allowed me the freedom to design and execute experiments with continuous guidance, providing better direction for this dissertation. With a background in predictive toxicology, I was always interested in in-silico research. I designed similar project for my qualifying exam for targeting Prx4. I later wanted to execute same project for targeting Srx in our lab. I am thankful to Dr. Wei to allow me to execute this project in lab that lead us to identification of ISO1. This is the kind of independence I always wanted in my PhD. I am grateful to find a mentor who gave me that level of functional independence. I thank my dissertation committee, Dr. Xianglin Shi, Dr. Mary Vore, and Dr. Edward Hall for their guidance in improving the study and challenging my critical thinking. Thanks to my doctoral committee ex-members, Dr. Christian Paumi and Dr. Liya Gu, who provided guidance during conception of this dissertation.

I would like to thank Dr. Natasha Kyprianou, Dr. Vivek Rangnekar, Dr. Alan Daugherty, and Dr. Daret St. Clair for allowing me to rotate in their labs during 1st year and helping me in my professional development. I thank Dr. Hong Jiang, Dr. Lisha Wu, and Hedy Chawsheen whose continuous help and support in the lab provided a pleasant work environment.

I thank Dr. John J. Irwin at the University of California, San Francisco, for help with accessing subsets of data with DockBlaster. I thank Mr. Daniel Binzel, College of Pharmacy, and Dr. Janice Ortega Rodriguez, Department of Toxicology and Cancer Biology, both at the University of Kentucky, for helping with acquisition of SPR data using ProteOn. I also thank Dr. Gary F. Ross at Bio-Rad for his assistance in troubleshooting the SPR studies. I thank University of

Kentucky Writing/Language Editing Center for proof reading this dissertation and providing insights related to language and grammar.

The work presented in this dissertation was supported financially by a National Cancer Institute (NCI) grant and the University of Kentucky.

Finally, I would like to thank my family and friends for their unending support. I thank my parents for allowing me to study and live my dream, especially since no one else in my family has ever pursued a degree in biological sciences or any applied sciences or a graduate degree in any field. I want to thank my brother, Kanhaiya, and sister, Ramita, for staying with my parents while I was busy with my education. I thank my wife, Shohana, for all the support she provided during my stay in Lexington. You were always there when I needed a family member most, so you deserve the greatest thanks. You were the one who always supported my ambitious nature and provided your best support to make me a better professional. I would like to thank my friends, Rakesh Nankar for helping me with finances when I was coming to USA. You showed true friendship and trust in me, when many others did not. I thank my other friends, Pravin Shinde and Vijay Rathod, for helping me in selecting *in silico* tools that I later used during my dissertation. I am thankful to my friends, Ketan Patil and Brajesh Tiwari, who helped me early in my career. I am also thankful to Dr. Debanjan Chakrabarty for being like a fresh breath of air in Lexington. I will always remember Lexington for the fun we had together. I thank Ghanshyam Sinha, Hemendra Vekaria, Mayuresh Moghe, Sheetal kumar Dacha, Ram Roy, Pranav Aramane, Aman Gupta and anyone I missed for keeping Lexington entertaining for all these years. I am blessed to have a great set of friends like you guys. Thanks to anyone I missed in this acknowledgement, who helped me anytime during my journey. Thank you everyone for your support, I truly appreciate it.



# TABLE OF CONTENTS

LIST OF FIGURES.....	VIII
LIST OF TABLES.....	X
CHAPTER 1: INTRODUCTION.....	1
1.1 Background .....	1
1.1.1 Peroxiredoxin .....	2
1.1.2 Sulfiredoxin .....	5
1.1.3 Enzymatic roles of Srx .....	7
1.1.4 Molecular characteristics of the Srx-Prx interaction .....	10
1.1.5 The role of the Srx-Prx axis in cell-signaling and carcinogenesis .....	14
1.1.6 Summary and future directions .....	26
1.2 Scope of dissertation .....	29
1.2.1 Hypothesis .....	29
1.2.2 Specific aims.....	29
CHAPTER 2: EFFECT OF SULFIREDOXIN DEPRIVATION ON THE URETHANE-INDUCED LUNG TUMORIGENESIS .....	30
2.1 Synopsis .....	30
2.2 Introduction .....	31
2.3 Materials & methods .....	32
2.3.1 Cell culture and western blot.....	32
2.3.2 Quantitative reverse transcription and polymerase chain reaction.....	33
2.3.3 Lentiviral ShRNA knockdown of Srx in BEAS2B cells.....	34
2.3.4 Soft agar colony formation assay.....	35
2.3.5 Srx knockout mice genotyping.....	36
2.3.6 Urethane protocol .....	36
2.3.7 Immunohistochemistry staining and <i>in situ</i> apoptosis assay .....	37
2.3.8 Statistical analysis .....	38
2.4 Results.....	38
2.4.1 CSC enhances the expression of antioxidant proteins.....	38
2.4.2 Urethane enhances expression of antioxidant protein .....	40

2.4.3 Urethane treatment transforms BEAS2B cells in an Srx-dependent manner.....	44
2.4.4 Srx knockout mice are resistant to urethane-induced lung cancer .....	46
2.4.5 Urethane induces the expression of antioxidant proteins in mouse lung.....	49
2.4.6 Depletion of Srx reduced cell proliferation and increased apoptosis in the urethane treated groups .....	50
2.5 Discussion.....	53
2.6 Summary .....	58
<b>CHAPTER 3: THE BIOLOGY OF SULFIREDOXIN (SRX)-PEROXIREDOXIN1 (PRX1) INTERACTION: STRUCTURE TO MOLECULAR INSIGHTS .....</b>	
3.1 Synopsis .....	59
3.2 Introduction .....	60
3.3 Materials and methods.....	61
3.3.1 Homology modeling and protein-protein docking studies.....	61
3.3.2 Western blot and immunoprecipitation (IP) assay in HEK293T cells.....	62
3.3.3 Purification of recombinant proteins.....	62
3.3.4 <i>In vitro</i> IP using purified recombinant proteins .....	64
3.3.5 Study of the Srx-Prx interaction kinetics using surface plasmon resonance (SPR).....	64
3.3.6 Statistical analysis .....	65
3.4 Results.....	65
3.4.1 Complete 3D-structure of full length proteins were predicted using homology modeling .....	65
3.4.2 Protein-protein docking output identified a possibility of steric hindrance for the Srx-Prx interaction.....	69
3.4.3 IP assay confirms the differences in interaction of Srx with individual Prx .....	69
3.4.4 Srx binds more efficiently to Prx1 <sup>mutant</sup> than Prx1 <sup>wildtype</sup> .....	72
3.4.5 Deletion of Prx C-terminal arm leads to faster Srx-Prx association with minimal effect on dissociation .....	74
3.5 Discussion.....	77
3.6 Summary .....	84
<b>CHAPTER 4: TARGETING SRX-PRX INTERACTION USING SMALL-MOLECULE INHIBITORS .....</b>	
4.1 Synopsis .....	85
4.2 Introduction .....	86
4.3 Materials and methods.....	88

4.3.1 Cell lines, plasmids, antibodies and chemicals .....	88
4.3.2 Virtual screening to identify the Srx-Prx interaction inhibitor.....	89
4.3.3 Small molecule assay for Srx inhibitory activity.....	91
4.3.4 Western blotting, IP, and phosphokinase profiling .....	91
4.3.5 Colony formation, cell proliferation assay and cell cycle analysis.....	92
4.3.6 Surface plasmon resonance study of Srx-Prx interaction kinetics.....	92
4.3.7 Wound healing assay .....	93
4.3.8 Statistical analysis .....	93
4.4 Results.....	93
4.4.1 Srx contains a good druggable pocket suitable for virtual screening.....	93
4.4.2 <i>In silico</i> studies led to selection of four chemicals for <i>in vitro</i> testing.....	94
4.4.3 Two molecules showed inhibition of Srx activity.....	96
4.4.4 Two molecules inhibit cell growth and colony formation in lung and colon cancer cells .....	101
4.4.5 Surface plasmon resonance studies indicate higher affinity of Srx for ZINC64002748 and ISO1 compared to Prx1 .....	101
4.4.6 ISO1 inhibits Srx-mediated phosphokinase signaling .....	106
4.4.7 ISO1 arrests cell growth in G <sub>2</sub> phase.....	108
4.4.8 ISO1 inhibits cell-migration in wound healing assay .....	108
4.5 Discussion.....	110
4.6 Summary .....	115
CHAPTER 5 OVERALL DISCUSSION .....	116
5.1 Summary of dissertation.....	116
5.2 Conclusions and future directions .....	125
APPENDIX 1 .....	126
Abbreviations .....	126
APPENDIX 2 .....	128
Copyrights .....	128
REFERENCES.....	129
VITA.....	143

## LIST OF FIGURES

Figure 1-1: Sulfiredoxin reduces over-oxidized peroxiredoxin and acts as a switch to regulate antioxidant vs chaperone function of peroxiredoxin .....	4
Figure 1-2: Mechanism of the deglutathionylation function of sulfiredoxin .....	9
Figure 1-3: Oxidative stress stimulates sulfiredoxin expression by activating AP-1 and Nrf2 activity.....	17
Figure 1-4: Peroxiredoxin may act as a tumor-suppressor or oncogene depending on the tumor type. ....	22
Figure 2-1: Cigarette smoke condensate (CSC) induces the expression of antioxidant proteins .....	39
Figure 2-2: Cigarette smoke condensate regulates the transcription of the Srx and Prx	41
Figure 2-3: Urethane treatment enhances antioxidant protein expression in BEAS2B cells .....	42
Figure 2-4: Urethane transforms BEAS2B cells in an Srx-dependent manner .....	45
Figure 2-5: Srx null mice are resistant to urethane toxicity.....	47
Figure 2-6: Srx null mice are resistant to urethane-induced carcinogenesis.....	48
Figure 2-7: Immunohistochemistry staining showing expression of different proteins in urethane-treated lung tissue.....	51
Figure 2-8: Srx enhances tumor cell proliferation and reduces tumor cell apoptosis in urethane-induced lung carcinogenesis .....	52
Figure 2-9: Prospective mechanism of urethane-induced lung carcinogenesis.....	56
Figure 3-1: Protein purification using pRSET B vector.....	63
Figure 3-2: Representative images of Srx and Prx1 .....	66
Figure 3-3: Representative images of typical 2-Cys Prxs other than Prx1 .....	68
Figure 3-4: The C-terminal arm hinders Srx binding to Prx1 .....	70
Figure 3-5: Effect of H <sub>2</sub> O <sub>2</sub> treatment on Srx interaction with various typical 2-Cys Prxs in HEK293T cells .....	71
Figure 3-6: Prx C-terminal arm deletion enhances the Srx-Prx interaction.....	73
Figure 3-7: C-terminal deletion mutation increases the Srx-Prx affinity .....	76
Figure 3-8: Extending C-terminal arm of Prx covers the Srx-Prx interface and may cause steric hindrance for Srx access to Prx .....	79
Figure 3-9: The Srx-Prx complex showing crystal structure with truncated Srx N-terminal .....	83
Figure 4-1: Predicted pockets in Srx and Prx1 .....	95
Figure 4-2: Representative images of docked small molecules in Srx-binding pocket. ...	98
Figure 4-3: Effect of individual small molecules on Prx-SO <sub>3</sub> reduction.....	99
Figure 4-4: Effect of ZINC64002748 and ISO1 on pull-down of Prx1 and Prx-SO <sub>3</sub> along with Srx .....	100
Figure 4-5: Effect of ZINC64002748 and ISO1 on cell growth.....	102
Figure 4-6: Small molecules inhibit anchorage-independent cell growth .....	103

Figure 4-7: Surface plasmon resonance curves of Srx interaction with small molecules .....	104
Figure 4-8: ISO1 inhibits phosphokinase signaling.....	107
Figure 4-9: ISO1 inhibits lung cancer cell growth and migration .....	109

## LIST OF TABLES

Table 1-1: Expression pattern of the Srx-Prx system in different cancer types as evident from microarray data available at Oncomine .....	15
Table 3-1: The C-terminal deletion of Prx1 increases its affinity for Srx .....	75
Table 4-1: Filters applied to shortlist virtually screened hits and their significance .....	90
Table 4-2: List of 4 chemicals selected on the basis of virtual screening .....	97
Table 4-3: Srx has higher binding affinity for chemical inhibitors than Prx1 (SPR analysis).....	105

## CHAPTER 1: INTRODUCTION

### 1.1 Background

Redox signaling is signaling involving oxidation-reduction cycles of molecules leading to cell signal transduction. Redox signaling is an essential component of cellular processes involved in the maintenance of physiological homeostasis. It is an integral part of eukaryotic as well as prokaryotic cell signaling. The physiological activities regulated by redox signaling include (but are not limited to) growth factor signaling such as epidermal growth factor (EGF) [1] and insulin-like growth factor [2] as well as important energy metabolism and hormonal signaling [3]. Reactive oxygen/nitrogen species (ROS/RNS) are highly reactive oxygen/nitrogen containing species. ROS/RNS have a very short half-life, partly due to their highly reactive nature and the presence of antioxidants in host organisms. Any imbalance in production and utilization of ROS/RNS leads to abnormal accumulation of these particles. This abnormal accumulation of highly reactive molecules is known as oxidative stress. Oxidative stress contributes to multiple disorders in humans, including diabetes, Alzheimer's disease, Parkinson's disease, hepatic diseases, and various types of cancer [4, 5]. Antioxidants are molecules that are preferentially oxidized under oxidative stress conditions. They can be internal housekeeping molecules (expressed in intracellular or extracellular compartments of animal tissue) or external molecules (part of daily diet or supplements). Every organism expresses many antioxidant molecules at intracellular and extracellular sites to protect it from oxidative damages. Thiol-based antioxidants are major internal housekeeping antioxidant

molecules that act as redox switches to maintain physiological homeostasis [6]. Peroxiredoxins (Prxs) and sulfiredoxin (Srx) are part of the thiol-based antioxidant system.

### **1.1.1 Peroxiredoxin**

Prx is a class of thiol-based peroxidases ubiquitously found in prokaryotes as well as eukaryotes. Prx was first discovered about 27 years ago in yeast [7]. These proteins initially had multiple names, for example, protector protein, thiol-specific antioxidants, thioredoxin-linked thiol peroxidase and thioredoxin peroxidase. Finally, they were classified and widely accepted as peroxiredoxin [7-12]. There are six different isoforms of Prxs expressed in humans (i.e., Prx1-6) [13]. These Prx are involved in the regulation of cell proliferation, apoptosis, embryonic development, lipid metabolism, immune response, and other functions. [14]. All human Prx have one enzymatic cysteine called peroxidatic cysteine ( $C_P$ ) on their N-terminus. Five out of six human Prxs also have another cysteine called resolving cysteine ( $C_R$ ) on their C-terminus. Classification of Prx is largely based on the presence and the behavior of  $C_R$ . Human Prx are classified into three groups: (i) typical 2-Cys Prx (i.e. Prx1-4), (ii) atypical 2-Cys Prx (i.e. Prx5), and (iii) 1-Cys Prx (i.e. Prx6) [15]. A few publications reported the N-terminus as a reference for location of  $C_P$  and  $C_R$ . However, distance between  $C_P$  and  $C_R$  is not the same among different typical 2-Cys Prxs. From the comparison of typical 2-Cys Prxs, we found that the C-terminal of Prxs can be a better reference for  $C_P$  and  $C_R$  as their distance from the C-terminal end is approximately fixed across all typical 2-Cys Prx. For example, the  $C_P$  is at a



distance of 148-149 amino acids from the C-terminal end whereas the C<sub>R</sub> is at a distance of 27-28 amino acids from the C-terminal end. The Prx family of proteins reduces hydrogen peroxide (H<sub>2</sub>O<sub>2</sub>), alkyl hydroperoxides and peroxyxynitrite into water and other harmless metabolites. In this reaction, the thiol group of C<sub>P</sub> is oxidized to sulfenic acid. The cysteine-sulfenic acid group can be enzymatically reduced back by the glutaredoxin or thioredoxin (Trx)-thioredoxin reductase system [16, 17]. The pK<sub>a</sub> of most biological cysteines is in the range of 8-9 if it is not stabilized by other molecular factors, while the pK<sub>a</sub> of C<sub>P</sub> falls in a lower range of 5-6 due to stabilization by the conserved arginine and threonine residues in neighboring positions [18]. There is no evidence of stabilization of C<sub>R</sub> by any intramolecular factors. Therefore, the pK<sub>a</sub> of C<sub>R</sub> should remain in the same range as other non-stabilized biological cysteines (i.e., 8-9). The difference in pK<sub>a</sub> values makes C<sub>R</sub> resistant to oxidation compared to C<sub>P</sub>. The rate constant (k) of Prx-thiol oxidation is higher than most other thiol-based antioxidant proteins. It is the main reason why Prx are 10<sup>5</sup>-10<sup>7</sup> times more efficient antioxidants compared to other thiol-based antioxidants such as glutathione, Trx, glyceraldehyde-3-phosphate dehydrogenase (GAPDH), protein-tyrosine phosphatase 1B (PTP1B), etc. [19]. Higher rate constant and lower pK<sub>a</sub> are indicators of the Prx's ability to reduce ROS that are present even in minute amounts. If the oxidative stress level is high and/or the amount of Prx is low, the C<sub>P</sub> can become over-oxidized to sulfinic (-SOOH) or sulfonic acid (-SOOOH) forms, leading to the loss of antioxidant activity [20]. Figure 1-1 shows this reaction along with Srx mechanism of action.

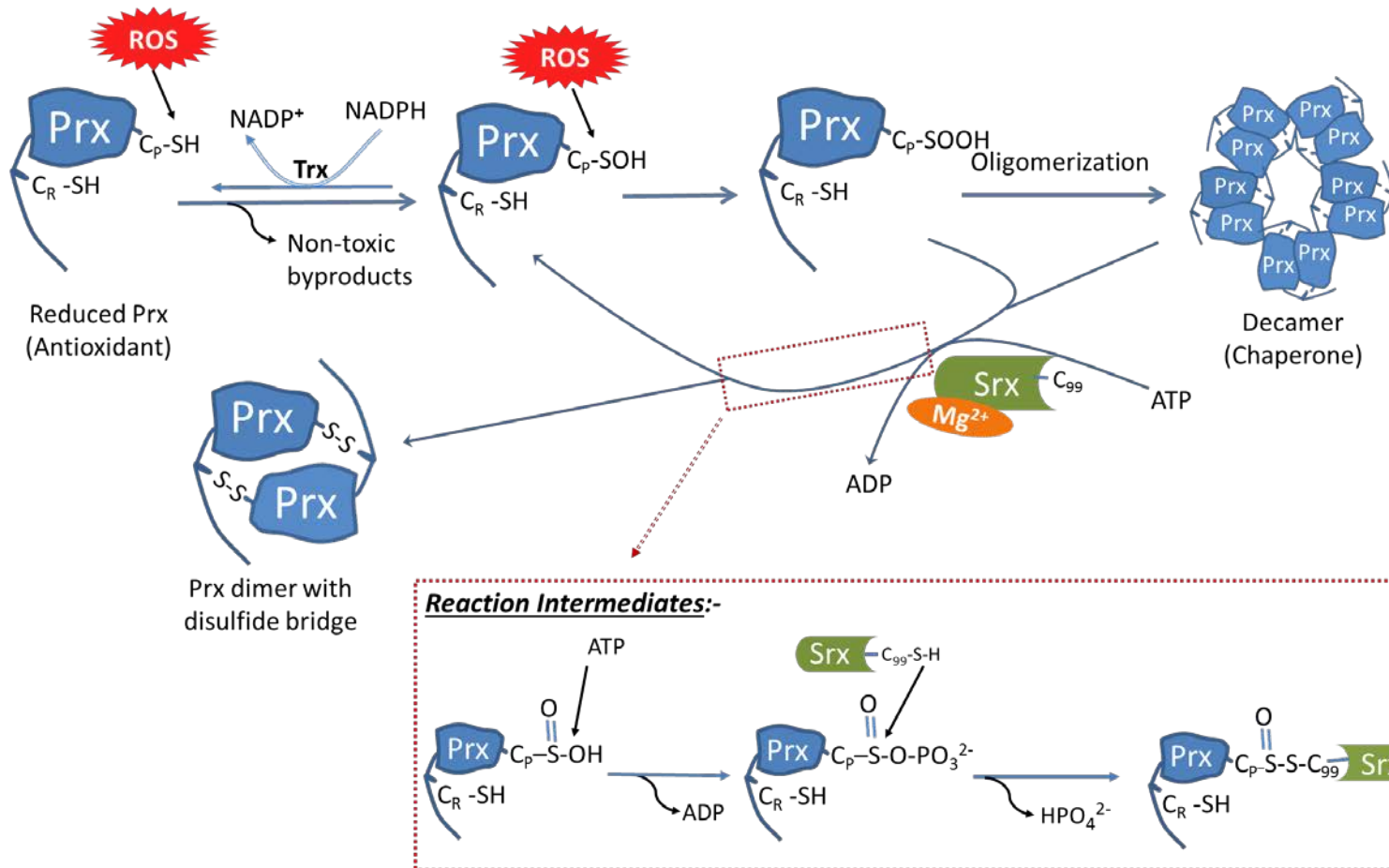


**Figure 1-1: Sulfiredoxin reduces over-oxidized peroxiredoxin and acts as a switch to regulate antioxidant vs chaperone function of peroxiredoxin** : Figure shows the relative location of  $C_P$  in Prx monomer and its role in the reduction of ROS. It also shows how the Srx forms phosphoryl esters and thiosulfinate intermediate finally leading to reduction of Prx Cys-sulfinic (-SOOH) form to Cys-sulfenic (-SOH) acid form.

Over-oxidation of Prxs is detectable in almost all eukaryotes and a few prokaryotes such as cyanobacteria [21]. Earlier literature indicated that the hyperoxidation of Prxs is a unique property of eukaryotic Prxs. However, the latest reports present evidence of this phenomenon in prokaryotes too [21]. Hyperoxidation and loss of antioxidant function is not a disadvantage for the host. The hyperoxidation of Prxs adds an additional molecular chaperone function to a few members of this class [22]. However, the molecular basis behind gain of chaperone function is yet to be identified. Further research is required to identify proteins whose folding is assisted by Prx. The chaperone function of Prx was considered a unique property of eukaryotic Prx until similar activity was detected in prokaryotes such as *Helicobacter pylori* [23].

### **1.1.2 Sulfiredoxin**

Experts long wondered about the existence of enzymes having the potential to reduce over-oxidized Prxs until Srx was identified in *Saccharomyces cerevisiae* [24] and was later found to be conserved in higher eukaryotes and a few prokaryotes (e.g. cyanobacteria). Srx plays a role in the reduction of over-oxidized Prxs and hence acts as a regulator of oligomerization of these Prxs. Rate constants from two independent studies indicate that the reduction of oxidized Prxs by Trx (rate constant  $10^6 \text{ M}^{-1}\text{s}^{-1}$ ) is much faster than the rate of reduction of over-oxidized Prxs by Srx (rate constant approximately  $2 \text{ M}^{-1}\text{s}^{-1}$ ) [25, 26]. Therefore, reduction of over-oxidized Prx by Srx can be considered a rate-limiting step in the reduction of over-oxidized Prxs.

The closest prokaryotic counterpart of Srx is a functionally unrelated protein called 'ParB' in bacteria, which carries out the function of chromosome partitioning [27]. The '*Oncogenic suppressive activity*' or 'Osa' protein is probably a connecting link between ParB and Srx. Osa contains both the DNase domain [18] of ParB and the ATPase domain of Srx [28]. Srx requires ATPase domain for ATP hydrolysis required for Prx reduction. The 'ParB' is a chromosome partitioning protein that requires a DNase domain for its function. In normal human tissues, Srx is present in kidney, lungs, and pancreas [29]. Srx is mainly a cytosolic protein that can translocate into mitochondria under oxidative stress conditions [30]. Recent research suggests that mitochondrial Srx level follows circadian rhythm [31]. In this manner, Prx3 along with Srx plays an important role in the management of mitochondrial redox balance.

The Srx-Prx axis can be explored as a therapeutic target as well as a therapeutic tool depending on its role in a particular pathological condition. For example, individual Prx can be considered as a good therapeutic targets in lung cancer [32], glioblastoma [33], colorectal cancer [34], and prostate cancer [35], where they protect tumor cells. It is important to evaluate the risk-benefit ratio of targeting individual members of the Srx-Prx axis as they also have a protective role in normal (non-tumor) tissue. Srx null mice have a normal phenotype under laboratory conditions [34]. Prx3 knockout mice are born and mature normally [36]. Prx4 knockout mice have mild prostate atrophy [37]. Prx1 and Prx2 knockout mice are reported to have some issue with erythropoiesis [38, 39] but they are otherwise normal. Hence, the majority of proteins in the Srx-Prx axis can

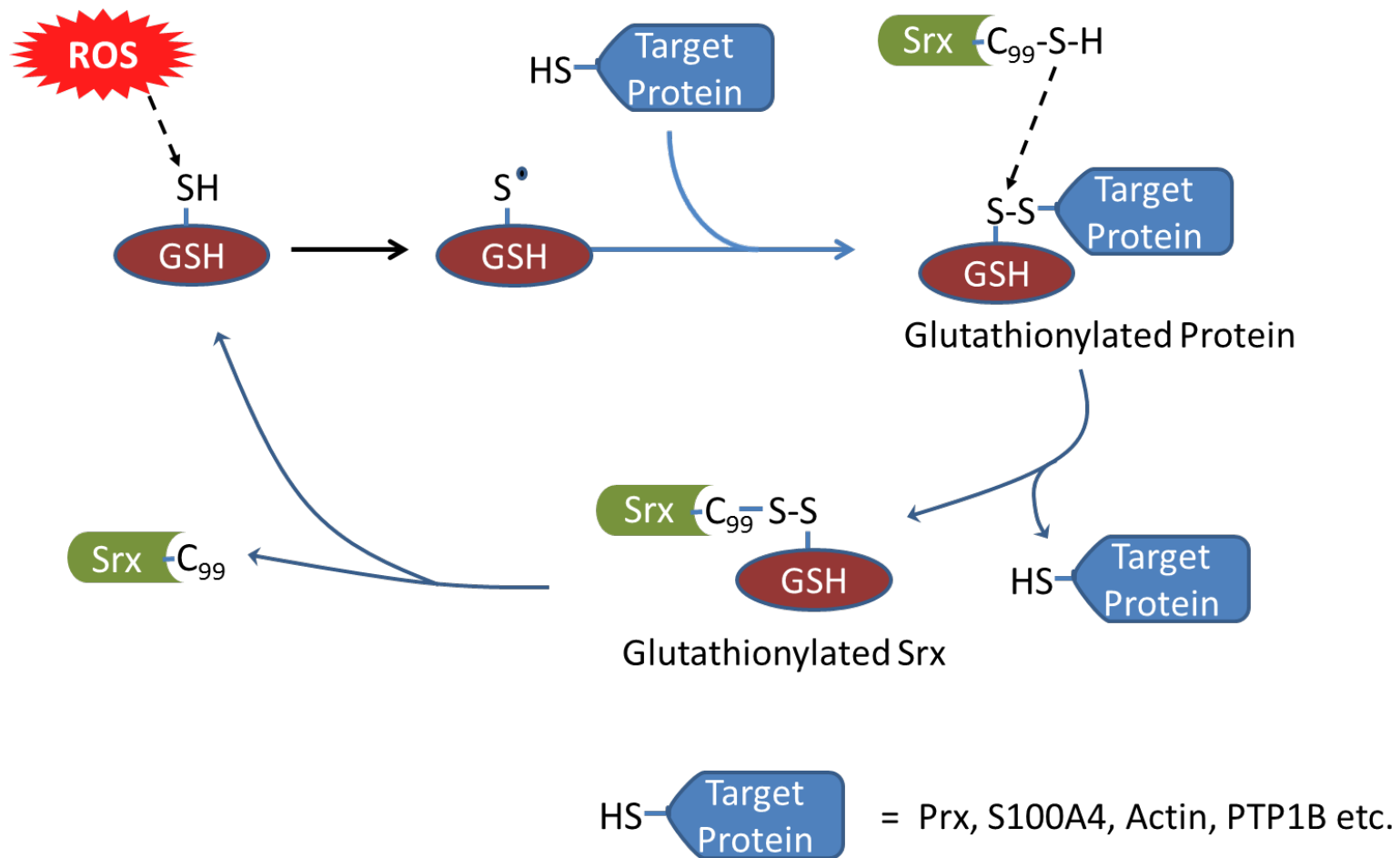
be knocked-out without any life-threatening issue under non-stress conditions. Considering the risk associated with cancer, it is worth exploring targets that can prolong the lives of patients by a few extra years. Hence, the benefits associated with targeting Srx or individual Prx outweigh the associated risk; therefore, the Srx-Prx system can be considered as therapeutic target in cancer. On the other hand, individual Prxs can be explored as a therapeutic or diagnostic tool in Parkinson's disease, Alzheimer's disease, and diabetic complications [40-44]. These differential properties of individual components of the Srx-Prx system draw our attention to differences in molecular properties of individual Prx that gives them the ability to play such diverse roles. An improved understanding of these molecular differences will help us in therapeutic intervention of the Srx-Prx system.

### **1.1.3 Enzymatic roles of Srx**

Human Srx has a length of 137 amino acids [45]. Srx is present in mammals, birds, and many (not all) other eukaryotic organisms [46]. It is an exclusive enzyme that acts as an antioxidant to reduce the sulfinic acid form of typical 2-Cys Prxs [47]. Biteau and colleagues identified how adenosine triphosphate (ATP)-bound yeast Srx in the presence of  $Mg^{2+}$  approaches the over-oxidized Prx1, phosphorylates it, and forms thiosulfinate intermediate, which can be further reduced by other thiol-reducing enzymes [24]. Yeast Srx has cysteine at two locations in its primary sequence; the first cysteine (Cys<sup>48</sup>) helps the enzymatic cysteine (Cys<sup>84</sup>) by recycling the thiosulfinate intermediate [48]. However, human Srx has only one cysteine, i.e. Cys<sup>99</sup> (a homologue of Cys<sup>84</sup> of

yeast). Therefore, it needs an external source of thiol, such as Trx or glutathione, to reduce the thiosulfinate intermediate [48, 49]. The evolution of an ATP consuming process to reactivate Prxs after deactivation of their peroxidase function by  $H_2O_2$  provides a unique advantage to the host organism. The  $H_2O_2$  and Srx act as an On-Off switch for the chaperone and peroxidase functions of various Prx. The excess of  $H_2O_2$  enhances the chaperone function and reduces the peroxidase function of Prxs, whereas an excess of Srx reverses this process [50]. Figure 1-1 depicts the mechanism by which Srx performs the aforementioned antioxidant function. The Prx structure in this figure is designed to give a rough idea about the positions of individual cysteine in a typical 2-Cys Prx. The C-terminal  $C_R$  is shown in the C-terminal arm and the other cysteine in Prx indicates the N-terminal  $C_P$ .

Another important action of Srx involves the deglutathionylation of several substrates in eukaryotes [45]. Most of the Prx-independent and a few Prx-dependent functions of Srx are mediated by this mechanism. Figure 1-2 depicts the role of Srx in the deglutathionylation process. Srx can regulate the chaperone function of Prx1 by controlling its levels of glutathionylation. The glutathionylation of Cys<sup>83</sup> of Prx1 favors formation of dimer over decamer, resulting in the loss of chaperone activity [51]. Although it is a general consensus that Prx-reducing activity of Srx is more important than its deglutathionylation function, more mechanistic studies are required to assess the individual contribution of Prx reduction and deglutathionylation processes in regulating the chaperone function of Prx1 or other typical 2-Cys Prxs.



6

**Figure 1-2: Mechanism of the deglutathionylation function of sulfiredoxin** : Figure shows how glutathione assists sulfiredoxin in carrying out this function.

There is no evidence of tissue specific predominance of one Srx function over the other. However, there is a great scope for exploration of Srx deglutathionylation function. The lack of extensive biochemical studies in this field may be a possible reason behind the difficulty in ranking the importance of antioxidant vs. deglutathionylation functions of Srx. Unlike the antioxidant function of Srx, which is exclusive to Prxs, the deglutathionylation carried out by Srx does not seem to be limited to Prxs. S100A4, actin and PTP1B are examples of substrates other than Prx whose glutathionylation levels can be regulated by Srx [22, 52]. There may be other intracellular targets of Srx that can be deglutathionylated by Srx. Identification of those substrates may help to identify different mechanisms of Srx signaling.

#### **1.1.4 Molecular characteristics of the Srx-Prx interaction**

The Cys<sup>99</sup> of human Srx is not involved in Srx-Prx binding but it is directly involved in the antioxidant and deglutathionylation functions of Srx [47, 50, 53]. Amino acids adjacent to Cys<sup>99</sup> (i.e., Gly<sup>97</sup>, Gly<sup>98</sup>, His<sup>100</sup>, and Arg<sup>101</sup>) are considered to play a supportive role for the enzymatic activity of Srx [54]. Pro<sup>52</sup>, Leu<sup>82</sup>, Phe<sup>96</sup>, Val<sup>118</sup>, Val<sup>127</sup>, and Tyr<sup>128</sup> are amino acids that form a hydrophobic pocket in Srx that acts as the interface for Srx-Prx interaction [54, 55]. The hydrophobic pocket formed by the active site of Srx forms a depression that wraps around the slightly protruding active site of Prx [54]. It acts as a lock and key model of Srx-Prx interaction.

The Prx family of proteins is one of the most abundant and most efficacious antioxidants in the human body. The enzymatic cysteine of Prx is called



peroxidatic cysteine ( $C_P$ ). A few Prx isoforms also contain a cysteine called  $C_R$ . Classification of Prx is based mainly on the presence and behavior of  $C_R$  in different Prx-isoforms [15]. Individual Prxs also contain cysteines other than peroxidatic and  $C_R$ , which may play some regulatory role in these Prx. For example, Cys<sup>83</sup> of Prx1 mediates the formation of a decameric complex of Prx1 that differentiates the functions of Prx1 from Prx2 [56]. Despite sharing 78% sequence similarity with other typical 2-Cys Prx, one cysteine of Prx1 (Cys<sup>83</sup>) plays an especially important role as it is a highly efficient chaperone compared to other Prx [56]. One report indicates that Cys<sup>83</sup>-Cys<sup>83</sup> disulfide bond formation is not essential for rat Prx1, in particular, as it forms a decameric structure through hydrophobic interactions and van der Waals bonds [57]. Glutathionylation of Cys<sup>83</sup> has been reported to negatively affect the chaperone function of Prx1 [51]. However, the way the glutathionylation impacts the chaperone activity of other typical 2-Cys Prxs remains to be understood.

The number of amino acids between the peroxidatic and  $C_R$  is critical for the formation of the Prx dimer. All human typical 2-Cys Prx have 121 amino acids between the  $C_P$  and  $C_R$ . This 121 amino acid distance imparts the ability to form an intermolecular disulfide bond between the  $C_P$  of one typical 2-Cys Prx monomer and the  $C_R$  of another monomer and viceversa. The bond results in the formation of a homodimer of Prx in which the two Prx monomers are oriented in an antiparallel manner. Under reduced state, these typical 2-Cys Prx are still present in the form of a homodimer but the process involves only non-covalent interaction [58]. In atypical 2-Cys Prxs, there is a 104 amino acid

distance between C<sub>P</sub> and C<sub>R</sub> [47]. This distance helps the Prx5 form an intramolecular disulfide bond. The distance of C<sub>P</sub> and C<sub>R</sub> from the GGLG and YF motif is another highly conserved feature of typical 2-Cys Prxs. The GGLG motif is located between the C<sub>P</sub> and C<sub>R</sub>, 42 amino acids downstream of the C<sub>P</sub>. The YF motif is localized between the C<sub>R</sub> and the N-terminus (i.e., 20 amino acids downstream of C<sub>R</sub>). GGLG and YF motifs bestow these Prx with the unique ability to become over-oxidized by H<sub>2</sub>O<sub>2</sub> [59]. The YF motif interacts with the GGLG motif, which hinders interaction between the C<sub>P</sub> of oxidized Prx and the C<sub>R</sub> of the other monomer. This allows the second H<sub>2</sub>O<sub>2</sub> molecule to react with the C<sub>P</sub> of the first Prx monomer in a timely manner, resulting in the formation of over-oxidized Prx [60]. In the absence of the GGLG and YF motifs, Prx will not become over-oxidized, thus they are important for the chaperone function of Prxs [59]. The GGLG and YF motifs were also identified in prokaryotic Prx [21]. The chaperone function is gained by the formation of higher molecular weight complexes that look like a stack of rings in transmission electron microscopy and X-ray crystallography studies [61]. In some species, hyperoxidation of the C<sub>P</sub> is not required for the gain of chaperone function, as their Prx can form a high-molecular weight structure in the absence of hyperoxidation [62]. However, human Prxs have been known to gain chaperone function only after the C<sub>P</sub> is over-oxidized. Susceptibility to hyperoxidation varies among the typical 2-Cys Prxs. For example, Prx3 is considered more resistant to hyperoxidation than other isoforms [63]. The conservation of amino acids around the C<sub>P</sub> probably indicates their importance for the enzymatic activity or a particular behavior of a

Prx isoform. For example, most Prx have a proline and a threonine (occasionally serine) before the C<sub>P</sub>, forming a PXXXTXXC motif. This may be important for the enzymatic activity of Prxs [64]. In human typical 2-Cys Prx, amino acids around the C<sub>P</sub> (i.e. PLDFTFVCPTEI motif) and the C<sub>R</sub> (i.e. HGEVCPAXW motif) are highly conserved [65]. This conserved sequence of amino acids around C<sub>P</sub> and C<sub>R</sub> may indicate their importance for Prx function [66]. However, the significance of these amino acids has not been experimentally proved yet and may be of interest for further studies. Although all typical 2-Cys Prx are generally considered substrates of Srx, the affinity of Srx to individual Prx is not the same [32]. Srx has the highest affinity for Prx4 among all the typical 2-Cys Prxs [32]. However, the way this high affinity of interaction affects the kinetics of Prx4 reduction compared to other Prx still needs to be studied. Members of the Prx family may have different subcellular localizations, and their abundance in different tissues also varies. The interaction between Srx and different isoforms of Prx is thus also affected by their subcellular localization. For example, the Srx-Prx3 interaction becomes significant only under higher oxidative stress conditions. At higher oxidative stress, the mitochondrial wall gets damaged. Hence, Srx may translocate from cytosol to mitochondria through those damaged mitochondrial walls [30]. At lower oxidative stress conditions, the Srx-Prx3 interaction is not noticeable. An alternative explanation of this phenomenon is proposed in the literature: Prx3 can be over-oxidized only at higher oxidative stress levels due to its high resistance to over-oxidation [63]. There may be some molecular characteristics of reduced Prx3 that does not allow its interaction with

Srx. Hence, the molecular rearrangement during over-oxidation of Prx3 becomes necessary for facilitation of Srx-Prx3 interaction. However, more mechanistic studies are required to clarify whether this is the case. All these molecular factors affect signaling of the Srx-Prx axis. Differential affinity of Srx for individual Prx as well as molecular characteristics of individual Prx allows them to regulate a wide range of cell signaling, which I will discuss in detail in the next few sections.

#### **1.1.5 The role of the Srx-Prx axis in cell-signaling and carcinogenesis**

The main function of the Srx-Prx system is to protect host cells from oxidative damages. This property of the Srx-Prx system becomes harmful to the host organism when it starts protecting the survival of tumor cells. As per the data from Oncomine (an online microarray database) [67] and other published literature, the Srx-Prx system is altered in multiple types of cancer. Table 1-1 summarizes different types of cancer in which expression of individual members of the Srx-Prx system is altered. The information in Table 1-1 indicates changes in mRNA expression. Up-regulation indicates more than a 1.5 fold increase in mRNA levels whereas down-regulation indicates more than a 1.5 folds decrease in mRNA levels. Apart from mRNA, alterations at the protein level are also reported for multiple tumor types. Information about expression changes at places other than those shown in Table 1-1 are mainly based on studies of their protein levels. The correlation between patient survival and protein expression changes has not been studied. From published data, the Srx-Prx system predominantly functions as an activator or enhancer of oncogenic signaling to promote cancer development.

**Table 1-1: Expression pattern of the Srx-Prx system in different cancer types as evident from microarray data available at Oncomine:** Up-regulation is classified as more than a 1.5 fold increase in expression compared to normal non-tumor cells; Down-regulation is classified as more than a 1.5 fold decrease in expression compared to normal non-tumor cells. Data summarized here can be confirmed by other independent studies

<b>Protein</b>	<b>Up-Regulation</b>	<b>Down-Regulation</b>
Srx	Breast cancer, Colorectal cancer, Lung cancer, Prostate cancer, Skin cancer	Esophageal Cancer
Prx1	Bladder cancer, Colorectal cancer, Gastric cancer, Leukemia, Liver Cancer, Lymphoma, Breast cancer, Pancreatic cancer, Sarcoma	Esophageal Cancer, Head & Neck cancer, Myeloma
Prx2	Colorectal cancer, Lung cancer, Lymphoma, Myeloma, Ovarian cancer	Brain & Central Nervous System (CNS) cancer, Esophageal cancer, Head & Neck cancer, Kidney cancer, Leukemia, Pancreatic cancer, Sarcoma
Prx3	Gastric cancer, Head & Neck cancer, Lymphoma, Prostate Cancer	Bladder cancer, Brain & CNS cancer, Kidney cancer, Leukemia, Pancreatic cancer
Prx4	Bladder cancer, Brain & CNS cancer, Breast cancer, Cervical cancer, Colorectal cancer, Head & Neck cancer, Kidney cancer, Lung cancer, Lymphoma, Melanoma, Prostate Cancer, Sarcoma	Leukemia, Liver cancer, Pancreatic cancer

A few reports have also indicated a tumor suppressor function of the Prx family. Hence, Prx may function as a double-edged sword in tumorigenesis. The exact role of the individual components of the Srx-Prx system in cancer can be complicated, and should be considered in the context of specific cancer and cell types.

#### **1.1.5.1 Srx in cell-signal transduction and tumorigenesis**

The expression of Srx is regulated by factors at both the transcriptional and translational levels. Redox signaling is the major component that activates Srx expression. Figure 1-3 summarizes how the expression of Srx is regulated by redox signaling. Activation of transcription factors, such as nuclear factor erythroid 2-related factor 2 (Nrf2), induces Srx expression [68]. Activator protein-1 (AP-1) also up-regulates Srx expression [69]. c-Jun is a component of the AP-1 complex and its activation stimulates Srx expression. TAM67 is an N-terminal deletion mutant of c-Jun that acts as a c-Jun antagonist. Therefore, TAM67 negatively regulates Srx expression by inhibiting the AP-1 complex [70]. Multiple intracellular and extracellular factors such as nitric oxide, cigarette smoke, dietary derived electrophiles, and tumor promoters like 12-O-tetradecanoylphorbol-13-acetate (TPA) lead to the activation of Nrf2 or AP-1 and have the potential to stimulate the expression of Srx [70, 71]. In mouse macrophages, treatment with lipopolysaccharide strongly induces Srx expression in an Nrf2 and AP1 dependent manner [72]. Besides these transcriptional regulations, Srx expression is negatively regulated at the translational level by cAMP-PKA (cyclic AMP-protein kinase A) through the eIF2 kinase Gcn2 [73].

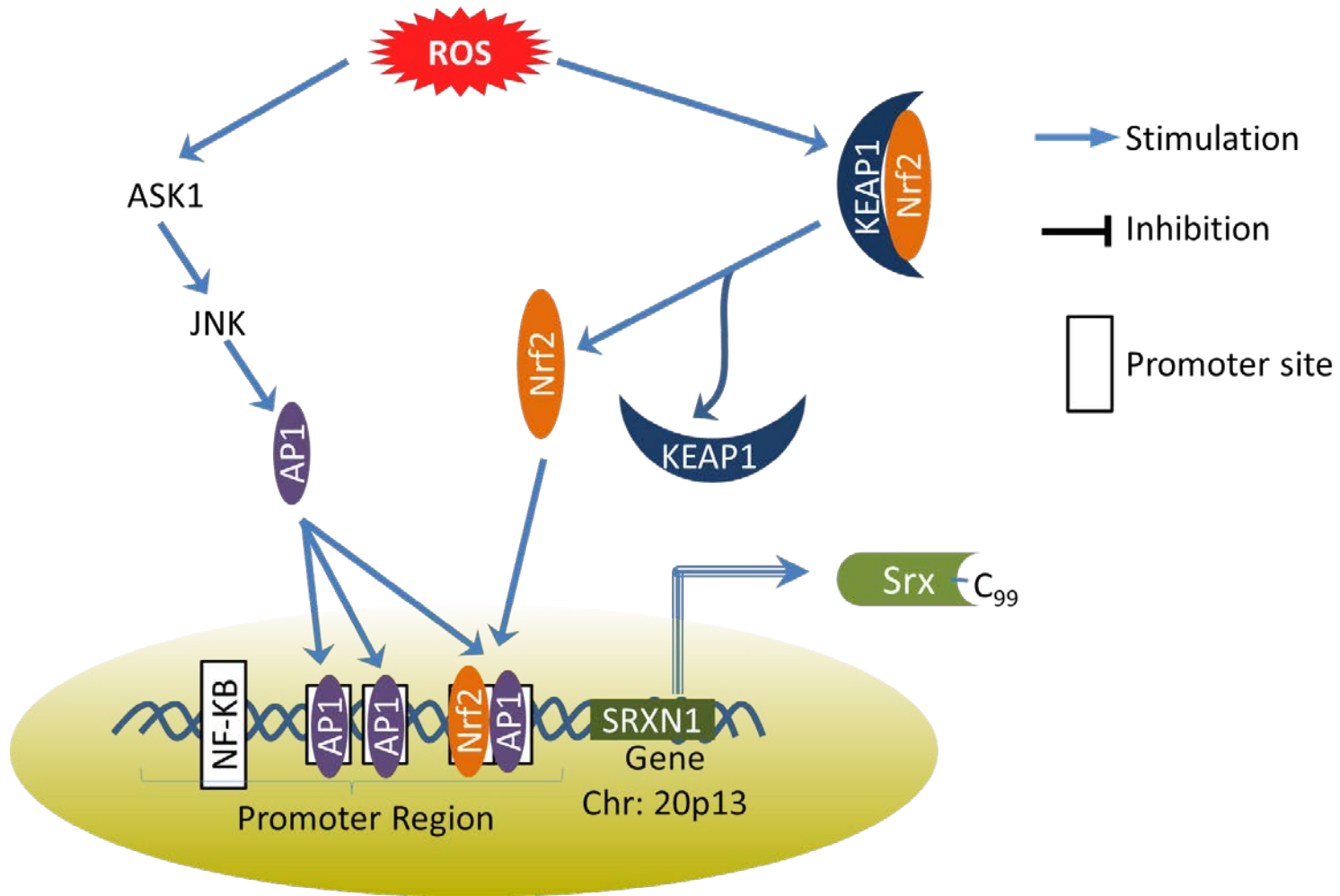


**Figure 1-3: Oxidative stress stimulates sulfiredoxin expression by activating AP-1 and Nrf2 activity:** AP-1 and Nrf2 transcriptionally regulates the sulfiredoxin expression.

Srx is over-expressed in a variety of cancers and it may promote carcinogenesis in a Prx-dependent or independent manner [32, 52]. It promotes tumor progression in lung cancer by enhancing intracellular phosphokinase signaling such as mitogen-activated protein kinase (MAPK) and AP-1/MMP9 (matrix metalloproteinase 9) signaling in a Prx4-dependent manner [32].

Srx may also enhance cell migration in lung cancer in a Prx-independent manner by interacting with S100A4 (a calcium binding protein) and non-muscle myosin IIA [52]. Aberrant expression of Srx in lung squamous cell carcinoma, lung adenocarcinoma, and pancreatic cancer is correlated with poor survival in patients [74-76]. Srx is also over-expressed in renal cell carcinoma where it is proposed to be a good target for antibody to induce tumor cell death [77]. Srx expression is stimulated by TPA via MAPK/JNK (c-Jun N-terminal kinase) pathway in skin carcinogenesis and Srx depletion at least partially protects mice against DMBA (7,12-dimethylbenz[a]anthracene) / TPA-induced skin carcinogenesis [78]. Srx is also necessary for colon carcinogenesis as it is highly over-expressed in colon tumor tissue compared to normal human colon, and Srx null mice are highly resistant to azoxymethane/dextran sulfate sodium-induced colon carcinogenesis [34]. Although the importance of Srx in various tumor types is well established, research is needed to understand the mechanism by which Srx plays a role in tumor progression and metastasis. Considering lung cancer as an example, the antioxidant and deglutathionylation activities of Srx may work in tandem to enhance the chances of tumor promotion and metastasis [32, 52]. However, more studies are required before we can rank their individual contributions toward cancer. Unraveling the



mechanistic details of Srx signaling will further help us design better approaches to target tumors in which Srx plays an essential role.

#### **1.1.5.2 Prx1 in cell-signal transduction and tumorigenesis**

Prx1 is mainly localized in the cytoplasm and can translocate to the nucleus [79]. The expression of Prx1 is regulated at both transcriptional and post-transcriptional levels. At the transcriptional level, Nrf2 directly activates its expression [80]. Focal adhesion kinase is also reported to be involved in transcriptional regulation of Prx1 [81]. In one study, Prx1 null mice were shown to be prone to spontaneous tumor development [38], suggesting that Prx1 may function as a tumor suppressor. However, Prx1 null mice developed in another lab were normal and free of tumor development [82]. The tumor suppressor function of Prx1 may be mediated by its regulation of PTEN (phosphatase and tensin homolog) levels as indicated in a mouse breast cancer model [83]. Also, PTEN null mouse embryonic fibroblasts are resistant to ROS-mediated induction of Prx1/Prx2 expression [84]. Prx1 may also be required for ROS-mediated activation of the K-Ras/ERK pathway that contributes to lung tumorigenesis [85]. Moreover, Prx1 along with Prx4 plays an essential role in the regulation of c-Jun and AP-1 mediated promoter activity in lung cancer cells [86]. Activation of Prx1 by histone deacetylase inhibitor (FK228), results in induction of apoptosis in esophageal tumor cells [87]. Furthermore, Prx1 helps reactivate DEP-1 (a protein tyrosine phosphatase that functions as tumor suppressor) by reducing the levels of ROS [88]. These mechanisms are a few examples of how Prx1 functions as a tumor suppressor.

On the other hand, there are many reports indicating that Prx1 has an essential pro-oncogenic role in cancer. For example, Prx1 promotes vascular endothelial growth factor expression in a toll-like receptor 4-dependent manner. This effect of Prx1 enhances angiogenesis and results in an environment favorable for tumor cell proliferation and promotes tumor progression in prostate cancer [89, 90]. Prx1 is over-expressed in esophageal cancer cells and has an auto-immunogenic activity [91]. Prx1 protein is also found aberrantly increased in early stage endometrial cancer where its functional significance is yet to be established [92]. Prx1 induces TRAIL (tumor necrosis factor–related apoptosis-inducing ligand) resistance by suppressing the redox-dependent activation of caspase [93]. TRAIL is a biological agent that induces apoptosis of cancer cells and is considered a promising anticancer agent [94]. Down-regulation of Prx1 (using RNA interference or chemical agents like dioscin) results in induction of apoptosis in tumor cells [95, 96]. Also, in A549 lung adenocarcinoma cells, Prx1 enhances the transforming growth factor (TGF)- $\beta$ 1 induced epithelial-mesenchymal transition (EMT) by stimulating the expression of snail and slug—two transcription factors that inhibit E-cadherin expression [97]. For this function, the Cys<sup>51</sup> (C<sub>P</sub>) of Prx1 is essential, as replacement of Cys<sup>51</sup> by Ser nullifies this effect [97]. A study using murine hepatocytes as well as human esophageal and lung cancer cell lines reports that TGF- $\beta$ 1 enhances ROS production by up-regulating the levels of ferritin heavy chain and intracellular labile iron pool [98]. It can be inferred from these studies that ROS produced by TGF- $\beta$ 1 signaling probably oxidizes the C<sub>P</sub> of Prx1 and this oxidation is essential for the role of Prx1 in EMT. Therefore, higher levels of ROS may promote the

progress of EMT. Whether and how the hyperoxidation of Prx1 and its molecular chaperone activity are involved in the process of EMT is largely unknown. Figure 1-4 depicts how Prx can perform both tumor suppressor and oncogenic functions. The factors that determine the dominance of one role over another are yet to be identified. Possibly, Prx1 functions as a tumor suppressor before transformation, but after transformation it promotes tumor cell proliferation by protecting against ROS-induced cell death. Other possible explanations may be related to the single nucleotide polymorphism or allelic variants of Prx1, but these factors need further investigation.

#### **1.1.5.3 Prx2 in cell-signal transduction and tumorigenesis**

Prx2 is the second member of the typical 2-Cys Prx. It is mainly present in cytosol [79] and is one of the most efficient H<sub>2</sub>O<sub>2</sub> scavengers in cells compared to the majority of other antioxidants [99]. In red blood cells, the oxidation-reduction cycle of Prx2 correlates with the circadian rhythm resulting in circadian rhythm dependent oligomerization of Prx2 [100]. This oscillation in levels of over-oxidized Prx2 is not controlled at the transcriptional level since red blood cells do not have a nucleus [100]. It is also not likely controlled by Srx, as the oscillations exist in Srx null mice [101]. Rather, it is controlled by hemoglobin autoxidation and 20S proteasome in red blood cells that are in turn regulated by circadian rhythm [101]. Extensive methylation of CpG islands in the promoter region of the Prdx2 gene is one of the mechanisms to control Prx2 expression in melanoma [102]. Prx2 expression is also regulated by transcription factor Hand1/Hand2 [103].

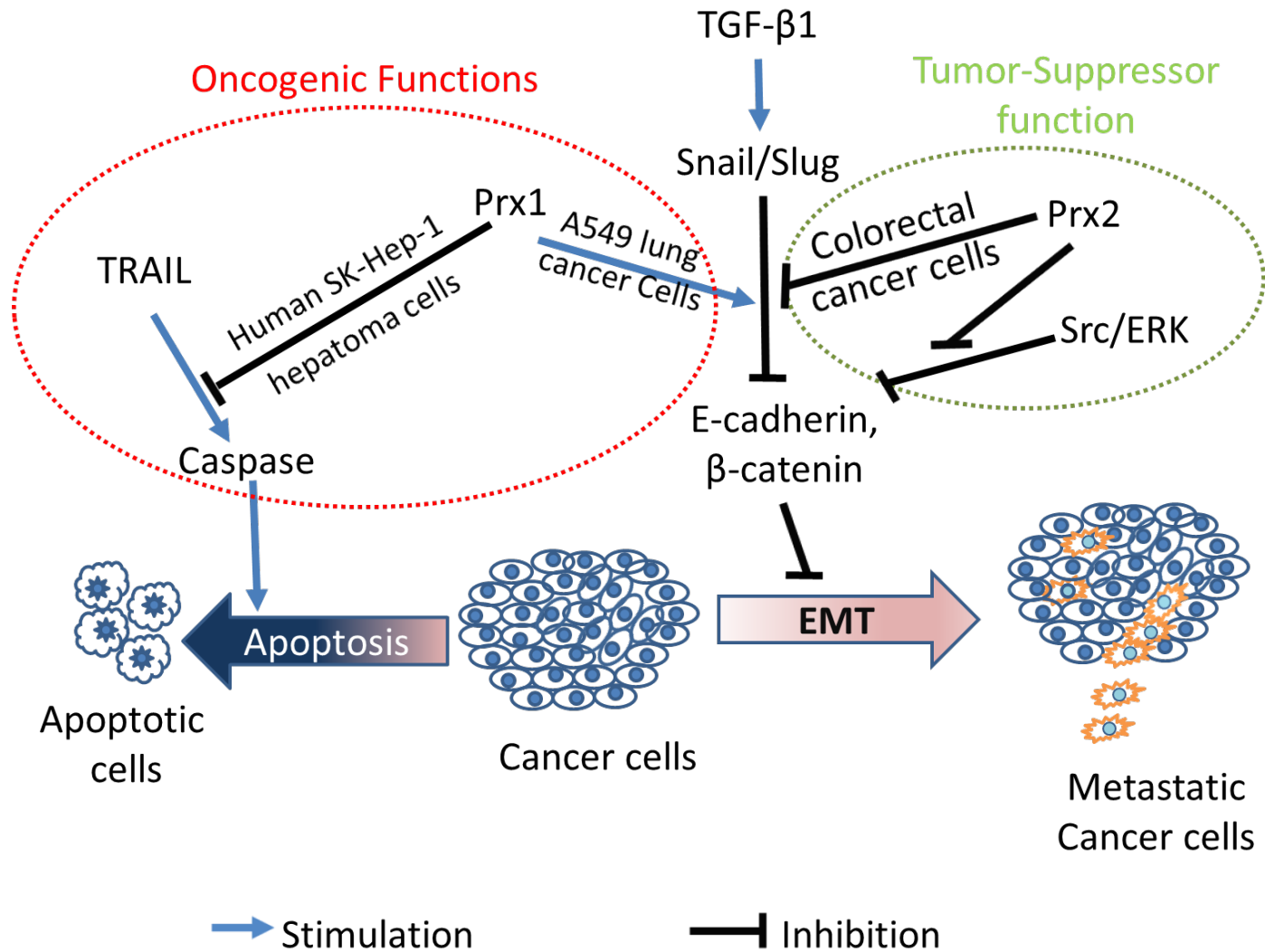


Figure 1-4: Peroxiredoxin may act as a tumor-suppressor or oncogene depending on the tumor type.

In mouse embryonic fibroblasts, Prx2 is induced by ROS in a PTEN dependent manner [84]. As mentioned earlier, PTEN activation is regulated by Prx1; therefore, it can be assumed that Prx1 may have potential to affect Prx2 expression too. Prx2 is down-regulated in a few cancers where Prx1 is up-regulated, but the exact mechanism behind the differential expression is not yet known [104, 105]. Whether or not PTEN is responsible for this relationship between Prx1 and Prx2 expression in those tissues remains a question. Nitrosylation of Tyr<sup>193</sup> in the YF motif of Prx2 is an important post-translational modification that plays a critical role in regulation of disulfide bond formation under oxidative stress conditions [106]. Glutathionylation is another post-translational modification of Prx2 that may affect its localization to the extracellular compartment [107]. Extracellular Prx2 is glutathionylated under oxidative stress conditions and the glutathionylated form induces TNF $\alpha$  production, leading to oxidative stress dependent inflammatory reaction [107]. In this manner, Prx2 plays a role in cytokine mediated inflammation. Serum levels of Prx2 in colorectal cancer are correlated with survival of patients [108]. In human papillomavirus related cervical cancer, increased expression of Prx2 is proposed to mediate carcinogenesis in cervical tissue [109, 110]. However, more studies are required to establish whether alteration of Prx2 is a cause or effect of carcinogenesis. Prx2 is the main factor determining the metabolic stress and oxidative stress response of breast cancer cells metastasized to lung [111]. It also regulates the activation of transcription factor STAT3 by transferring the oxidative equivalents to the latter, resulting in generation of a disulfide-linked

inactive STAT3 oligomer [99]. Prx2 reduces the chances of metastasis by negatively regulating Src/ERK activation, resulting in increased E-cadherin expression and  $\beta$ -catenin retention [112]. Prx2 overexpression also reduces the chances of TGF- $\beta$ 1 induced EMT and cell migration in colorectal cancer cells [113]. It is interesting to note that the effect of Prx2 on TGF- $\beta$ 1 induced EMT in colorectal cancer cells is exactly opposite to the effect of Prx1 on the same signaling pathway in A549 cells, which is discussed earlier in this review and depicted in Figure 1-4. However, it is not clear yet whether these activities are regulated in a tissue-specific manner or they co-exist in the same cancer type.

#### **1.1.5.4 Prx3 in cell-signal transduction and tumorigenesis**

Prx3 is primarily a mitochondrial Prx. The expression of Prx3 is enhanced by SirT1 in partnership with FoxO3a and PGC1 $\alpha$ , and the absence of either leads to its down-regulation [114]. SirT1 enhances the complex formation of FoxO3a with PGC1 $\alpha$  and this complex regulates the expression of Prx3 as well as multiple other antioxidant proteins [114]. Prx3 expression is also regulated by superoxide dismutase through an unknown mechanism [115]. Prx3 is a downstream target of c-Myc transcription factor and it acts as a major mediator for the regulation of c-Myc functions in cell transformation, tumor progression, and apoptosis [116]. In medulloblastoma, Prx3 is a target of MiR-383 (a microRNA), and its expression reduces cell proliferation [117]. In cervical cancer, Prx3 is over-expressed and its levels are correlated with an increased rate of cell proliferation [118]. Single nucleotide polymorphism RS7082598 of the PRDX3 gene is correlated with a reduced risk of cervical cancer [119]. In lung squamous cell carcinoma, Prx3 is

over-expressed along with increased Srx in an Nrf2 dependent manner, which indicates a potentially important role of the Srx-Prx3 axis in these tumors [74].

#### **1.1.5.5 Prx4 in cell-signal transduction and tumorigenesis**

Prx4 is the fourth member of typical 2-Cys Prx family and resides mainly in endoplasmic reticulum. There is also a low molecular weight secreted form of Prx4 that can be found in extracellular matrix and plasma. Although there are a few reports about the post-transcriptional regulation of Prx4, how this protein is regulated at the transcriptional level is yet to be studied. Calpain (a calcium-dependent cysteine protease) can enhance the expression of Prx4 through post-transcriptional regulation [120].

Besides its regular antioxidant function, Prx4 also mediates the oxidative folding of various endoplasmic reticulum proteins through its chaperone function. Chaperone function is accomplished through cooperation with protein disulfide isomerase [121]. Data in our lab indicate that Prx4 is susceptible to hyperoxidation at very low levels of oxidative stress. Hence, the chaperone function of Prx4 may be facilitated at lower oxidative stress levels. Prx4 improves insulin synthesis by enhancing the endoplasmic reticulum folding of insulin and thus improves pancreatic  $\beta$ -cell function [122]. In pancreatic cancer, Prx4 is reported to be down-regulated [67]. However, it is not clear whether the Prx4 down regulation is a cause or effect of pancreatic cancer. Expression of Prx4 promotes the metastatic potential of lung adenocarcinoma cells [86]. Prx4 along with Srx increases RAS-RAF-MEK signaling by enhancing intracellular phosphokinase signaling [32]. The RAS-RAF-MEK pathway is well-known for

controlling cancer cell proliferation and metastasis in various types of cancer. Therefore, the ability of the Srx-Prx4 system to modulate this pathway indicates their importance in cancer development. The exact mechanism of regulation of RAS-RAF-MEK pathway by Srx or Prx4 is not identified yet. Theoretically, a ROS dependent mechanism may be involved since Srx restores the antioxidant function of Prx4 [32]. Moreover, Prx4 is a downstream mediator of Srx in lung cancer development. The Prx4 knockdown recapitulates the phenotypes of Srx knockdown cells (i.e. reduction in anchorage independent colony formation, cell migration, and invasion) [32]. There are a few other typical 2-Cys Prx-isoforms that may have similar effects in other pathological or physiological conditions, but such a strong relationship of Srx with other Prx is not reported yet. Furthermore, Prx4 is over-expressed in the majority of cancers where Srx is overexpressed (refer to Table 1-1) [67]. In prostate cancer, over-expressed Prx4 enhances the rate of cell proliferation [123]. In oral cavity squamous cell carcinoma, expression of Prx4 enhances cancer metastasis [124]. In colorectal cancer, high expression of Prx4 correlate with poor survival of patients [125]. As mentioned before, Srx is also highly expressed in colon cancer and is required for chemical-induced colon carcinogenesis [34]. Therefore, it may be of interest to study the significance of Srx and Prx4 in colon cancer.

### **1.1.6 Summary and future directions**

The Srx-Prx axis plays a critical role in a variety of physiological and pathological conditions involving redox signaling. Some information is available about cross-talk between the Srx-Prx axis and other signaling pathways. However, the factors



that affect this cross-talk are largely unknown. The way an individual isoform of Prx contributes to different signaling pathways remains elusive. It is necessary to differentiate the contributions of the antioxidant function of Prx and its molecular chaperone function in terms of their impact on signal-transduction. Further research will help to unravel the list of proteins whose folding is assisted by Prx. Such research will provide a direction to identify different signaling pathways that are modulated by the chaperone function of Prx. Classification of signaling pathways regulated by chaperone and antioxidant functions of Prx will help us design a better targeting strategy against Prx in tumor cells. Prx is clearly shown to play a protective role in cardiovascular and neurological diseases. However, its role in cancer is still controversial due to both tumor-suppressor and oncogenic roles played by Prx-isoforms in different cancer types. Special attention needs to be paid to the mechanism by which the same Prx-isoform can play different, and sometimes opposite roles in different cancer types. Post-translational modifications of Prx may be one of the mechanisms that contribute to the dual behavior of Prx. Other possible explanations may include the presence of allelic variants or single nucleotide polymorphism of the Prx genes. More in-depth mechanistic studies in the future will help to unravel the interweaved behavior of Prx and lead to development of better therapeutic strategies for cancer prevention or treatment.

The Srx itself plays an oncogenic role in many types of cancer, including skin, colon, and lung cancer, to name a few. The biochemistry of Srx function has been studied in great detail. However, discerning the role of Srx in

carcinogenesis requires a deeper understanding that can only be fulfilled by future research. Considering the oncogenic role of Srx, it will be worth exploring Srx inhibitors as molecules of choice for chemoprevention and/or chemotherapy. Our existing understanding of the Srx-Prx interaction can help in designing good targeting strategies against Srx. However, more details regarding Srx deglutathionylation activity will be of great help for defining future directions. The hydrophobic pocket of Srx or other amino acids present at the Srx-Prx interface can be defined as a target for inhibitor screening. Virtual screening tools and other computational methods of drug-discovery can help reduce the cost and time required for identifying a good inhibitor. In short, Srx can be explored as a therapeutic target in cancer and targeting Srx using small molecules can be a valuable strategy for development of future chemotherapeutic molecules.

## **1.2 Scope of dissertation**

### **1.2.1 Hypothesis**

The majority of Srx functions are mediated through the Srx-Prx interaction. Previous publications from our research group have demonstrated the oncogenic role of the Srx-Prx interaction in tumor promotion and metastasis. The general hypothesis of the research described in this dissertation is that Srx plays a critical role in lung carcinogenesis and targeting the Srx-Prx axis or Srx alone may facilitate future development of targeted therapeutics for prevention and treatment of human cancer.

### **1.2.2 Specific aims**

To test the stated hypothesis, the following specific aims were designed:

**Specific Aim 1:** Demonstrate that Srx enhances urethane-induced lung carcinogenesis.

**Specific Aim 2:** Demonstrate the molecular domains in Srx and Prx that can be used as a target site to modulate Srx-Prx interaction or inhibit Srx.

**Specific Aim 3:** To demonstrate the potential of ISO1 as an inhibitor of the Srx-Prx interaction.

## CHAPTER 2: EFFECT OF SULFIREDOXIN DEPRIVATION ON THE URETHANE-INDUCED LUNG TUMORIGENESIS

### 2.1 Synopsis

Sulfiredoxin (Srx) is the exclusive enzyme that reduces the over-oxidized form of typical 2-Cys peroxiredoxins (i.e. Prx1-4). It has been found to be over-expressed in human non-small cell lung cancer. Cigarette smoke induces lung carcinogenesis and is a mixture of multiple carcinogens that work together to promote tumorigenesis. Urethane is a component of cigarette smoke and has been known to induce lung tumors in mice. We first tested the effect of cigarette smoke condensate on Srx expression *in vitro*. Both cigarette smoke and urethane induced Srx expression *in vitro*. To study the effect of Srx on lung tumorigenesis *in vivo*, we tested the effect of Srx-knockout on urethane-induced lung tumorigenesis in mice. Srx knockout mice were generated on FVB background and lung tumorigenesis was induced by urethane protocol. We found significantly lower tumor multiplicity in Srx knockout (Srx<sup>-/-</sup>) mice compared to wild type (Srx<sup>+/+</sup>) or heterozygous (Srx<sup>+/-</sup>) siblings. Urethane treated BEAS2B cells indicated increased expression of Srx, Prx1, Prx2, and Nrf2. Histopathological analysis revealed that loss of Srx decreases tumor cell proliferation and enhances apoptosis. This data indicates that loss of Srx protects mice against urethane-induced lung tumorigenesis. Hence, Srx has a critical oncogenic role in lung tumorigenesis.

## 2.2 Introduction

Sulfiredoxin (Srx) is an exclusive enzyme that reduces over-oxidized typical 2-Cys peroxiredoxins [24]. Srx utilizes ATP and magnesium ( $Mg^{2+}$ ) or manganese ( $Mn^{2+}$ ) as cofactors and forms sulfinic phosphoryl ester followed by thiosulfinate intermediate to reduce over-oxidized Prx [24, 126]. Srx is evolutionarily conserved in the majority of eukaryotes, but is rare in prokaryotes, with few exceptions (e.g. cyanobacteria). Apart from its antioxidant function, Srx can catalyze the deglutathionylation of actin, Prx2, and protein phosphatase [45, 53]. There may be other unidentified substrates that are deglutathionylated by Srx. Biochemistry of the Srx-Prx interaction and enzymatic activity of Srx has been studied in great detail (*please refer to chapter 1*); however, the physiological and pathological significance of Srx has not been fully revealed. Srx expression is altered in many types of human cancer. Our previous work has demonstrated oncogenic association of Srx with skin, colon, and lung tumorigenesis, where it is found to be highly over-expressed in tumors compared to adjacent normal tissue [32, 34, 78, 86, 127].

Lung cancer is the leading type of cancer-related deaths worldwide [128, 129]. Smoking multiplies the risk of lung cancer according to amount and quality of exposure. To understand the effect of cigarette smoke on antioxidant protein expressions, we treated BEAS2B cells with cigarette smoke condensate (CSC) and studied its effect on the expression of various antioxidant proteins. CSC induced expression of various antioxidant proteins, including Srx. Cigarette smoke is a complex mixture of more than 5,000 chemicals [130]. To further study

the effect of cigarette smoke on tumorigenesis, we decided to test one of its components, urethane, which is a well-known lung carcinogen [131, 132]. Urethane is also present in a variety of fermented food and beverages, including alcoholic beverages [133]. Urethane-induced lung carcinogenesis is a well-established model in mice. Mechanistic studies identified Nrf2, AP-1, STAT3, and many other oxidative stress induced proteins as mediators of urethane's carcinogenic activity [134, 135]. Previous studies have indicated that oxidative stress related induction of Srx expression is mediated through Nrf2 as well [69, 78]. Therefore, we hypothesized that Srx may be a mediator of urethane-induced lung cancer. Whether Srx is involved in urethane-induced lung carcinogenesis has not yet been studied. Therefore, we studied the functional significance of Srx in urethane-induced lung carcinogenesis. We used Srx knockout mice and a well-established urethane-induced lung carcinogenesis model for this study. The model provides an important experimental strategy to study the pathological significance of Srx in urethane-induced lung carcinogenesis. Our data suggest that loss of Srx protects mice from urethane-induced lung tumorigenesis.

## **2.3 Materials & methods**

### **2.3.1 Cell culture and western blot**

Human lung/bronchus epithelial BEAS2B cell line was commercially obtained from American Type Culture Collection (ATCC; Manassas, VA). Cells were cultured in our laboratory less than 6 months after resuscitation. All experiments were conducted with BEAS2B cells within 10 passages in 6 months. Cells were

maintained in Dulbecco's Modified Eagle Medium (DMEM) (Lonza Walkersville, Inc., Walkersville, MD) containing 5% fetal bovine serum.

Cigarette smoke condensate was obtained from Dr. Chandra Gary Gairola's laboratory at the University of Kentucky. Urethane and N-acetyl cysteine were commercially obtained from Sigma-Aldrich (St. Louis, MO). The cells were treated with CSC concentrations of 10 µg/mL, 20 µg/mL, and 40 µg/m for 48 hours. To mimic chronic exposure to urethane from a variety of food, beverages, and cigarette smoke, we treated cells with urethane for 5 days. The media was changed daily and fresh urethane added each time the media was changed. For western blot, cells were lysed in radioimmunoprecipitation assay (RIPA) buffer containing protease inhibitors (Santa Cruz Biotech, Dallas, TX). Protein bands were separated using sodium-dodecyl sulfate-polyacrylamide gel electrophoresis and western blotting was performed following standard protocol. The primary antibodies used included anti-Srx (Proteintech, Chicago, IL; Catalog 14273-1-AP), anti-Prx I (Abcam, Cambridge, MA; Catalog ab41906), anti-Prx II (Santa Cruz Biotech; Catalog SC-33574), anti-Prx III (Santa Cruz Biotech; Catalog SC-59661), anti-Nrf2 (Santa Cruz Biotech; Catalog SC-722), anti-Prx IV (Abcam; Catalog ab133872), anti-p-c-Jun (Cell Signaling, Billerica, MA; Catalog 9261L) and anti-β-actin (Sigma–Aldrich; Catalog A2228).

### **2.3.2 Quantitative reverse transcription and polymerase chain reaction**

BEAS2B cells were treated with CSC or urethane. Vehicle treated cells were used as control. RNA was extracted using the RNeasy Kit (Qiagen, Valencia, CA). RNA (200 ng) was used for cDNA synthesis and polymerase chain reaction

(PCR). The following primers were used in the process: mSRX forward 5'- AAA GTG CAG AGC CTG GTG G-3', mSRX reverse 5'-CTT GGC AGG AAT GGT CTC TC-3'; mNRF2 forward 5'-AGT GGA TCT GCC AAC TAC TC-3'; mNRF2 reverse 5'-CAT CTA CAA ACG GGA ATG TCT G-3'; mPrx1 forward 5'- ACC TCT TCC TGC GTT CTC AC-3', mPrx1 reverse 5'-TGT CCA TCT GGC ATA ACA GC-3'; mGAPDH forward 5'-ACA ACT TTG GCA TTG TGG AA-3', mGAPDH reverse 5'-GAT GCA GGG ATG ATG TTC TG-3'. Reverse transcription and PCR were carried out using standard protocol [78]. The PCR product was mixed with SYBR green and 6X running buffer. This mixture was run on 3% agarose. The bands were quantitated using ImageJ software 1.49. Quantitative results were normalized by level of GAPDH mRNA.

### **2.3.3 Lentiviral ShRNA knockdown of Srx in BEAS2B cells**

BEAS2B cells were treated with 5 mM urethane for 3 generations. This treatment induced expression of Srx and other antioxidant proteins in those cells. ShRNA-based knockdown experiments were planned and performed according to previously published methods [86]. All ShRNA constructs, including MISSION® pLKO.1-puro control vector (vector control), MISSION® non-target shRNA (ShNT), and ShRNAs specifically targeting Srx (ShSrx), were commercially obtained (Sigma-Aldrich). Commercial sequencing services were utilized to confirm the sequence. Lentiviral particles expressing ShRNA were produced in HEK293T cells using the provider's plasmid packaging system and FuGENE 6 transfection reagent following suggested transfection and virus production procedures. The titer of virus-containing medium was determined by measuring



the level of p24 using ELISA and Lenti-X GoStix kits (Clontech, Mountain View, CA). To establish stable knockdown, urethane-treated BEAS2B cells were infected with lentiviral particles. Cells were subsequently maintained in puromycin-containing medium to establish stable cells.

### **2.3.4 Soft agar colony formation assay**

BEAS2B cells were treated with 5 mM and 10 mM urethane for 5 days. The control group was treated with phosphate buffer saline (PBS) as vehicle control. Each of these groups was harvested and cell numbers were counted using a Luna<sup>TM</sup> automated cell counter. The cells were suspended in 0.3% agar. The cell culture (6-well) plates were pre-coated with 1 mL of 0.6% agar and 15,000 cells were plated per well for each group. Urethane was added to the treatment group and PBS to the vehicle control group 24 hrs after plating. Medium was changed every 4 days and fresh urethane/vehicle was added each time the media was changed. The plates were incubated for 6 weeks. The soft agar colonies were stained using 0.25% crystal violet staining and images were taken using Amscope 3.7 software with a digital camera. The size and number of colonies were counted using OpenCFU 3.8.11 software.

To study the role of Srx in the urethane-induced BEAS2B cell transformation, we knocked-down Srx expression in urethane-treated BEAS2B cells using the lentiviral method. The BEAS2B cells were first treated for 3 generations with 5 mM urethane to enhance Srx expression. These cells were subjected to lentiviral infection to knockdown Srx. Vector-infected cells were used as control. These cells were subsequently maintained on 5 mM urethane along with puromycin-

containing media to get stable transfection. Srx expression in non-treated BEAS2B cells, along with multi-generation urethane-treated ShV and ShSrx cells were measured using western blot. We carried out the colony formation assay after stable knockdown was confirmed. Both ShVector (empty vector transfected) and ShSrx (Vector loaded with Srx shRNA transfected) cell colonies were treated with 5 mM urethane and puromycin throughout the incubation period. The rest of the procedure was the same as the procedure used for normal BEAS2B cells.

### **2.3.5 Srx knockout mice genotyping**

Mouse breeding and animal protocols were performed following the guidelines of the University of Kentucky's Institutional Animal Care and Use Committee. Srx knockout mice were generated on FVB background using Srx<sup>-/-</sup> B6/129 mice backcrossed onto an FVB mice strain [34]. After backcrossing on FVB background for seven generations, the inbred offspring were used for experiments. Genomics DNA from tail clip was extracted using genomic DNA extraction kit (Qiagen). This genomic DNA was used for PCR-based genotyping as previously reported [136].

### **2.3.6 Urethane protocol**

A randomized double-blind experimental design was applied to eliminate potential subjective bias. Briefly, mice at 7 week of age, including wild type (Wt), heterozygous, and knockouts, were given once weekly intraperitoneal injection for 3 weeks, with 1 mg/g body weight of urethane (Sigma-Aldrich) dissolved in saline [137, 138]. The mice were weighed before every administration of

urethane during the first 3 weeks. After the third administration of urethane, mice were weighed once weekly. Mice were maintained on a normal diet and ad libitum water for 10 weeks following the first injection. During this period of 10 weeks, mice with signs of severe suffering were euthanized. At the end of 10 weeks, all mice were humanely sacrificed. Mouse lungs were perfused with PBS followed by multiple rinses in PBS. Tumors were counted using a magnifying glass. This counted all the tumors on the surface of lung. Mouse lungs were fixed in 4% paraformaldehyde and stored in 70% ethanol before being processed with standard paraffin embedding and sectioning. For histological assessment, all lobes of each lung were sectioned for 15 slides and the first slide was stained by hematoxylin and eosin (H&E) staining.

### **2.3.7 Immunohistochemistry staining and *in situ* apoptosis assay**

Immunohistochemistry was performed using Vectastain Elite ABC kit #PK-6100 (Vector Laboratories, Inc., Burlingame, CA) with hematoxylin counterstaining. Antibodies used include anti-Srx (1:200, Proteintech, Chicago, IL; Catalog 14273-1-AP), anti-Prx1 (1:300, Abcam, Cambridge, MA; Catalog ab41906), anti-Nrf2 (1:200, Santa Cruz Biotech, Inc., Dallas, TX; Catalog SC-722) and anti-Ki67 (1:20, Abcam, Cambridge, MA; Catalog ab16667). Terminal deoxynucleotidyl transferase-mediated dUTP nick end labeling (TUNEL) assay was performed using TACS 2TdT-DAB In Situ Apoptosis Detection Kit (Trevigen, Gaithersburg, MD) to assay apoptosis in mouse lung. Following manufacturer's protocol, all samples were counterstained with methyl green, dehydrated, and mounted before microscopic visualization. Images of immunohistochemistry were taken

using a digital camera with AmScope 3.7 software attached to a Zeiss Axioplan 2 Imaging microscope (Carl Zeiss Microscopy, LLC, Thornwood, NY). The IHC images were quantitated using the Aperio Imagescope and the quantitative values were plotted in the form of bar graph for comparison.

### **2.3.8 Statistical analysis**

Quantitative data were presented as sample mean  $\pm$  standard deviation ( $\bar{x} \pm SD$ ). Data were analyzed with the indicated statistical methods using SigmaPlot (version 13.0). For calculation of the p-value, parameters of two-tailed 95% confidence interval were used for all analyses. A p-value of  $\leq 0.05$  was considered statistically significant.

## **2.4 Results**

### **2.4.1 CSC enhances the expression of antioxidant proteins**

BEAS2B cells were selected to study the effect of urethane on protein expression as they are an immortalized normal (non-cancer) lung cell line that is considered suitable to study chemical-induced carcinogenesis of lung cells. BEAS2B cells (human lung Broncho epithelial cell line) were treated with CSC at concentrations of 10  $\mu\text{g/mL}$ , 20  $\mu\text{g/mL}$ , and 40  $\mu\text{g/mL}$ . The two higher concentrations significantly enhanced expression of Srx and other antioxidant proteins after 48 hours of treatment (Figure 2-1A & B). The expression of all Prx (except Prx3) showed significant increase in concentration at all 3 concentrations. The Prx3 expression did not show significant increase in expression. We further tested whether this over-expression of the Srx-Prx axis is mediated by oxidative stress.

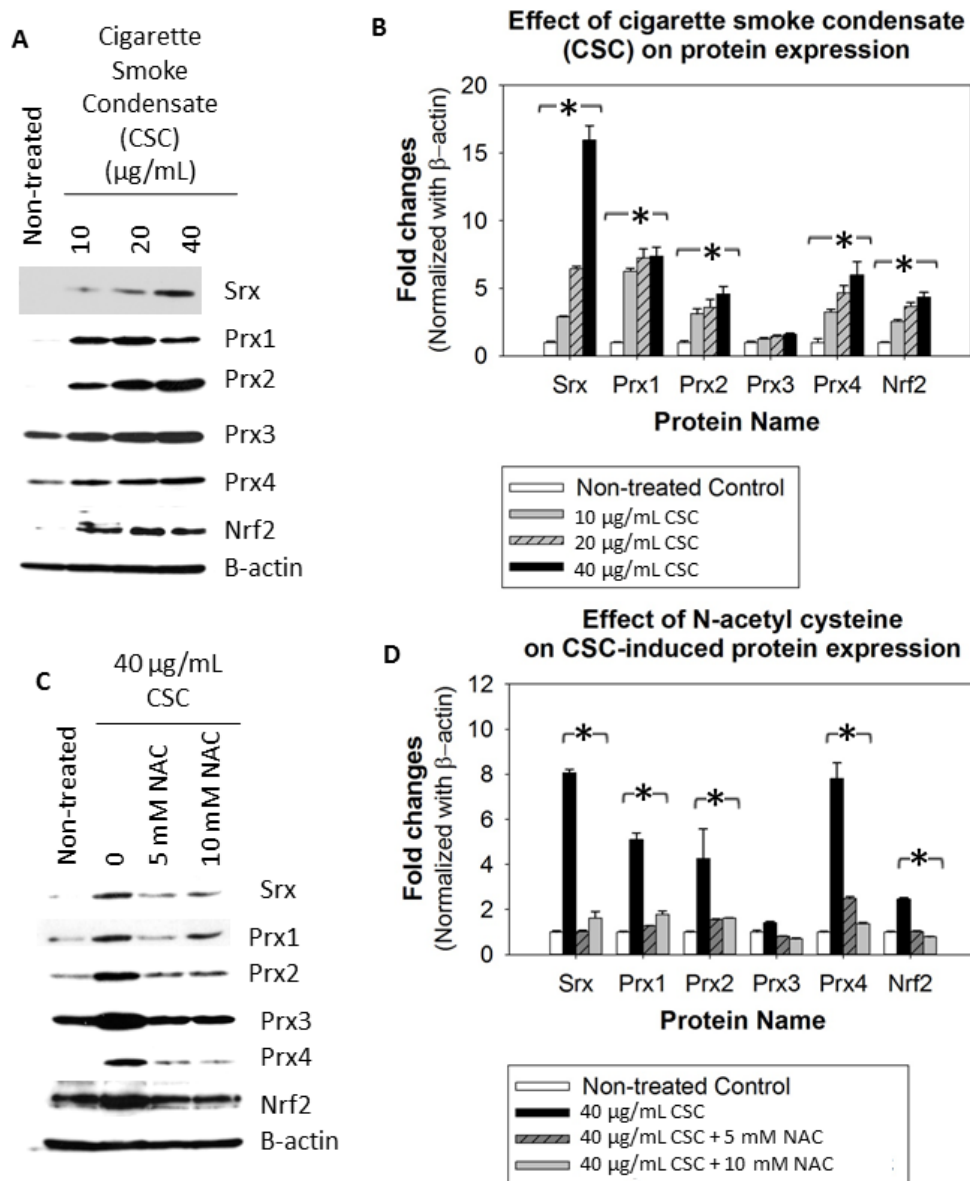


**Figure 2-1: Cigarette smoke condensate (CSC) induces the expression of antioxidant proteins:** CSC increases the expression of Srx, Prx, and Nrf2 in a dose-dependent manner and this effect can be reversed by co-exposing cells with N-acetyl cysteine: (A) western blot and (B) quantification graph showing expression of different proteins in BEAS2B cells treated with CSC for 48 hours; (C) western blot and (D) quantification graph showing the effect of N-acetyl cysteine on CSC-induced protein expression. The statistical significance is achieved for differences in all three treatments compared to control in panel (B) and both NAC treated group compared to CSC only group in panel (D). Statistically significant difference was not observed in case of Prx3. One way ANOVA followed by Holm-Sidak post hoc test was utilized to test statistical significance ( $p \leq 0.05$ ).

We co-treated a group of BEAS2B cells with N-acetyl cysteine (antioxidant) along with CSC for 48 hours. N-acetyl cysteine reversed the enhanced expression of these proteins (Figure 2-1C & D). Hence, CSC-induced overexpression of the Srx-Prx axis is mediated through oxidative stress. To confirm whether the regulation of protein expression is at a transcriptional or translational level, we studied the mRNA expression of individual proteins using reverse transcription followed by polymerase chain reaction (RT-PCR). The RT-PCR results indicated increased transcription of antioxidant proteins (Figure 2-2A & B). The highest increase in transcription was observed in Nrf2, Srx, and Prx1; transcription of Prx2 and Prx4 increased to a lesser extent. On comparing the changes in protein expression with mRNA expression, we found that the effect of CSC on protein expression was much stronger than its effect on mRNA expression. Hence, apart from transcriptional regulation, there can be other mechanisms by which CSC enhances protein expression.

#### **2.4.2 Urethane enhances expression of antioxidant protein**

Urethane is a component of cigarette smoke and fermentation products. We selected urethane to confirm whether it can enhance Srx expression in the same way as CSC. To mimic chronic human exposure conditions, we treated BEAS2B cells with urethane for 5 days. This 5-day chronic treatment induces the expression of sulfiredoxin in a dose-dependent manner (Figure 2-3 A&B). Urethane also enhances the expression of typical 2-Cys Prxs, especially Prx1 and Prx2. The levels of over-oxidized Prxs (i.e., Prx-SO<sub>3</sub>) were also found to be enhanced in urethane treated cells too.

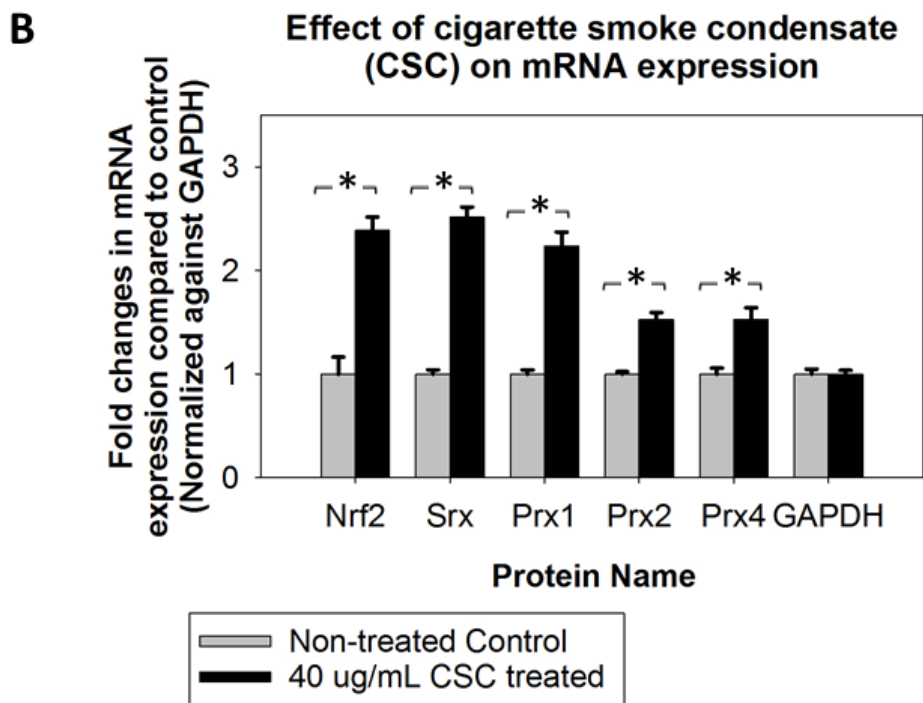
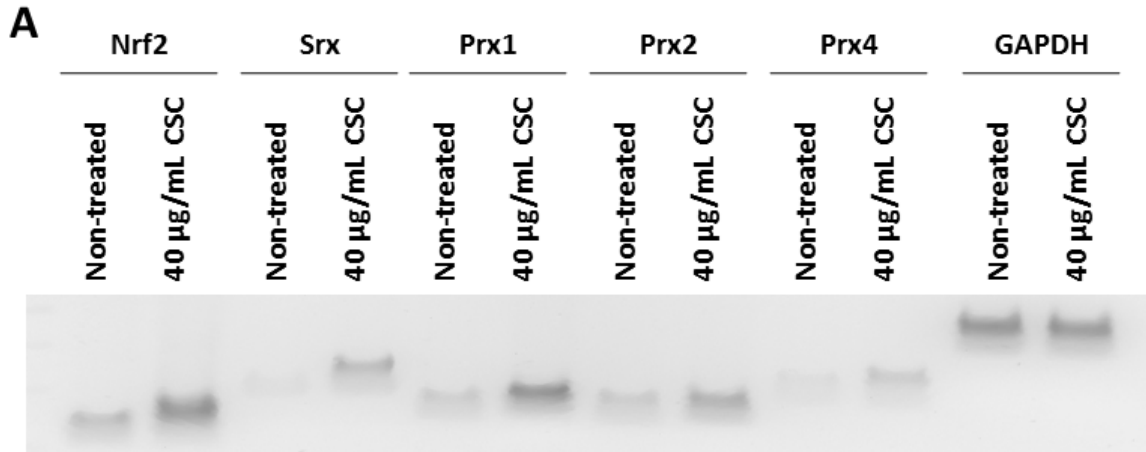


**Figure 2-2: Cigarette smoke condensate regulates the transcription of the Srx and Prx:** Cigarette smoke condensate transcriptionally regulates the expression of antioxidant transcripts. (A) RT-PCR gel showing mRNA expression of individual proteins; (B) graph showing quantification of bands. T-test was applied to analyze the statistical difference in mRNA expression (\* $p \leq 0.05$ ).

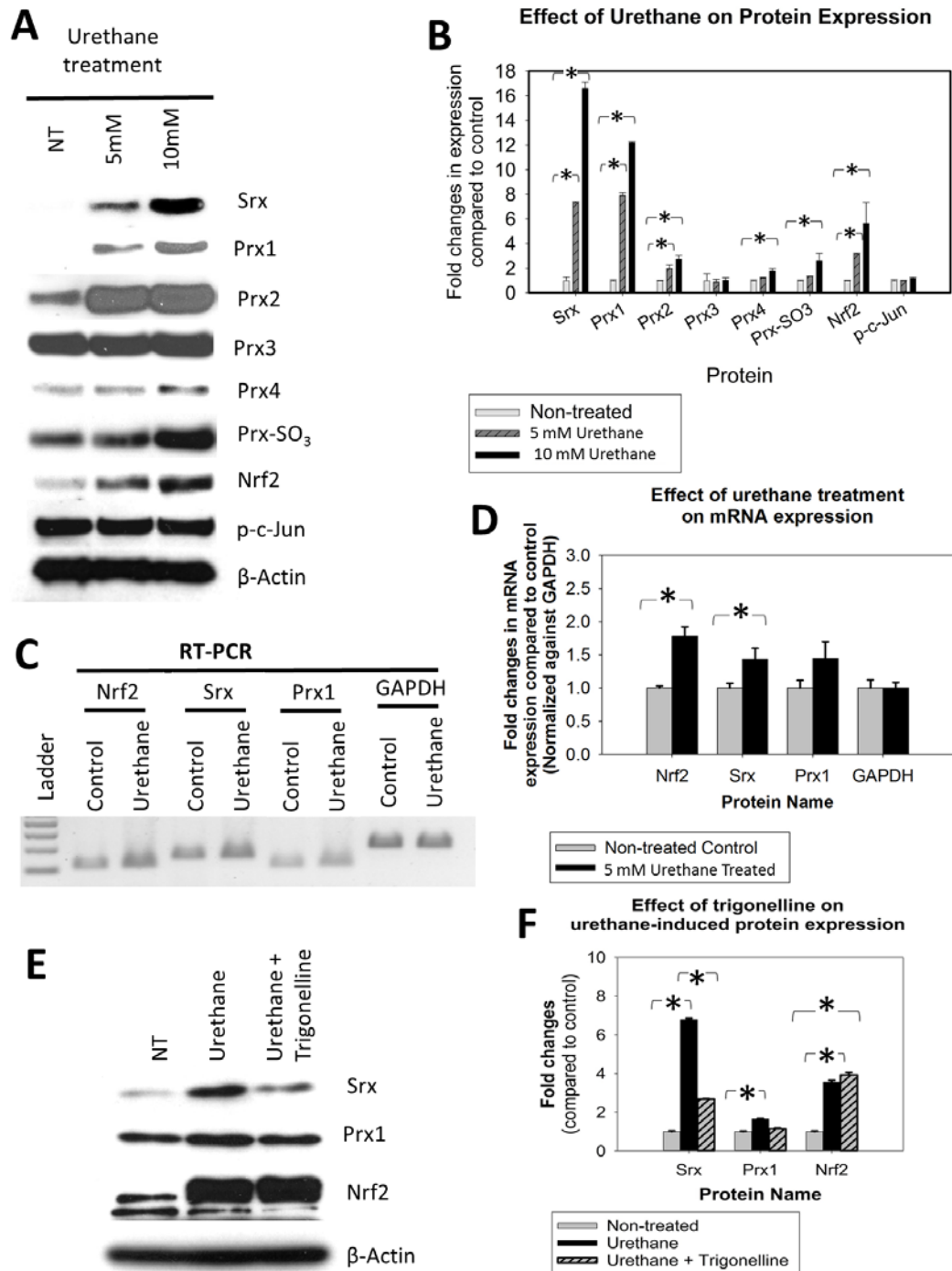


**Figure 2-3: Urethane treatment enhances antioxidant protein expression in BEAS2B cells:** (A & B) Effect of urethane on protein expression; (C&D) effect of urethane on mRNA expression; (E&F) effect of trigonelline on urethane-induced protein expression. One-way ANOVA on Ranks followed by Dunn's test was applied for analysis of protein expression. T-test was applied to analyze the statistical difference in mRNA expression (\* $p \leq 0.05$ ).



On comparison on increase in total Prx expression to increase in Prx-SO<sub>3</sub> expression, we concluded that Prx-SO<sub>3</sub> expression probably due to increased levels of total Prx and not due to higher oxidation of Prxs. Nrf2 signaling can be considered the most plausible mechanism of Srx and Prx1 induction by urethane treatment, as Srx was found to have higher expression in urethane-treated cells compared to control. The expression of Prx3 and Prx4 did not change substantially after 5 days of urethane treatment. To confirm the mechanism of Srx and Prx1 induction we next carried out reverse transcription-polymerase chain reaction. BEAS2B cells treated urethane for 5 days showed increase in mRNA transcription of antioxidant proteins (i.e. Srx, Prx1 and Nrf2). The increase in mRNA expression in the group treated with 5mM urethane was found to be statistically significant (two tailed t-test,  $p \leq 0.05$ ) for Nrf2 and Srx, but not for Prx1 compared to respective non-treated BEAS2B control (Figure 2-3 C&D). Similar to CSC treatment, the effect of urethane on protein expression was stronger compared to its effect on mRNA expression. Ergo, there can be non-transcriptional mechanisms by which urethane can regulate the expression of these proteins.

Earlier literature has indicated that the Nrf2 enhances the Srx transcription. Hence, a Nrf2 inhibitor should reduce the Nrf2 induced Srx and Prx1 expression. We studied the effect of trigonelline (Nrf2 inhibitor) on Srx and Prx1 expression in urethane treated cells. Trigonelline inhibited Srx expression in urethane treated cells (Figure 2-3 E & F). It confirms that urethane-induced Srx expression is mediated through Nrf2. Trigonelline inhibited Prx1 expression to a lesser extent.

Hence, urethane-induced Prx1 expression is (at least partially) mediated through Nrf2.

### **2.4.3 Urethane treatment transforms BEAS2B cells in an Srx-dependent manner**

After confirming the effect of urethane treatment on protein expression, we tested the effect of this treatment on BEAS2B cell transformation. Our initial study indicated that 5-day urethane treatment induces Srx expression in BEAS2B cells. Therefore, we initially treated cells for 5 days with 5 mM or 10 mM urethane, followed by treatment in soft agar plate with respective urethane concentrations or vehicle (phosphate buffer saline)-treated control. As expected, the vehicle-treated control group showed low anchorage-independent colony formation. However, the urethane-treated group produced multiple colonies. The numbers of colonies were higher in the 10 mM urethane-treated group compared to the 5 mM urethane-treated group, which indicates the dose-dependence of urethane's effect (Figure 2-4A & C). Statistically significant differences were observed in a number of colonies in the 10 mM urethane-treated group (but not the 5 mM urethane-treated group) compared to vehicle-treated control.

To study the role of Srx in the urethane-induced BEAS2B cell transformation, we studied the effect of Srx-knockdown on colony formation in the urethane-treated cells. The cells treated with urethane for multiple generations followed by Srx knockdown showed lower incidences of colony formation compared to vector infected control (Figure 2-4 B & D). Hence, urethane induced cell transformation is mediated through induction of Srx expression.

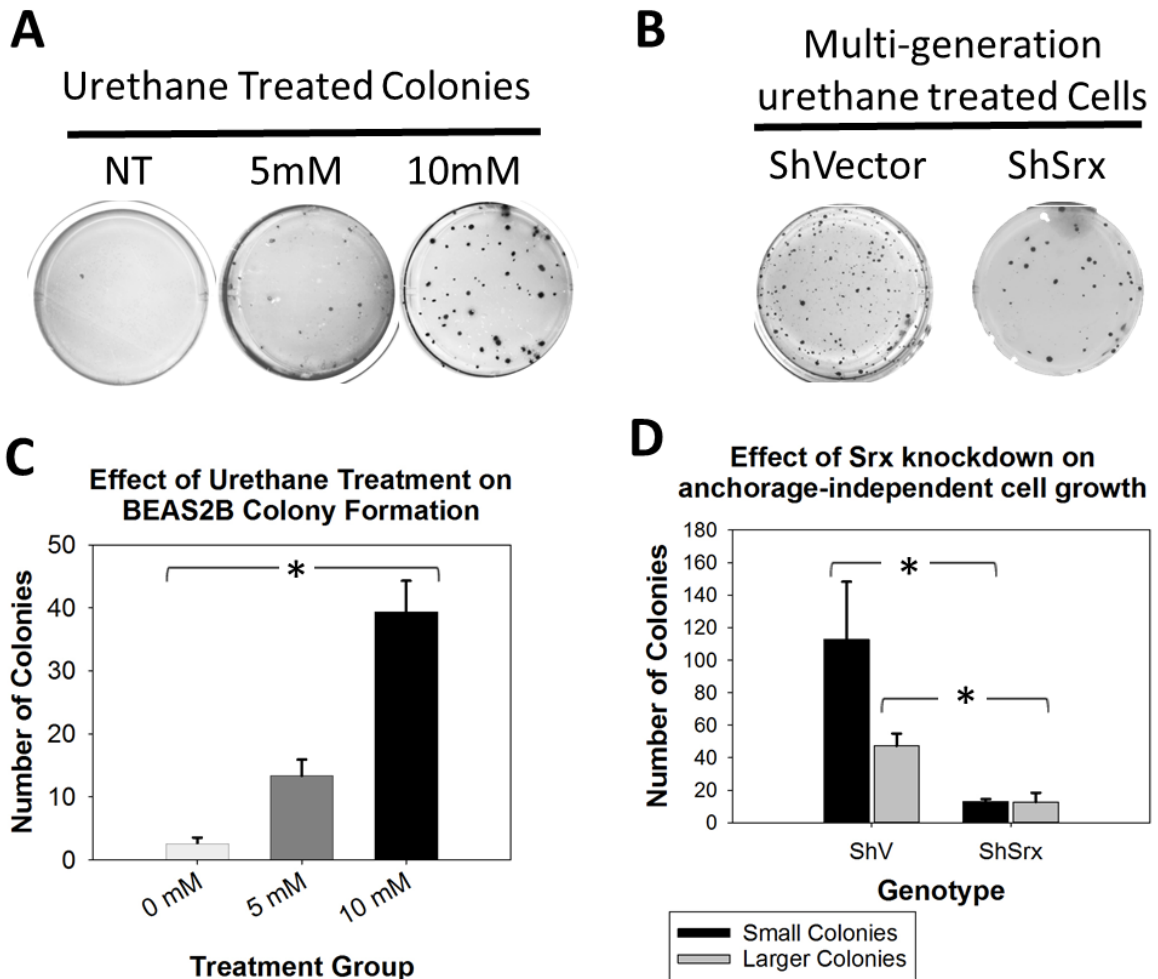


**Figure 2-4: Urethane transforms BEAS2B cells in an Srx-dependent manner:** Urethane enhances anchorage independent cell growth in a dose-dependent manner (A & C). Urethane-induced cell transformation is partially mediated through Srx, as knockdown of Srx results in reduced potential of colony formation (B & D). Each treatment group represents data from triplicates (n= 3). Statistical methods used were (C) one-way ANOVA and Holm-Sidak post-hoc analysis (\*p ≤ 0.05), and (D) t-test (\*p ≤ 0.05)

Srx-knockdown reduced the number of small and large colonies compared to vector control. The differences in number of colonies were statistically significant ( $p \leq 0.05$ ) irrespective of colony size. Hence, our data shows that urethane transforms BEAS2B cells and enhances anchorage-independent colony formation. Our data also confirms that the aforementioned transformation is partially reversible by knockdown of Srx. Hence, Srx plays an important role in urethane mediated cell transformation of BEAS2B cell.

#### **2.4.4 Srx knockout mice are resistant to urethane-induced lung cancer**

Srx knockout mice on FVB background were completely normal under normal laboratory conditions. To study the role of Srx in *in vivo* lung tumorigenesis, a well-established urethane-induced mouse lung tumorigenesis protocol was applied (Figure 2-5A). Mean mouse weight was plotted on a time scale. Srx knockout and heterozygous mice showed a statistically significantly ( $p < 0.001$ ) better weight profile compared to wild type mice (Figure 2-5B). The differences in weight profile over weeks were not statistically significant between heterozygous and knockout mice groups ( $p = 0.148$ ). To minimize mouse suffering, all mice were humanely sacrificed 10 weeks after the first urethane administration.

We examined the tumor incidence in mice lungs. Representative images of mice lungs with tumors and H&E staining of tumors are shown (Figure 2-6A & C). All mice had lung tumors at this stage. The number of tumors was counted using a magnifying glass. The intra-tissue tumors limited the detection of those tumors. However, they should follow the same pattern as the surface tumor while comparing the effect of Srx expression.

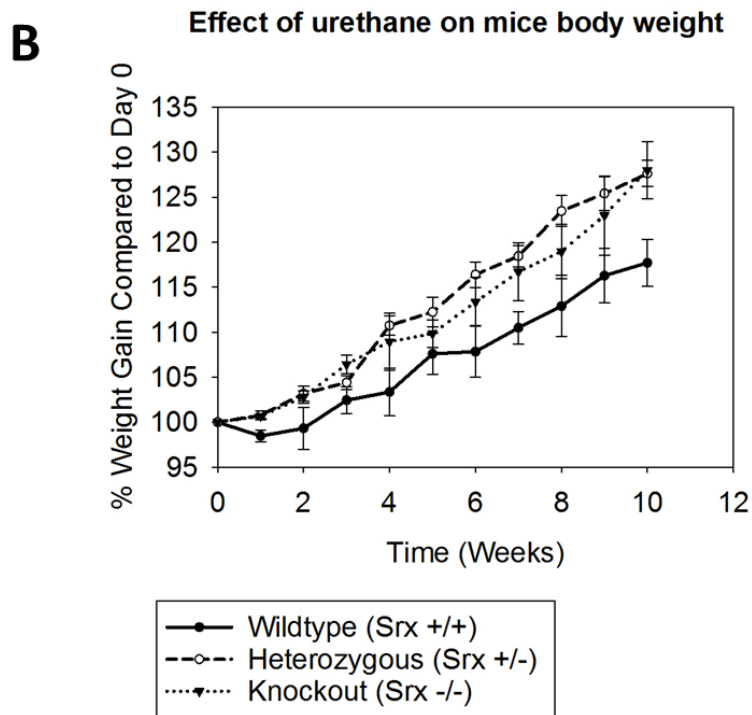


**Figure 2-5: Sr x null mice are resistant to urethane toxicity:** (A) Schematic presentation of the urethane protocol; (B) effect of urethane treatment on mouse body weight. The Sr x genotype did not affect weights of non-treated mice. Statistical methods used were two-way ANOVA and Holm-Sidak post-hoc analysis (\* $p \leq 0.05$ ).

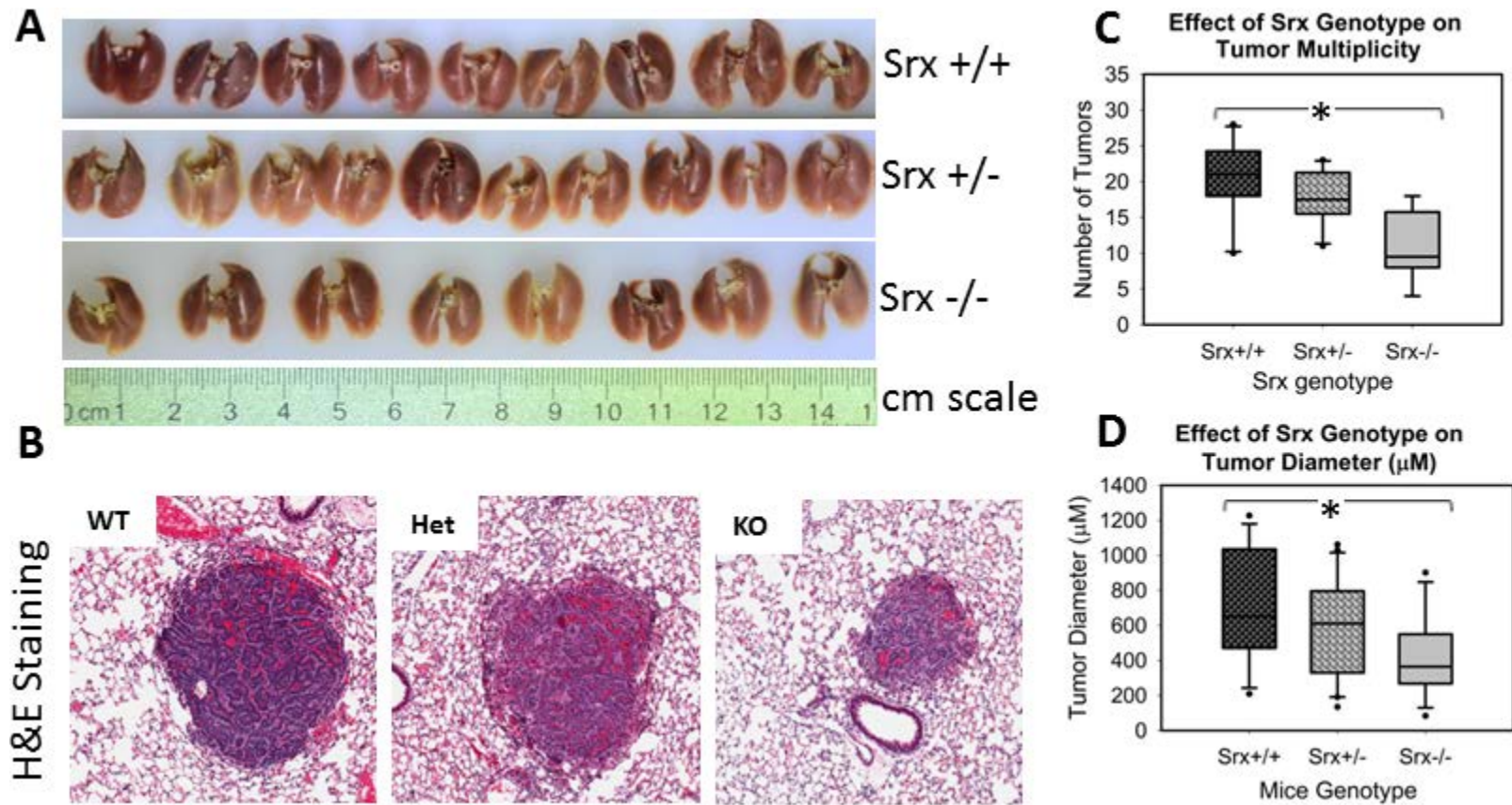


**Figure 2-6: Srx null mice are resistant to urethane-induced carcinogenesis:** (A) Whole lung tissue; (B) 10X images of Hematoxylin and Eosin stained mouse tumors; (C) average tumor multiplicity in Srx Wt, Het, and knockout mice, (D) average tumor size in Srx Wt, Het, and knockout mice. We started with equal number of mice in each group. Due to mice fighting and injury, few mice needed to be sacrificed. Hence, we had different number of lungs in different genotype. The dots above and below error bars indicate outliers (C & D). Statistical methods used were one-way ANOVA (C-D) and Holm-Sidak post-hoc analysis ( $*p \leq 0.05$ ).

The number of tumors per lung tended to be lower in Srx knockout (-/-) mice compared to wild type ( $p=0.001$ ) or heterozygous ( $p=0.012$ ) mice (Figure 2-6C). The average tumor multiplicity in Srx knockout mice was reduced by approximately 2-fold compared to wild type mice. Smaller tumor size and tumor location hindered accessibility for measurement of tumor diameter. Therefore, we used the longest diameter of each tumor from the H&E stained slides. These tumor diameters ( $\mu\text{M}$ ) were used for comparison of tumor sizes in all three groups. The average diameter in Srx knockout mice tended to be lower than wild type and heterozygous mice, although statistically significant differences were found only on comparison of wild type with knockout mice ( $p=0.022$ ) as opposed to wild type vs. heterozygous ( $p=0.199$ ) or heterozygous vs. knockout ( $p=0.174$ ) mice (Figure 2-6D). Our data indicate that Srx knockout mice had a significant reduction in tumor multiplicity and tumor diameter compared with their wild type or heterozygous counterparts. Therefore, these data suggested that genomic loss of increases the mice resistance to urethane-induced lung tumorigenesis.

#### **2.4.5 Urethane induces the expression of antioxidant proteins in mouse lung**

To investigate why Srx depletion in mice led to lower tumor multiplicity, we examined the effect of urethane treatment on the expression of Srx in mouse lung tumors. An immunohistochemical method that specifically detected Srx in formaldehyde-fixed tissue was applied as previously reported [139]. Previous reports from our group indicate that Srx is barely detectable in normal human lung tissue. After urethane treatment, the majority of lung tissue, including tumor

tissue from Srx (+/+) or (+/-) mice, showed strong positive Srx-staining (Figure 2-7A). There were differences in strength of staining in Wt vs. Het mouse tissue as well, with Wt showing stronger staining. Lack of positive staining in the lung and tumors of Srx knockout mice further validated the specificity of anti-Srx staining (Figure 2-7A & D). We also tested Prx expression in these lungs and found positive staining for Prx1 (Figure 2-7B&E). Prx expression was lower in Srx+/- and Srx-/- mice compared to Srx+/+ mice.

As Nrf2 transcriptionally up-regulates the expression of Srx as well as Prx1, we stained these lung tumors for Nrf2 using specific antibody. Our data confirmed the expression of Nrf2 in urethane-treated tumors (Figure 2-7C&F). The expression of Nrf2 was higher in Srx+/- and Srx-/- mice compared to Srx+/+ mice. These data suggest that application of urethane led to increased expression of antioxidant proteins in mouse lung and tumors.

#### **2.4.6 Depletion of Srx reduced cell proliferation and increased apoptosis in the urethane treated groups**

To identify the reasons behind reduction of tumor multiplicity and diameter in Srx knockout mice, we further investigated the effect of Srx depletion on cell proliferation and apoptosis. Mouse lung tumors from all three genotypes were stained with Ki67 (a cell proliferation marker). There was an enhanced staining for Ki67 in tumors from wild type mice as opposed to knockout and heterozygous, where the Ki67 staining was significantly lower (Figure 2-8A). The positive nucleus were counted using Aperio Imagescope software and plotted for quantitative comparison.



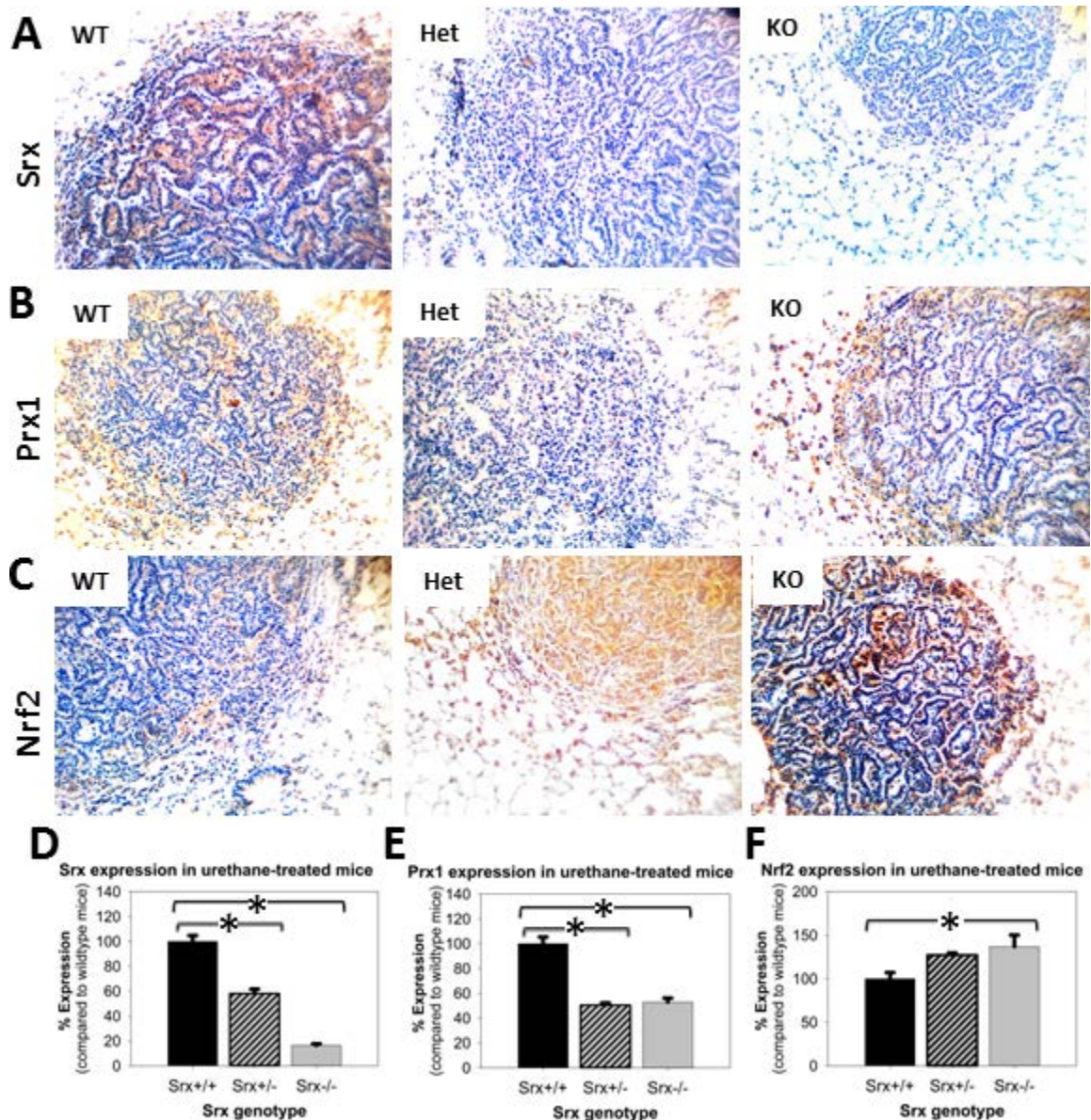


**Figure 2-7: Immunohistochemistry staining showing expression of different proteins in urethane-treated lung tissue:** 20X images of immunohistochemistry indicating expression in lung tumor from mice lungs of different SrX genotypes: (A) SrX, (B) Prx1, and (C) Nrf2. The staining was quantitated using Aperio Imagescope software. Quantitative values of 3,3'-diaminobenzidine (DAB) staining estimation are plotted for (D) SrX, (E) Prx1, and (F) Nrf2 expression. Statistical methods used were one-way ANOVA on Ranks and Dunn's post-hoc analysis (\* $p \leq 0.05$ ).

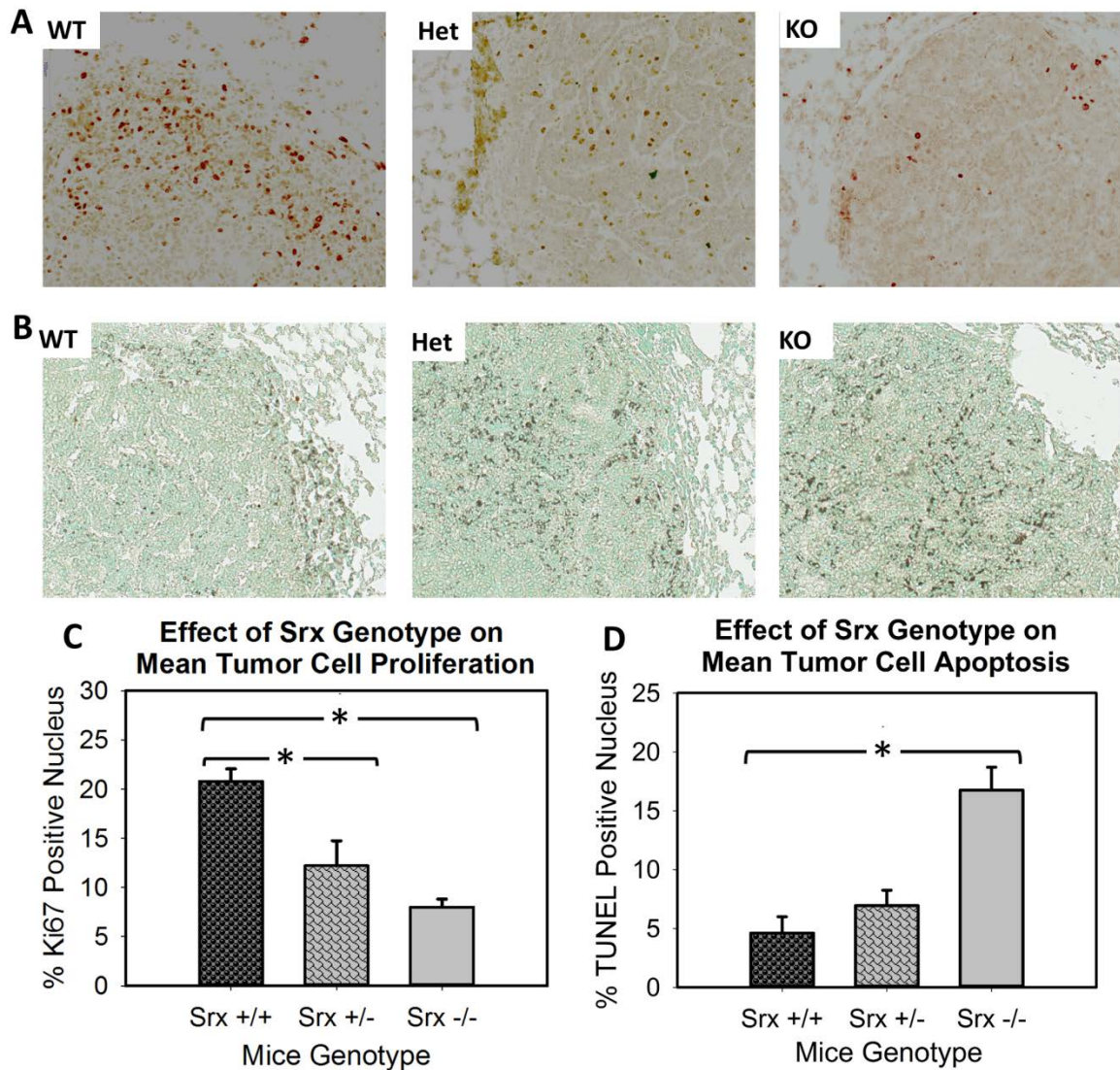


**Figure 2-8: SrX enhances tumor cell proliferation and reduces tumor cell apoptosis in urethane-induced lung carcinogenesis:** (A) 20X images of Ki67 staining as a tumor cell proliferation marker in tumors from different SrX genotype mice; (B) 20X images of TUNEL staining as an indicator of tumor cell apoptosis in tumors from different SrX genotype mice. The number of positive nucleus was quantitated using Aperio Imagescope software. (C) quantitative comparison of tumor cell proliferation index (Ki67 staining); (D) quantitative comparison of tumor cell apoptosis (TUNEL staining). Statistical methods used were one-way ANOVA (C & D) and Holm-Sidak post-hoc analysis (\* $p \leq 0.05$ )

Quantitatively, the difference in cell proliferation was statistically significant with a significantly lower number of positive nuclei in knockout ( $p < 0.001$ ) and heterozygous ( $p = 0.006$ ) compared to wild type mice (Figure 2-8A & C). A statistically significant difference could not be observed in Ki67 positive nuclei between the knockout vs. heterozygous groups.

We also examined intra-tumoral apoptosis using TUNEL staining. There were enhanced TUNEL positive cells in tumors from knockout mice as opposed to wild type and heterozygous (Figure 2-8B & D). Quantitatively, the differences in TUNEL positive nuclei were statistically significant with a significantly higher number of positive nuclei in knockout compared to wild type ( $p < 0.001$ ) as well as heterozygous ( $p = 0.001$ ) mice. Differences between TUNEL staining in heterozygous and wild type mice were not statistically significant.

## **2.5 Discussion**

The primary function of Srx is to reduce over-oxidized Prxs in host cells. Protein deglutathionylation is an alternative function [22]. Cellular antioxidants, such as glutaredoxin, Prx, Trx, and Trx-like proteins, as well as Srx, have been identified as over-expressed in a wide range of human cancers [69, 78, 140, 141]. These antioxidants promote cell survival through regulation of oxidative stress. Cigarette smoke is known to enhance susceptibility to lung cancer [142]. It is a complex mixture of chemicals that has potential to induce lung carcinogenesis. Many components of cigarette smoke act as direct or indirect lung carcinogens. We first checked the effect of cigarette smoke on expression of the Srx and Prxs. Cigarette smoke condensate enhanced the expression of Srx as well as

individual Prxs (Figure 2-1). This action of CSC could be reversed with the addition of chemical antioxidants such as N-acetyl cysteine. Hence, the effect of cigarette smoke on expression of Srx-Prx axis components is at least partially mediated through oxidative stress. This increase in expression of antioxidant proteins was regulated at the transcriptional level (Figure 2-2). However, the extent of change in mRNA expression is not as strong as the extent of change in protein expression. This may be an indicator of non-transcriptional mechanisms that cause the enhanced expression of Srx-Prx axis components in response to CSC treatment.

To further investigate the effect of the Srx-Prx axis on lung cancer, we selected a carcinogenic component of cigarette smoke. Urethane is a component of cigarette smoke and a well-known lung carcinogen in mice [138]. However, the urethane itself is not the carcinogen. Rather, urethane is metabolized to vinyl carbamate epoxide, which later causes the majority of urethane toxicity [143]. These mechanisms of urethane-induced lung carcinogenesis along with our data are summarized in Figure 2-9. Humans are mainly exposed to urethane from alcoholic beverages [144]. Alcohol increases the expression of CYP2E1 [145], which along with esterase are enzymes that play the main roles in metabolism of urethane [146]. CYP2E1 converts urethane to vinyl carbamate epoxide, whereas esterase converts it to ethanol [146]. Considering the stoichiometry of reaction, the presence of alcohol has potential to slow down the metabolism of urethane by esterase. Hence, the metabolism of urethane to vinyl carbamate epoxide becomes the predominant mechanism of metabolism partially due to increased

CYP2E1 expression and partially due to reduced rate of metabolism by esterase. Cigarette smoke is another major source of urethane [131, 132]. Many individuals consume alcohol and smoke cigarettes simultaneously [147]. This trend of alcohol consumption along with smoking has increased in recent years. Hence, the risk of urethane toxicity and urethane-induced lung cancer may be higher in individuals who smoke and consume alcohol simultaneously. Human lungs have a lower expression of urethane-metabolizing enzymes (i.e. CYP2E1) and esterase, compared to other tissue like liver and gastrointestinal tract [148, 149]. This multiplies the risk of the aforementioned stoichiometric inhibition of esterase in human lung. Hence, the risk of urethane conversion to carcinogenic metabolite increases under regular exposure conditions where lungs are simultaneously exposed to alcohol and cigarette smoke.

To study the role of Srx in lung carcinogenesis, we used the urethane model to mimic lung cancer development in humans. Srx knockout mice were established on an FVB background. Srx knockout mice were completely normal under standard laboratory conditions. We demonstrated that depletion of Srx rendered mice resistant to urethane-induced lung cancer, as Srx null mice showed reduced tumor multiplicity and tumor diameter compared to wild type mice. Srx null mice showed an almost 2-fold lower incidence of tumor multiplicity and roughly 1.5-fold reduction in median tumor diameter. In mechanistic studies, we found that Srx was strongly expressed in urethane-treated lung tumors and depletion of Srx led to reduction in cell proliferation.

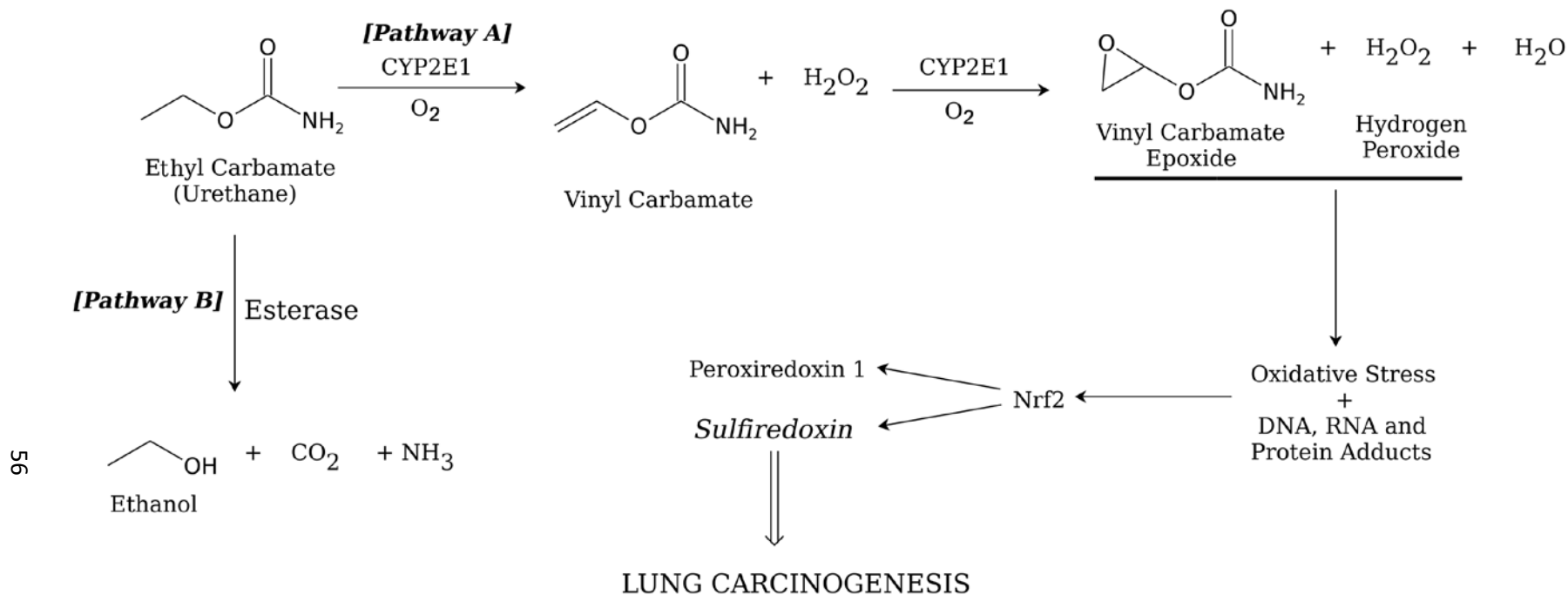


**Figure 2-9: Prospective mechanism of urethane-induced lung carcinogenesis:** CYP2E1 (Pathway A) and esterase (Pathway B) are the main enzymes that metabolize urethane. Pathway A predominates in metabolism of urethane as the majority of urethane exposure to humans is from alcoholic beverages; Pathway B is stoichiometrically inhibited/slowed down due to the presence of alcohol (an end product in Pathway B).

This study also demonstrates that depletion of Srx results in an enhanced rate of intra-tumoral apoptosis. Reduced cell proliferation and increased intra-tumoral apoptosis may contribute to the tumor-resistant phenotype of Srx knockout mice. As per data from the American Cancer Society publication 'Cancer Facts & Figures' and 'Global Cancer Statistics' reports, lung cancer is the leading cause of cancer related deaths in the USA and worldwide irrespective of gender [128]. Identification of novel therapeutic targets for lung cancer is therefore very important. Srx and Prx are highly expressed in human lung tumors. Srx expression is critical for the pathogenesis of several human diseases, including cancer. Our current and previous data clearly demonstrate that Srx plays a significant pathogenic role in human cancer development. The cellular levels of Srx may be regulated through AP-1 and Nrf2 [69]. In this study, we demonstrate that urethane directly stimulates the expression of Srx, Prx, and Nrf2. Nrf2 is involved in transcriptional regulation of Srx and Prx1 [69, 80]. Our data indicates that urethane induces Srx and Prx1 expression at the transcriptional level. Earlier researches as well as our current data indicate that Nrf2 acts as a mediator of urethane-induced carcinogenesis [134]. Hence, our finding establishes that urethane enhances Nrf2 expression and later transcriptionally regulates the expression of Srx and Prx1. These findings further establish the role of Srx as a mediator of urethane-induced lung carcinogenesis. Our findings of the tumor-resistant phenotype of Srx knockout mice may reflect a long-term accumulative effect of urethane exposure. It is not clear whether loss of Srx has any effect on the mutagenic potential of urethane. Nevertheless, our findings suggest that Srx

is one of the critical components that contribute to mouse lung tumorigenesis *in vivo*. Targeting Srx may thus be employed as a novel strategy for lung cancer prevention and/or treatment in the future.

## **2.6 Summary**

Urethane is a well-established lung carcinogen with potential to induce carcinogenesis in other tissues as well. It is a component of cigarette smoke and alcoholic beverages. Alcoholic beverages are the main source of urethane exposure for humans, while cigarette smoke is another major source. Vinyl carbamate epoxide is a metabolite of urethane that is responsible for the majority of its toxicities. Metabolism of urethane to vinyl carbamate epoxide is the preferred method of urethane metabolism in the presence of alcohol. Hence, the chances of urethane toxicity increase under normal human exposure conditions. The role of Nrf2 in urethane-induced lung carcinogenesis has been documented in the literature. This study identified the role of Srx in urethane-induced lung carcinogenesis: urethane causes enhanced expression of Nrf2, leading to transcriptional upregulation of Srx and Prx expression, in turn leading to lung tumorigenesis. Knockdown of Srx in FVB mice partially protects mice against urethane-induced lung tumorigenesis. The protection in Srx null mice is mainly due to a reduction in tumor cell proliferation and increase in tumor cell apoptosis. Hence, Srx plays an essential role in urethane-induced lung carcinogenesis and can be considered a novel target for lung cancer prevention and/or treatment.



## CHAPTER 3: THE BIOLOGY OF SULFIREDOXIN (SRX)- PEROXIREDOXIN1 (PRX1) INTERACTION: STRUCTURE TO MOLECULAR INSIGHTS

### 3.1 Synopsis

Typical 2-Cys Prx is the group of Prx that is reduced by Srx. Srx-Prx1 interaction is involved in pathogenesis of various oxidative stress-induced conditions, including cancer, inflammation, cardiovascular disorders, and neurological diseases. The purpose of this study was to understand the structural biology of the Srx-Prx1 interaction, which may be of significance as a molecular target site for a novel drug-discovery process. Homology modeling and protein-protein docking approaches were applied to examine the Srx-Prx1 interaction using *in silico* methods, including I-TASSER, Phyre2, Swissmodel, MZDOCK, and ZDOCK. Using *in silico* studies, a 26-amino acid motif at the C-terminus of Prx1 was identified that may cause a steric hindrance for the kinetics of the Srx-Prx1 interaction. These findings were tested *in vitro* using purified recombinant proteins, including Srx, Prx1, and Prx1<sup>Mutant</sup> (deleted C-terminal arm). We found that deletion of the C-terminal arm of Prx1 significantly enhanced its association with Srx (i.e. >1000-fold increase in  $k_a$ ) with minimal effect on dissociation ( $k_d$ ). These results were further validated in Prx4. These data confirms that the C-terminal arm of Prx is not required for Srx-Prx interaction. Taken together, these data add novel structural insights critical for understanding the biology of the Srx-Prx interaction.

### **3.2 Introduction**

The molecular characteristics of protein-protein interaction must be identified in order to design an effective targeting strategy for inhibition of such interactions. A 3-dimensional structure of a protein and its individual components can play a major or minor role in protein interaction. Understanding the molecular structure of individual proteins is the first criteria that must be fulfilled to study the effect of a 3-dimensional structure of individual proteins on protein-protein interaction. Protein structure can be predicted experimentally using X-ray crystallography and nuclear magnetic resonance studies. In the absence of experimental data, it can be predicted computationally by homology modeling. Homology modeling is one of the most popular methods for prediction of protein structures based on the known structure of homologous proteins with some sequence identity [150]. It is not trivial to predict the structure covering the full length of a protein using experimental methods, as crystallizing the whole protein is a cumbersome task that can be affected by myriad experimental factors leading to lower confidence in the predicted structure. The relative ease of predicting the structure covering the full protein sequence by homology modeling has led to popularity of this method. Homology modeling has already established its utility in hypothesis making for molecular studies [151, 152]. Protein structures predicted using this method can be used computationally for protein-protein docking studies.

Protein-protein docking is a unique computational tool to identify the points of contact during protein-protein interaction that can help in designing a targeting strategy to inhibit those interactions [153]. Predictions of docking studies can be

further confirmed experimentally using amino acid mutation and deletion studies. Recombinant proteins can be designed with mutations at individual points of contacts or deletion of a particular domain. These mutants can be used to study the effect of particular mutations on protein-protein interactions. Once confirmed, amino acids from these experiments can be defined as binding sites for protein-small molecule docking or virtual screening to identify the inhibitors of interaction. We carried out protein-protein docking studies followed by deletion mutation to confirm the role of the Prx C-terminal arm in Srx-Prx binding.

### **3.3 Materials and methods**

#### **3.3.1 Homology modeling and protein-protein docking studies**

Although the structures of Prx and Srx are available in the Protein Data Bank, none of the entries actually covers the full sequence of these proteins. Therefore, homology modeling was used to predict the full-length structures of all Prx and Srx. We used multiple online homology modeling programs in this experiment, including I-TASSER (iterative threading assembly refinement) [154, 155], Phyre2 [156] and Swissmodel [157]. We used M-ZDOCK [158] for prediction of dimeric structure from the monomeric structure predicted by I-TASSER and Phyre2. Followed by homology modeling studies, we carried out protein-protein docking studies using the ZDOCK [159] online server to identify structural characteristics of interaction. We analyzed the final output of these experiments using PyMOL visualizer and labeled the binding and catalytic site components.

### 3.3.2 Western blot and immunoprecipitation (IP) assay in HEK293T cells

HEK293T (human embryonic kidney) cells were transfected with pLV expression vector for FLAG-tagged Srx. The stable transfection was ensured by maintaining these cells on puromycin containing media. Cells were divided into three groups and were treated with vehicle, 500  $\mu\text{M}$   $\text{H}_2\text{O}_2$ , or 1000  $\mu\text{M}$   $\text{H}_2\text{O}_2$  for 10 minutes. The vehicle treated group was used as control. The cells were lysed using RIPA buffer for western blot and immunoprecipitation buffer for IP. The lysate were incubated with anti-Srx antibody overnight at 4° C. Next morning magnetic beads coated with anti-rabbit secondary antibody was incubated with samples for 2 hours. The sample was separated using magnetic bars. The beads were washed 3 times with fresh IP buffer. The protein was eluted using 1X LDS buffer by heating at 90° C for 10 minutes. Western blot was carried out using standard procedures as described earlier in this dissertation.

### 3.3.3 Purification of recombinant proteins

Srx, Prx1<sup>wildtype</sup>, Prx1<sup>mutant</sup> (in which the last 22 amino acids from the C-terminal were deleted), Prx4<sup>wildtype</sup>, and Prx4<sup>mutant</sup> were expressed in *E. coli* BL21(DE3) cells using pRSET B vector. Srx was inserted between the BamHI and EcoRI restriction sites of pRSET B. All the Prx wild type and Prx mutants were inserted between BamHI and HindIII restriction sites of pRSET B. Coomassie blue staining of different gels containing purified proteins is shown along with a pRSET B vector map in Figure 3-1. All proteins had a (His)<sub>6</sub> tag at the N-terminal. BL21(DE3) cells were cultured at 37° C in LB broth media (Sigma-Aldrich).

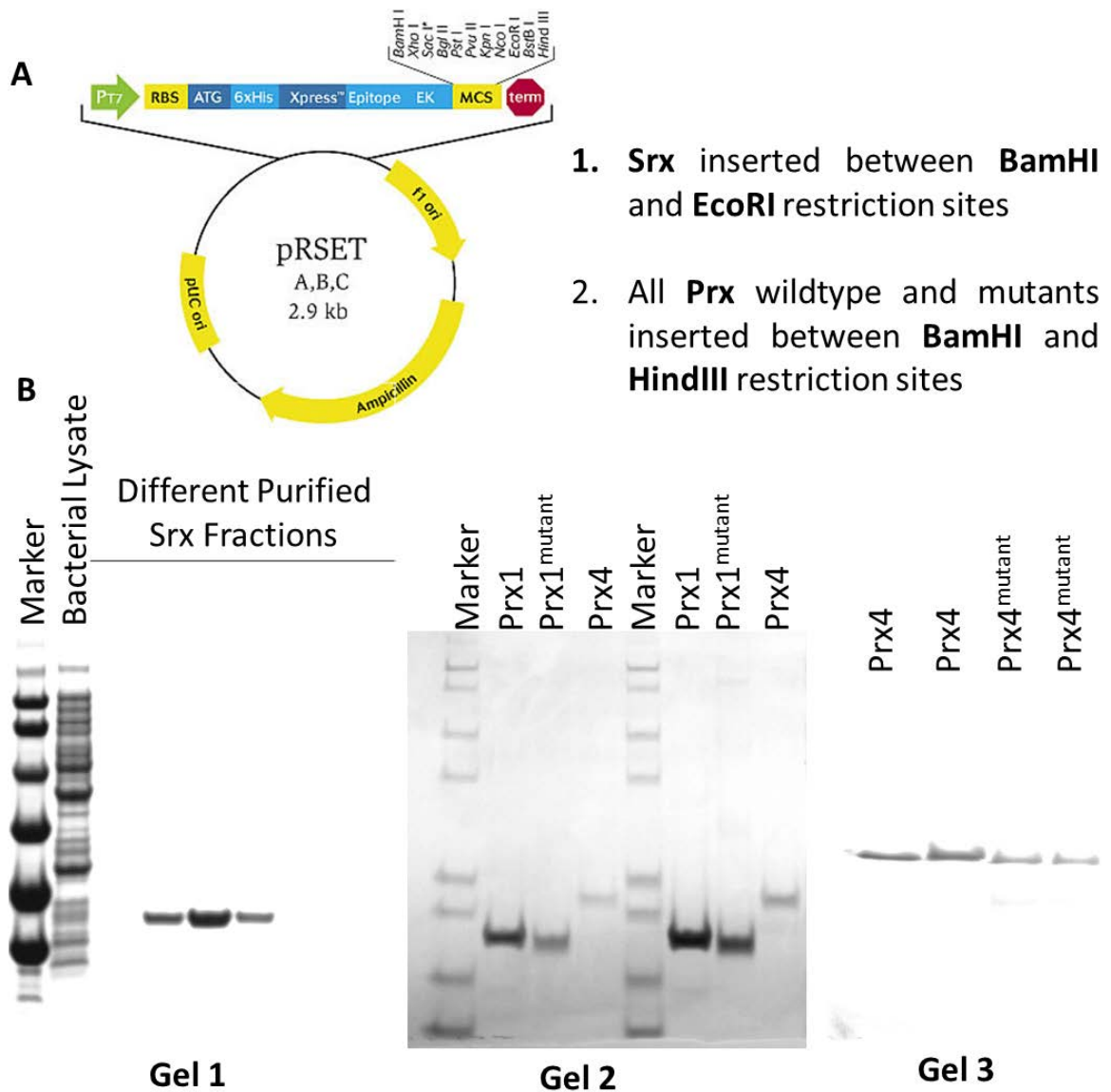


**Figure 3-1: Protein purification using pRSET B vector:** (A) Vector map; (B) coomassie blue stained gels showing pure protein bands. The replicate bands represents different preparation of proteins.

After addition of isopropyl-1-thio-D-galactopyranoside (1.0 mM), the cultures were incubated for 4 hours at room temperature. The cells were lysed using lysis buffer [8 M urea (pH 8.0), 100 mM monosodium phosphate, 10 mM Tris Base]. Protein purification was carried out using an Ni<sup>2+</sup> charged IMAC Select Affinity Gel [Sigma-Aldrich] column for purification of His-tagged proteins. The column was washed with wash buffer [20 mM imidazole (pH 8.0), 300 mM NaCl, and 50 mM monosodium phosphate]. The protein was eluted with elution buffer [300 mM imidazole (pH 8.0), 300 mM NaCl, and 50 mM monosodium phosphate] and was dialyzed in 20 mM Tris-HCl to remove extra salts and re-nature the protein.

#### **3.3.4 *In vitro* IP using purified recombinant proteins**

The Srx (2 µg) was incubated with multiple concentrations of Prx1<sup>wildtype</sup> and Prx1<sup>mutant</sup> (500 ng, 1µg, 2 µg, 4µg) in 500 µL of IP buffer for 2 hours at 4° C. The samples were incubated with anti-Srx antibody overnight at 4° C. Next morning magnetic beads coated with anti-rabbit secondary antibody was incubated with samples for 2 hours. The sample was separated using magnetic bars. The beads were washed 3 times with fresh IP buffer. The protein was eluted using 1X LDS buffer by heating at 90° C for 10 minutes. The western blot were carried out using standard procedures.

#### **3.3.5 Study of the Srx-Prx interaction kinetics using surface plasmon resonance (SPR)**

The interaction of Srx (analyte) with Prx1<sup>wildtype</sup> and Prx1<sup>mutant</sup> (ligand) was measured by surface plasmon resonance (SPR) technique using ProteOn™ XPR36 instrument (Bio-Rad). The ligands were immobilized on GLC sensor

chips (Bio-Rad) using the amine coupling method using BioRad standard manufacturer protocol. Ligand capturing on the GLC chip was performed as per the manufacturer's protocol. Several different concentrations of pure recombinant Srx (analyte) were used to evaluate the ligand-analyte binding. The data were acquired and processed by ProteOn manager software and the Langmuir 1:1 evaluation model was used for analysis.

### **3.3.6 Statistical analysis**

SPR data analyzed using the Langmuir 1:1 evaluation model. Quantitative data were presented as mean  $\pm$  standard deviation ( $\bar{x} \pm SD$ ). Data were analyzed with the indicated statistical methods using SigmaPlot (version 13.0). For calculation of the p-value, parameters of two-tailed 95% confidence interval were used for all analyses ( $p \leq 0.05$  was considered statistically significant).

## **3.4 Results**

### **3.4.1 Complete 3D-structure of full length proteins were predicted using homology modeling**

Multiple homology modeling programs were tested for prediction of dimeric structure. Swissmodel predicted a partial structure, which we could not use for our purpose. Phyre2 gave good results as well; however, I-TASSER proved to be the best for all proteins under this study. Although I-TASSER is time consuming, the capability of predicting the best structure from minimal information was appreciable. Therefore, we determined the structure of Prx1 and Srx monomer using I-TASSER (Figure 3-2). Prx1 monomers were uploaded to M-ZDOCK to predict the structure of Prx1 dimer.

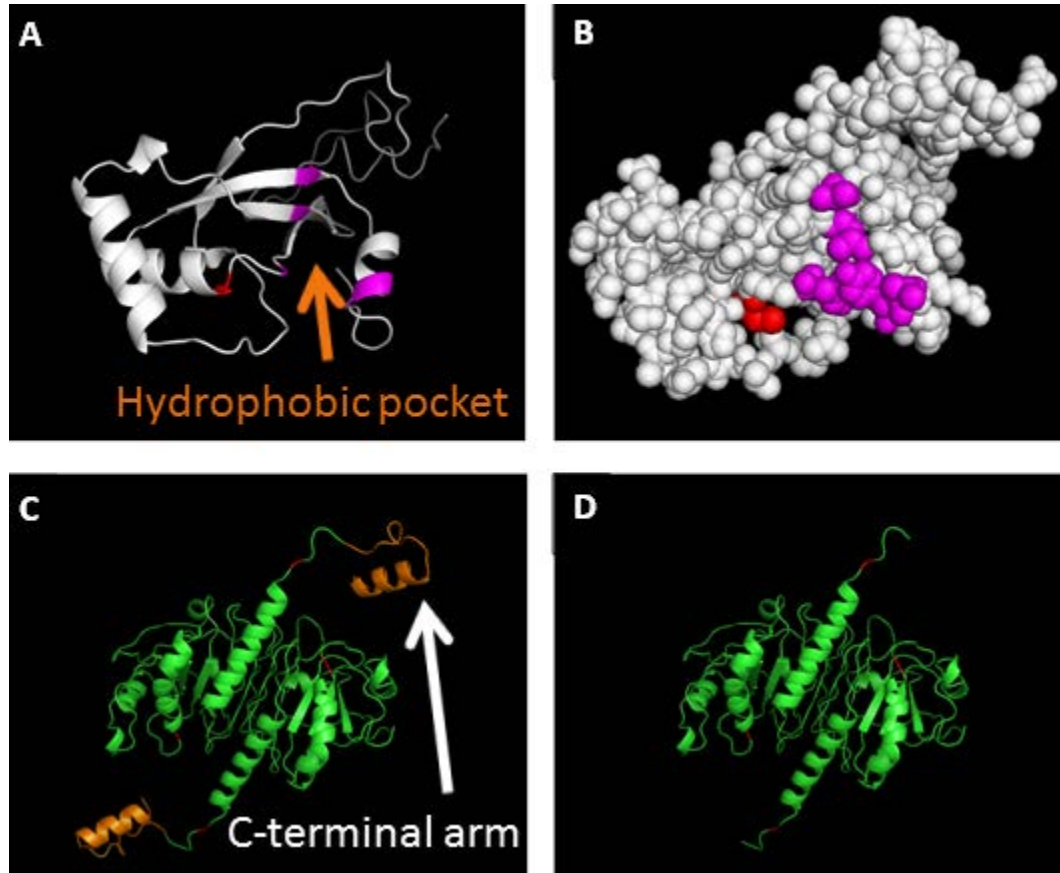


**Figure 3-2: Representative images of Srx and Prx1:** The Srx binding site forms a groove. Prx1 has a extending C-terminal arm of the Prx1 dimer. Prx1<sup>mutant</sup> is prepared by deletion of the last 22 amino acids from the C-terminal arm. The structure of (A) Srx (ribbon), (B) Srx (spheres), (C) Prx1 wild type dimer, and (D) Prx1<sup>mutant</sup> dimer, are shown, with important cysteines marked in red, other binding site amino acids marked in magenta, and the last 22 amino acids of Prx1 marked in orange. Srx is marked in white and Prx chains are marked in green



We received multiple structures with different scores for each of our predictions. A best guess for possible structures was made on the basis of the individual scores as well as information available in the literature. Different software has different score range that correlates with the confidence in structure. We compared the individual score and selected best structure for our study. A similar strategy was used to predict the 3-dimensional structures of Prx2-4. The structures of other Prxs were similar to Prx1 with slight differences in orientation of the C-terminal (Figure 3-3). We observed an extending C-terminal arm in Prx1 that covers the peroxidatic ( $C_P$ ) and resolving ( $C_R$ ) cysteine of Prx1 dimer (Figure 3-2C). Similar C-terminal arms are present in other Prxs with a slightly different orientation (Figure 3-3). The 3-dimensional structure of Prx1<sup>mutant</sup> (Figure 3-2D) was predicted by deleting the 22 amino acids from the C-terminal of both chains of the Prx1 dimer.



**Figure 3-3: Representative images of typical 2-Cys Prxs other than Prx1:** Full length structures of (A) Prx2 dimer, (B) Prx3 dimer, and (C) Prx4 dimer, produced by homology modeling. All important cysteines are marked in red, the last 22 amino acids of Prx are marked in orange, and the rest of the Prx chain amino acids are marked in green

### **3.4.2 Protein-protein docking output identified a possibility of steric hindrance for the Srx-Prx interaction**

All protein-protein docking studies were carried out using the ZDOCK online server. The hydrophobic pocket of Srx along with C<sub>P</sub> and C<sub>R</sub> of Prxs were defined as the binding site [55]. Docking output was visualized using the PyMOL visualizer. The results of docking indicated that the extending arm of Prx1 might create some steric hindrance for access of Srx to Prx1 (Figure 3-4A) as this arm covers the part of Prx1 that needs to be accessed by Srx for Prx1 reduction. Comparison of this phenomenon with Srx binding to other typical 2-Cys Prx indicated the possibility of steric hindrance in these Prx as well. However, the extent of hindrance may vary due to orientation of the C-terminal arm in an individual Prx. This may lead to differences in interaction affinity of Srx for individual members of the typical 2-Cys Prx family. Deletion of the C-terminal arm might reduce this steric hindrance (e.g. Srx may have easier access to Prx1<sup>mutant</sup>) (Figure 3-4B). Hence, deletion mutation may result in faster interaction between Srx and Prx.

### **3.4.3 IP assay confirms the differences in interaction of Srx with individual Prx**

The pull-down assay indicated differences in interaction between Srx and individual Prxs under normal and oxidative stress conditions. A multiple-fold increase exists in pull-down of Prx3 and Prx-SO<sub>3</sub> under oxidative stress conditions whereas the difference is less obvious in cases of Prx1, Prx2 and Prx4 (Figure 3-5A & B). It could be due to mitochondrial location of Prx3. Srx cannot translocate to mitochondria under non-stress conditions.

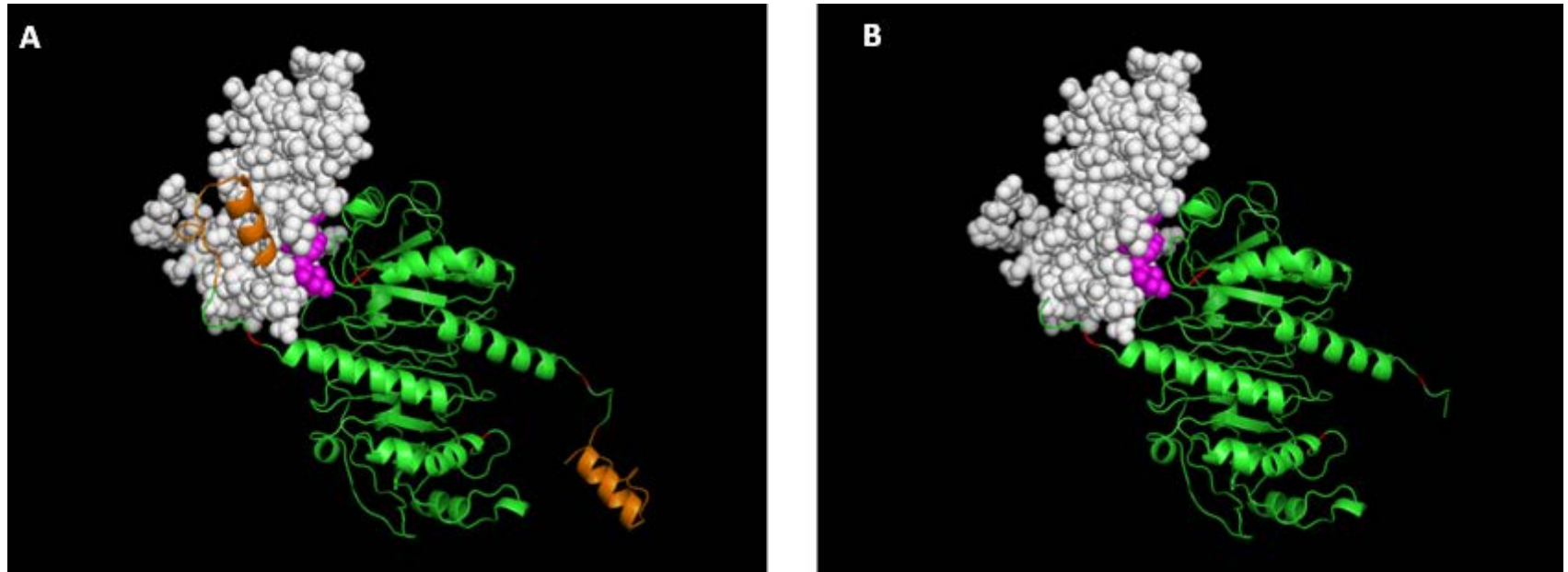


**Figure 3-4: The C-terminal arm hinders Srx binding to Prx1:** Structures of Srx bound to (A) Prx1<sup>wildtype</sup> dimer and (B) Prx1<sup>mutant</sup> dimer, with highlighted Srx binding site (magenta), Prx cysteine (red) and the last 22 amino acids of Prx (orange) to depict the ease of access of Srx binding site to C<sub>P</sub> of Prx1.

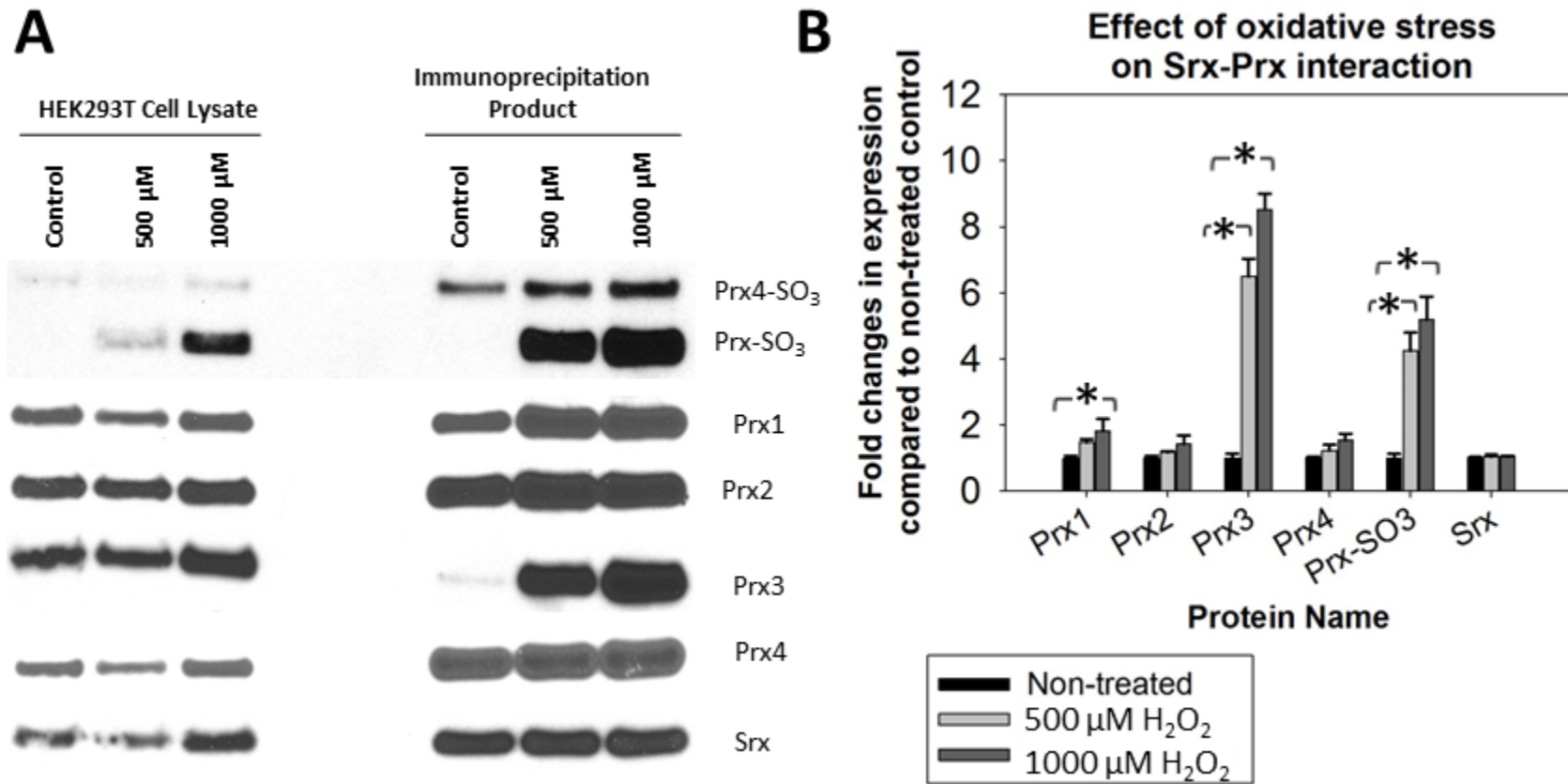


**Figure 3-5: Effect of H<sub>2</sub>O<sub>2</sub> treatment on Srx interaction with various typical 2-Cys Prxs in HEK293T cells:** (A) Western blot showing the relative amount of individual Prxs and oxidized Prx pulled down under oxidative stress conditions induced by 10 min treatment with 500  $\mu$ M and 1000  $\mu$ M H<sub>2</sub>O<sub>2</sub> compared to non-treated control; (B) band strength of individual Prxs under oxidative stress conditions compared to non-treated control as quantitated by ImageJ software. All bands show the same western blot gel. Quantitation is done for 4 different films. The quantitative comparison was carried out using One-way ANOVA followed by Holm-Sidak post-hoc analysis.

Under oxidative stress conditions, the mitochondrial wall's permeability increases leading to Srx translocation to mitochondria and hence, increased Srx-Prx3 interaction. Increased Prx-SO<sub>3</sub> is mainly due to increased oxidation of Prx under oxidative stress conditions. The C-terminal arm of Prx is known to re-orient itself once the Prx is oxidized [54]. These conformational changes can explain the differences in Srx-Prx interaction under different redox states. The difference in interaction of Prx3 may be partially due to its localization in the mitochondrial compartment where Srx cannot reach under normal culture conditions. However, no such factor plays a role in the case of Prx1, Prx2 and Prx4. Hence, differences in interaction of these Prxs to Srx under oxidative stress conditions could be attributed to molecular rearrangements in these Prxs. The difference between Srx interactions and individual Prxs may be partially due to the different orientation of the C-terminal arm in these Prxs, as predicted by homology modeling. However, these differences need to be confirmed by further evidence.

#### **3.4.4 Srx binds more efficiently to Prx1<sup>mutant</sup> than Prx1<sup>wildtype</sup>**

IP, which was carried out using recombinant Srx, Prx1<sup>wildtype</sup> and Prx1<sup>mutant</sup>, indicated the effect of the C-terminal arm on the Srx-Prx interaction. When equal amounts of Prx1<sup>wildtype</sup> and Prx1<sup>mutant</sup> were incubated with a fixed amount of Srx, more Prx1<sup>mutant</sup> was pulled-down by IP using anti-Srx antibody compared to Prx1<sup>wildtype</sup> (Figure 3-6A & B). The differences in binding are not as obvious at lower Prx concentrations since at such concentrations excess of Srx is available for each molecule of Prx1<sup>wildtype</sup> and Prx1<sup>mutant</sup>. Hence, differences in binding are compensated by the excess of Srx.

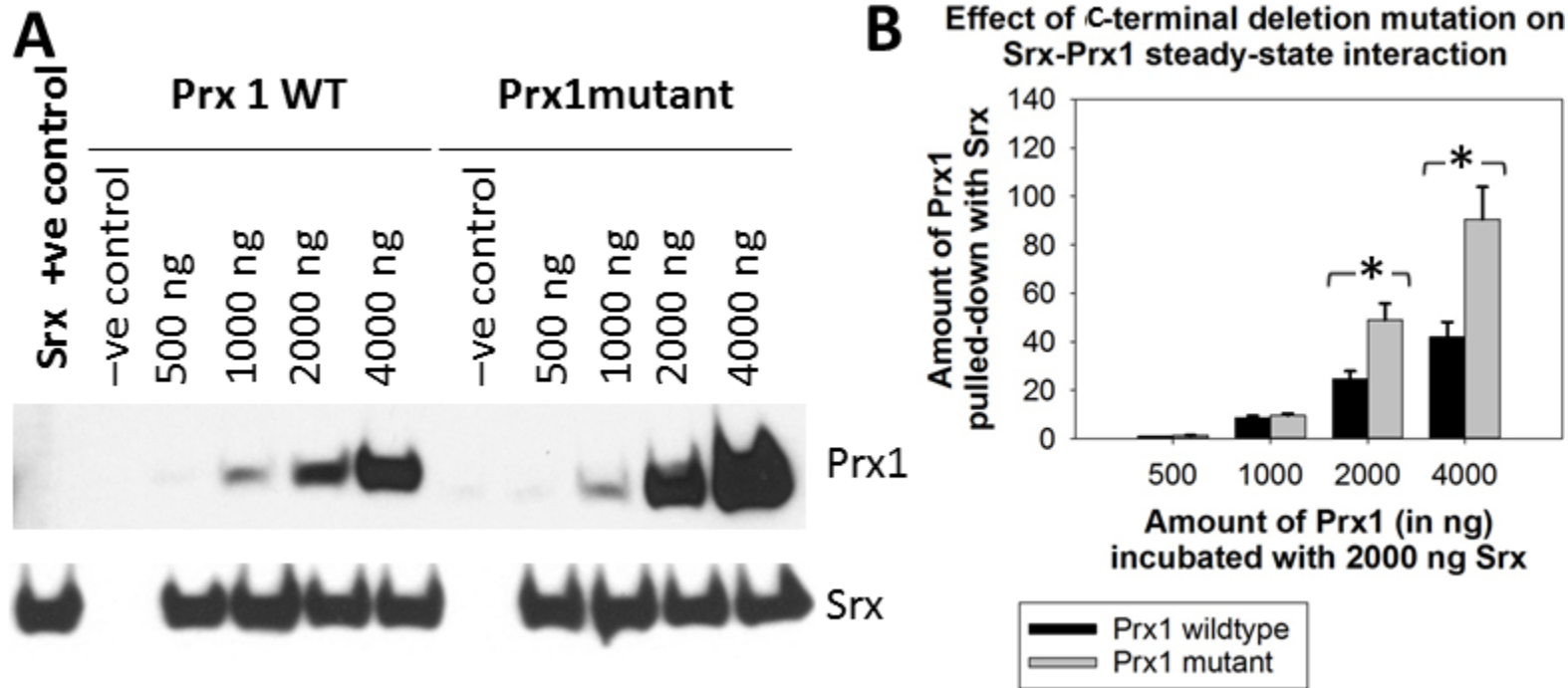


**Figure 3-6: Prx C-terminal arm deletion enhances the Srx-Prx interaction:** For the same amount of Prx1 wild type and mutant incubated with a fixed amount of Srx, more Prx1<sup>mutant</sup> is pulled-down along with Srx compared to Prx1<sup>wildtype</sup>. (A) Western blot showing amount of Prx1<sup>wildtype</sup> and Prx1<sup>mutant</sup> pulled down along with Srx; (B) quantitated values of Prx1<sup>wildtype</sup> and Prx1<sup>mutant</sup> pulled down at each concentration of Prx1. The quantitation represents bands from 4 different films. The positive (+ve) control contains only Srx, with no Prx. The negative (-ve) control contains only Prx1 wildtype or mutant, but no Srx.

The differences become quite obvious at higher Prx1 concentrations. As the Srx concentration becomes a limiting factor for interaction, a greater fraction of Prx with higher affinity (i.e. Prx1<sup>mutant</sup>) for Srx is pulled-down with anti-Srx antibody. These results confirm that Prx1<sup>mutant</sup> has higher steady-state interaction potential for Srx compared to Prx1<sup>wildtype</sup>. The results also emphasize the possibility that the C-terminal arm of Prx1 may cause some steric hindrance for Srx-Prx1 interaction.

#### **3.4.5 Deletion of Prx C-terminal arm leads to faster Srx-Prx association with minimal effect on dissociation**

The effect of C-terminal arm deletion on kinetics of the Srx-Prx interaction was studied using the SPR technique. The deletion mutation resulted in more than a 1,000-fold increase in association rate constant ( $k_a$ ) of the Srx-Prx1 interaction i.e. at equivalent molar concentrations of Prx1<sup>wildtype</sup> and Prx1<sup>mutant</sup>, the  $k_a$  for the Srx-Prx1<sup>mutant</sup> interaction was more than 1,000-fold higher compared to  $k_a$  for the Srx-Prx1<sup>wildtype</sup> interaction (Table 3-1; Figure 3-7 A & B). However, the deletion mutation did not significantly affect the dissociation rate constant ( $k_d$ ). Overall, the deletion mutation resulted in more than a 1,000-fold increase in interaction affinity. Based on homology modeling, we predicted slight differences in the orientation of the C-terminal arm in different Prx. Our predictions indicated that the C-terminal may cause steric hindrance to Srx access in all typical 2-Cys Prxs. However, the extent of steric hindrance could be different. To confirm our hypothesis, we deleted the same sequence of 22 amino acids from Prx4 and studied the interaction kinetics.



**Table 3-1: The C-terminal deletion of Prx1 increases its affinity for Srx** : The kinetic parameters calculated using SPR indicates faster rate of association and higher affinity of Srx for Prx1<sup>mutant</sup> compared to Prx1<sup>wildtype</sup>. E represents value of 10.  $k_a$  is association rate constant.  $k_d$  is dissociation rate constant.  $K_D$  is equilibrium dissociation constant.  $K_D$  has inverse relationship with affinity of interaction.

Parameters (Unit)	$k_a$ (1/Ms)	$k_d$ (1/s)	$K_D$ (M)	Comments
<b>Prx1<sup>wildtype</sup></b>	6.93 E <sup>-01</sup>	5.32 E <sup>-04</sup>	7.69 E <sup>-04</sup>	Prx1 has a slow rate of association but a very slow rate of dissociation. It results in a longer time required to form the Srx-Prx interaction but is a highly stable complex.
<b>Prx1<sup>mutant</sup></b> (last 22 amino acids from Prx1 C-terminal are deleted)	2.54 E <sup>+03</sup>	4.44 E <sup>-04</sup>	1.75 E <sup>-07</sup>	Deletion mutation results in more than 1,000-fold increase in rate of association with minimal effect on rate of dissociation.
<b>Prx4<sup>wildtype</sup></b>	5.09 E <sup>-01</sup>	1.66 E <sup>-03</sup>	3.26 E <sup>-03</sup>	Compared to Prx1 <sup>wildtype</sup> , the Srx-Prx4 complex dissociates faster.
<b>Prx4<sup>mutant</sup></b> (last 22 amino acids from Prx1 C-terminal are deleted)	9.04 E <sup>+01</sup>	2.69 E <sup>-03</sup>	2.97 E <sup>-05</sup>	Deletion mutation results in more than 100-fold increase in rate of association with minimal effect on rate of dissociation.

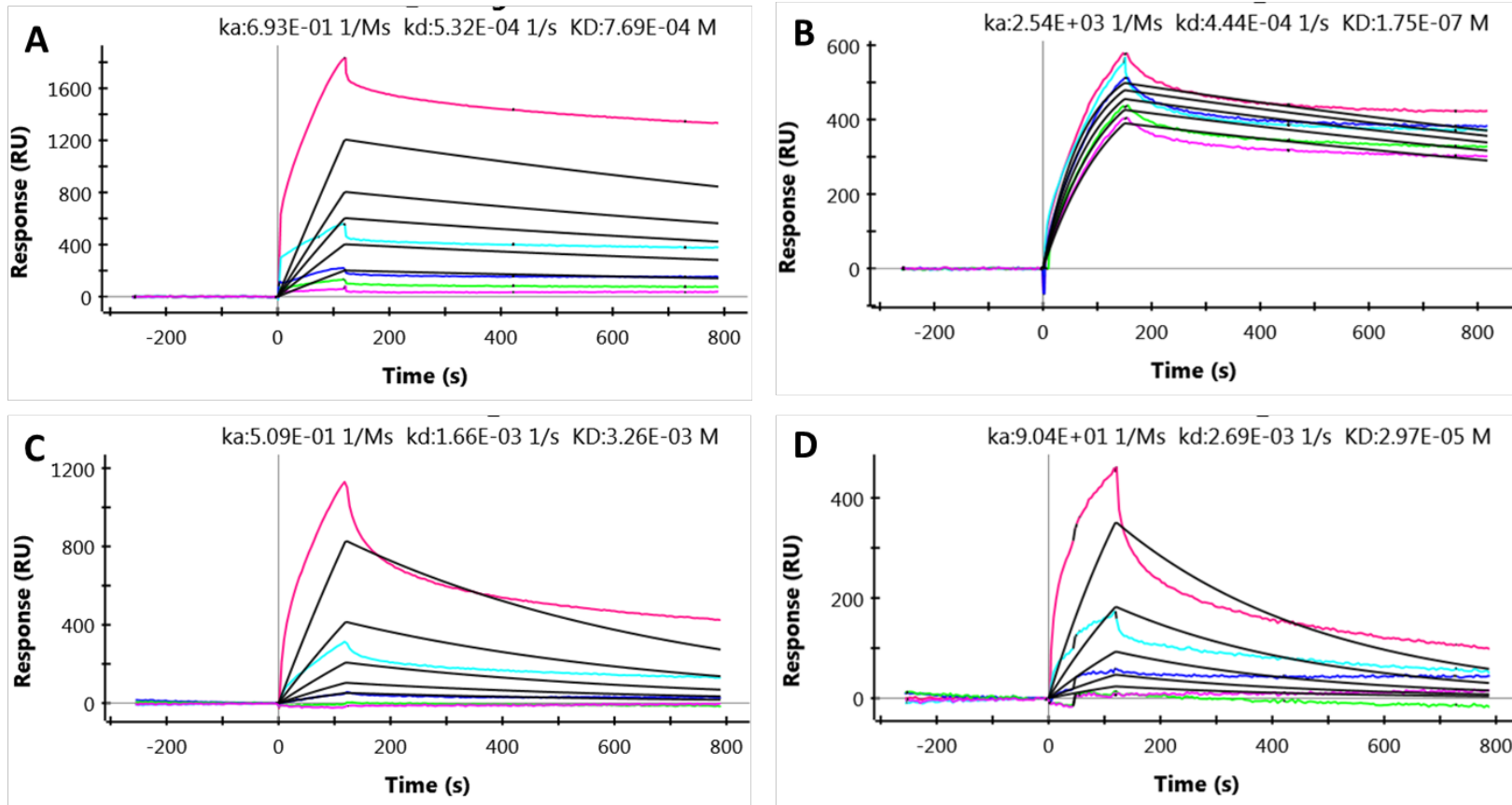


**Figure 3-7: C-terminal deletion mutation increases the Srx-Prx affinity:** The kinetic parameters calculated using SPR indicate a slower rate of association and lower affinity of Srx for (A) Prx1<sup>wildtype</sup> compared to (B) Prx1<sup>mutant</sup> as well as (C) Prx4<sup>wildtype</sup> compared to (D) Prx4<sup>mutant</sup>. Different color lines represent different concentrations of analyte. The dissociation rate is calculated from the peak of each curve i.e. the time we stop influx of protein for association. Hence, association and dissociation are measured at different times. Hence, two parameters are independent of each other.

Again the SPR analysis confirmed our hypothesis. Deletion of the C-terminal arm in Prx4 resulted in more than 100-fold faster association ( $k_a$ ) with minimal effect on dissociation ( $k_d$ ) (Table 3-1; Figure 3-7 C & D). Hence, both Prx1 and Prx4 deletion mutations confirm our hypothesis about the steric hindrance caused by Prx C-terminal site for Srx access to Prx. There is lower effect of Prx4 C-terminal deletion on Srx-Prx4 interaction, compared to effect of Prx1 C-terminal arm deletion on Srx-Prx1 interaction.

### **3.5 Discussion**

Proteomics is one of the fastest evolving fields in molecular biology. The molecular interaction of individual proteins can regulate a variety of cell signaling processes elucidating their role in physiological homeostasis as well as pathological conditions. The importance of these macromolecules has led to development of various tools that can provide insight from their molecular structure. Multiple experimental methods are available to study the structure of proteins; however, these methods have limitations in maintaining the conformation of a native protein in an environment suitable for structural prediction by nuclear magnetic resonance or X-ray crystallography. It takes years of research by a group of structural chemists to determine the structure of a simple protein. Often, these research efforts are insufficient to predict the complete structure of proteins.

The time and effort required for structural predictions using experimental methods and the limitations of these methods led to development of computational tools that can help structural chemists to temporarily fill the gap in

existing knowledge. Homology modeling is a computational method of protein structural prediction that provides great potential to fill the gap in existing data within acceptable limits of error [160]. Protein-protein docking is another computational method that provides insight into protein functions and molecular characteristics by filling the gap in existing knowledge about protein-protein interactions [161]. Both of these techniques are used in this study to help us understand the Srx-Prx interaction. A great amount of biochemical data related to Srx-Prx interaction is already available. We utilized experimental and computational prediction data to make a hypothesis that the C-terminal arm of typical 2-Cys Prxs may cause steric hindrance for the Srx-Prx interaction, as depicted in Figure 3-8. Experimental evidence from the existing literature suggests similar interaction of Srx with all 4 typical 2-Cys Prx. However, by virtue of being different proteins of the same subfamily, they also have minor differences in their characteristics. Our computational prediction indicated that those minor differences in interaction may be due to varying orientations of the C-terminal arm of Prx. To confirm our prediction of steric hindrance and the role of the Prx C-terminal arm in Srx-Prx interaction, we performed deletion mutation. Due to similarities in typical 2-Cys Prx and accepted conventions in the field, we decided to first study Prx1 molecular characteristics. The research in this field clearly establishes that differences in biochemistry of Srx interaction with individual typical 2-Cys Prx are minor. The major differences between typical 2-Cys Prx come from their subcellular localization, not their molecular characteristics [30]. The Prx C-terminal arm contains 26 amino acids.

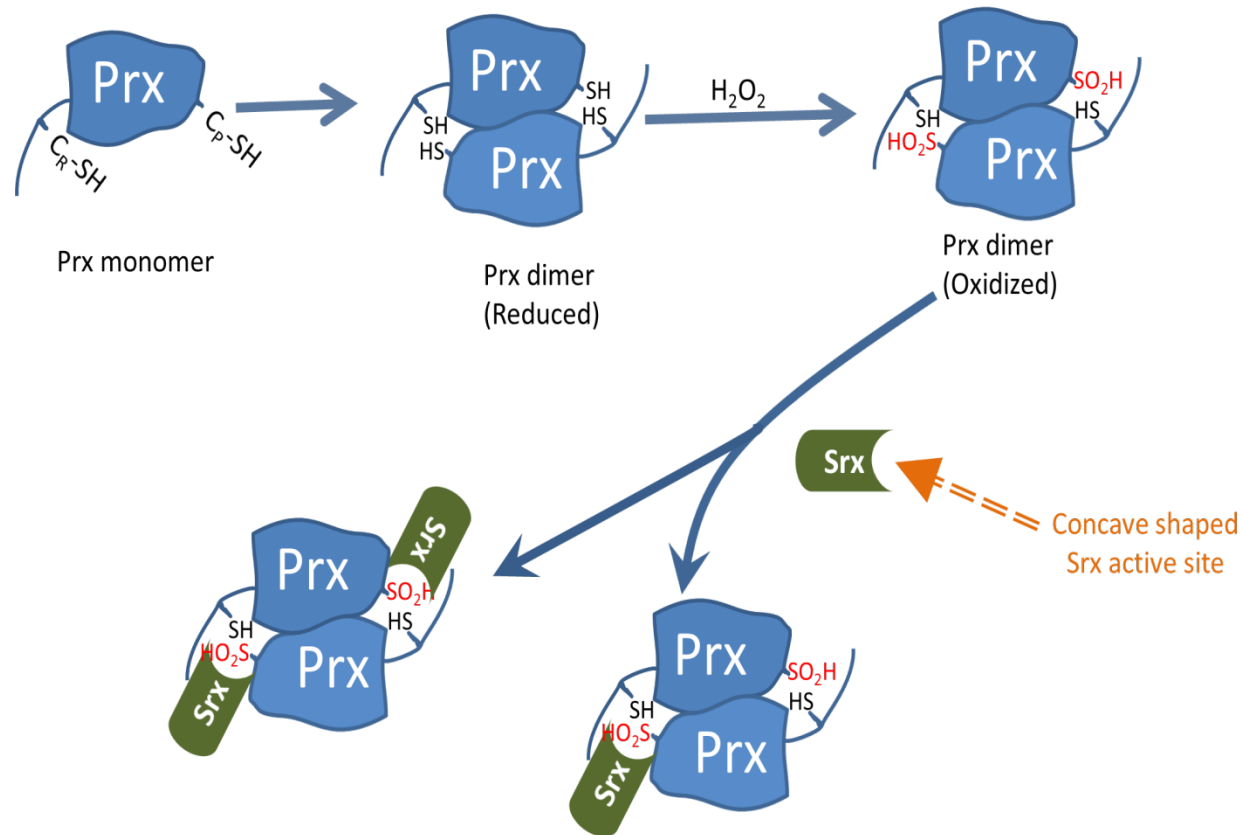


**Figure 3-8: Extending C-terminal arm of Prx covers the Srx-Prx interface and may cause steric hindrance for Srx access to Prx:** The figure depicts the relative location of the Prx C-terminal extending arm and location where the concave shape of the Srx-hydrophobic pocket needs to fit to carry out Prx reduction. In the presence of the C-terminal arm, Srx can access the Prx binding site only from a unique direction, leading to steric hindrance for Srx interaction. In absence of a C-terminal arm, Srx is freer to access Srx from different directions, which may result in faster association. The importance of inhibition of this interaction and its evolutionary values are mentioned in chapter 1 of this dissertation.

Out of those, the initial 4 amino acids are critical for Prx antioxidant function, while the last 22 amino acids do not affect the Prx antioxidant function. Hence, we deleted the last 22 amino acids of Prx1 C-terminal and studied its effect on Srx-Prx interaction. The effect of deletion mutation was studied on both steady-state Srx-Prx interaction and kinetics of the Srx-Prx interaction. The IP experiments indicated that the deletion mutation enhances the steady-state Srx-Prx interaction. It was not clear whether the effect on steady state interaction was due to changes in rate of association or dissociation or both. SPR is the technique of choice to study kinetics of protein-protein interaction [162]. This technique was used for studying the effect of C-terminal deletion on the kinetics of the Srx-Prx interaction. The SPR results indicated more than 1,000-fold increase in the association rate constant ( $k_a$ ) after deletion of the C-terminal arm. Higher  $k_a$  is a direct indicator of faster rate of association. Hence, C-terminal arm deletion leads to approximately 1000-fold faster rate of association. The deletion mutation resulted in a slight reduction in dissociation rate constant ( $k_d$ ). The ratio of  $k_d/k_a$  is equal to the equilibrium dissociation rate constant ( $K_D$ ) in SPR. The reciprocal of  $K_D$  is an indicator of affinity. Hence, lower  $K_D$  indicates better affinity of the Srx-Prx interaction. Deletion mutation reduces the  $K_D$  value of the Srx-Prx1 interaction by more than 1000-fold; hence, Prx1 C-terminal arm deletion results in more than 1000-fold increase in affinity of the Srx-Prx1 interaction.

To further confirm the applicability of these results to other typical 2-Cys Prxs, the effect of this same deletion mutation was studied in Prx4. Considering differences in C-terminal arm orientation (as predicted from homology modeling),

we expected that the extent of steric hindrance may be slightly different than what we saw in Prx1. This prediction was confirmed by SPR analysis of Srx interaction with Prx4<sup>wildtype</sup> and Prx4<sup>mutant</sup>. The deletion mutation in Prx4 resulted in roughly 100-fold increase in  $k_a$  with minimal effect on  $k_d$ . Again, the equilibrium dissociation constant ( $K_D$ ) for the Srx-Prx4<sup>mutant</sup> interaction was calculated to be approximately 100 times lower than the  $K_D$  for the Srx-Prx4<sup>wildtype</sup> interaction. The effect of differences in orientation of the C-terminal arm indicated a 10-fold difference in effect of C-terminal arm deletion (i.e. 1,000-fold in the case of Prx1 while only 100-fold in the case of Prx4). Hence, deletion of the C-terminal arm of Prx affects the rate of Srx-Prx association and these results can be extrapolated to other typical 2-Cys Prx. However, the extent of the effect may be different in other typical 2-Cys Prx.

While considering structural details of the Srx-Prx interaction published by Jonsson and colleagues, we found supportive evidence to our hypothesis [163]. The YF (tyrosine-phenylalanine) motif present in the C-terminal arm of Prx actually occludes the Srx-Prx interaction [163]. The YF motif is responsible for holding the C-terminal arm in a particular orientation, where it causes steric hindrance for the Srx-Prx interaction resulting in reduced rate of association. Jonsson and colleagues, also states a slight stabilizing effect of the C-terminal arm on the Srx-Prx complex. However, our data indicates very low effect of C-terminal arm deletion on dissociation rate constant ( $k_d$ ). We repeated these experiments 5 times and found very low effect on  $k_d$  in each repetition, whereas the effect on  $k_a$  was always multifold. On comparison of experimental methods,

we found that the Jonsson group used an N-terminal truncated Srx (amino acid 1-37 deleted) for their study, while we used the complete Srx sequence. The differences in the Srx-Prx complex stability (once it is formed) can be partially due to the presence of N-terminal in our protein which is present at the site where the Prx C-terminal arm wraps itself around Srx. Figure 3-9 shows representative images of these differences. Hence, it can be concluded from experimental data that the C-terminal arm of Prxs causes steric hindrance for Srx association with Prxs. However, it may have a slight stabilizing effect on the formed complex. Such a stabilizing effect should be minor compared to the multi-fold effect of Prx C-terminal on rate of association and it may have a minor effect on overall affinity. Taken together, these results give us some insight about the molecular characteristics of Srx-Prx interaction. Hence, this information about the Srx-Prx interaction interface can help us in successfully designing targeting strategies to inhibit the Srx-Prx interaction.



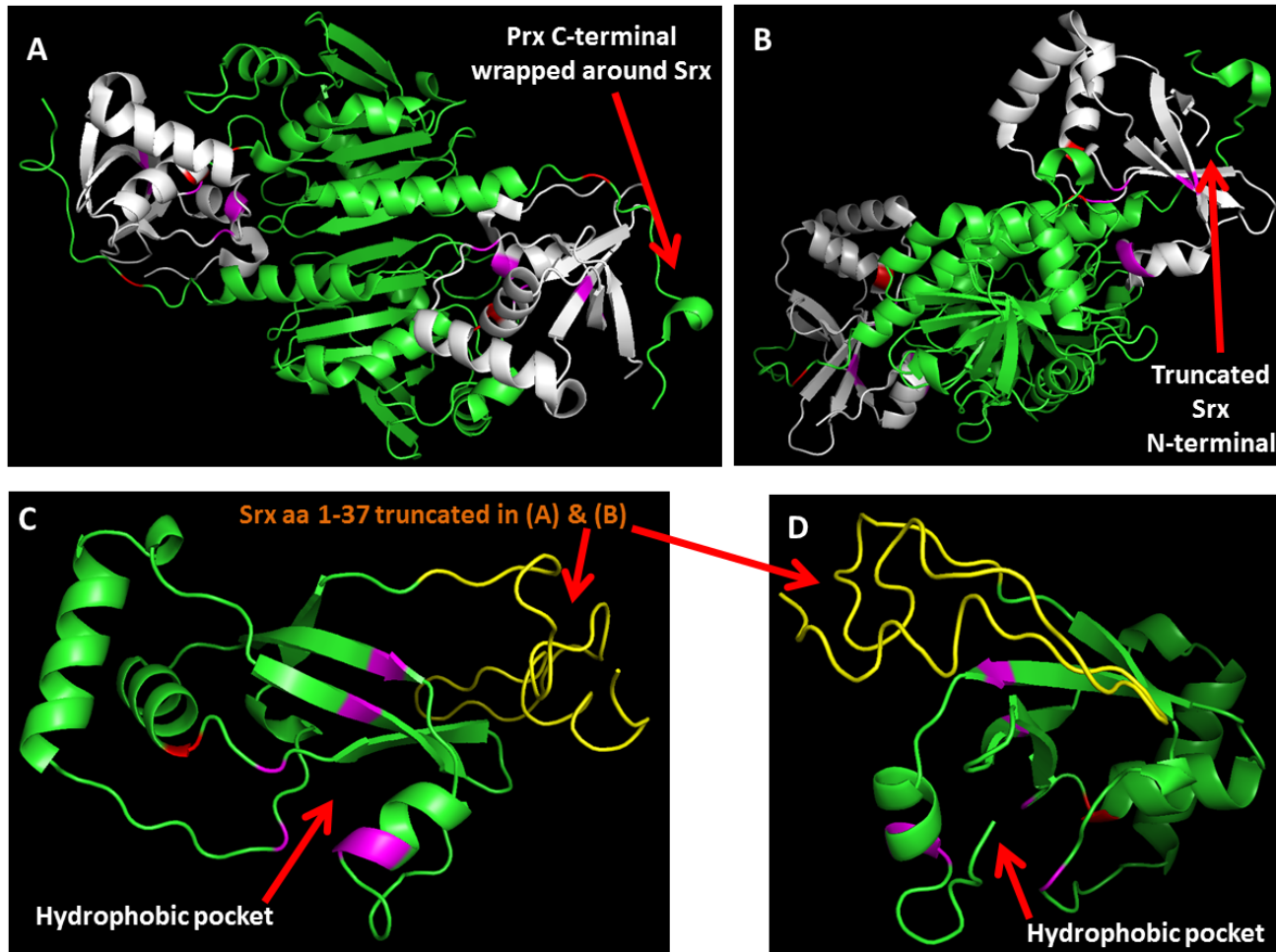


**Figure 3-9: The Srx-Prx complex showing crystal structure with truncated Srx N-terminal:** (A & B) The complete Srx structure predicted via homology modeling with N-terminal amino acids 1-37 marked yellow to represent the truncated part (C & D) and its orientation.

### **3.6 Summary**

Srx hydrophobic pocket formed by the Srx active site binds with a Prx homodimer in a region where  $C_P$  and  $C_R$  of alternate monomers is located. The C-terminal of the second monomer (the one with  $C_R$  in the binding site) covers the binding site and forms a pocket. This C-terminal arm can cause steric hindrance for Srx access to Prxs. Our data confirms this steric hindrance as deletion of the C-terminal arm results in increased steady state interaction between Srx and Prxs. Hence, Prx C-terminal arm is not required for Srx-Prx interaction. This data is further confirmed by kinetic studies which indicate that deletion mutation results in much faster association of Prxs with Srx with very low effect on dissociation. It results in overall higher affinity of the Srx-Prx interaction. Taken together, this study adds insight to the molecular characteristics of the Srx-Prx interaction and may help us design future targeting strategies for inhibition of the Srx-Prx interaction.

## CHAPTER 4: TARGETING SRX-PRX INTERACTION USING SMALL-MOLECULE INHIBITORS

### 4.1 Synopsis

The Srx-Prx axis is a critical component of the antioxidant system in eukaryotes. It is involved in pathogenesis of various oxidative stress-induced conditions that includes (but is not limited to) lung, skin, and colorectal cancer. The purpose of this study is to target the Srx-Prx interaction using small molecules that may further lead to development of novel therapeutics. We used *in silico* virtual screening and protein-small molecule docking to identify a few inhibitors of Srx-Prx interaction. Multiple *in silico* parameters were used as filters to minimize the number of small molecules to be tested. Molecules shortlisted on the basis of computational predictions were tested using *in vitro* techniques. These chemicals significantly reduced the chances of cell growth. ISO1 was found to be the best Srx inhibitor, with a  $K_D$  of 42 nM. Taken together, these data show a promising approach to identifying an Srx inhibitor that can be employed as a research tool as well as a therapeutic tool in the future.

## 4.2 Introduction

Macromolecular protein-protein interaction plays a very important role in several cell-signaling pathways, including redox signaling [164]. Srx-Prx interaction is one example of intracellular protein-protein interaction involved in redox signaling. Protein-protein interaction is one of the most complex macromolecular interactions inside cells and scientists have devoted decades of research to inhibit such interaction using small molecules [165]. Identification of a proper targeting strategy and target site is the most daunting task in the drug-discovery process. Decades of research from computational biologists have led to development of *in silico* tools that can be used to identify pockets or target sites in individual proteins that can be targeted using small molecules [166]. Molecular biologists can contribute to identification of proper targeting sites by identifying amino acids essential for protein function. In fact, contribution of molecular and computational biologists must complement each other for successful drug-discovery. Virtual screening is the process of screening a ligand library against a given target site or well-defined pocket or entire 3-dimensional structure of a given protein [167]. Virtual screening has proved to be a good computer-aided drug-designing tool in recent years as it helps to reduce the cost and time required for drug discovery. Virtual screening is a daunting task as identification of target sites and orientation of molecules that may lead to inhibition of a protein are still based on individual judgment of the researcher. Knowledge of molecular biology, and especially the molecular characteristics of particular protein-protein interaction, can prove to be a great asset for computational biologists as it helps to improve the accuracy of predictions and probability of success in later stages

of the drug-discovery process. Hits selected by virtual screening can either undergo further *in silico* screening for their pharmacokinetic properties or can be directly subjected to *in vitro* testing. The path taken for hits is selected based on availability of resources and prospective use of the molecules.

Molecular biology research reported in earlier chapters of this dissertation helped us identify a prospective pocket in typical 2-Cys Prxs. The amino acids of Srx that are involved in Srx-Prx interaction have been documented in the literature [127]. The amino acids form a groove/pocket in the Srx structure that can potentially be targeted by small molecules. The probability of small molecule binding sites can be predicted using pocket finder software, such as ConCavity and MetaPocket 2.0 [168, 169]. We used the aforementioned pockets of Srx and Prx for a virtual screening process. Screening 8,836,468 chemicals available in the ZINC online database against our targets returned 1,400 hits. We filtered these hits based on predicted pharmacokinetics and pharmacodynamics and shortlisted 100 molecules. Due to lack of funding, we decided to test only 4 molecules. I selected 4 molecules that covered 4 different chemical classes. One of them showed promising results. We named it inhibitor of sulfiredoxin oxidoreductase 1 (ISO1). ISO1 showed good efficacy against Srx. However, its pharmacokinetic profile needed improvement. ISO1 is an amphoteric molecule with lipophilicity outweighing hydrophilicity. Hence, we tested 3 more molecules while looking for a molecule with better pharmacokinetic profile. The main purpose of testing these molecules was to find an efficacious molecule with better pharmacokinetic profile. We finally tested these chemicals *in vitro*, using

lung cancer cell lines. As an aside, we later collaborated with the University of Kentucky College of Pharmacy for screening of more chemical libraries against the given target sites in Srx. We identified 41 more molecules with the help of Dr. Zhan's laboratory and these are being tested *in vitro*; however, those molecules are not part of this dissertation and their testing will be continued in the future.

Virtual screening and *in vitro* testing helped us identify the molecule that shows the most promising inhibition of cancer cell growth at minimal toxicity to normal organ control cells. It may be beneficial for future research to use QSAR techniques to design and test new molecules related to the one identified in our study, as this will help in identifying molecules with better efficacy and lower toxicity potential.

### **4.3 Materials and methods**

#### **4.3.1 Cell lines, plasmids, antibodies and chemicals**

Human lung cancer A549 cells were obtained from ATCC and cultured in RPMI medium containing 10% fetal bovine serum under standard conditions. All experiments were performed using cells within 10 passages from resuscitation. Primary antibodies used include rabbit anti-Srx (Proteintech, Chicago, IL; Catalog 14273-1-AP), rabbit anti-Prx I (Abcam, Cambridge, MA; Catalog ab41906), rabbit anti-PrxSO<sub>3</sub> (Abcam Catalog ab16830), mouse anti-β-actin (Sigma–Aldrich; Catalog A2228), mouse anti-Prx III (Santa Cruz Biotech; Catalog SC-59661), anti-pERK (Cell Signaling, Billerica, MA; Catalog 9101S), anti-ERK (Cell Signaling, Billerica, MA; Catalog 4376S), anti-p-c-Jun (Cell Signaling, Billerica, MA; Catalog 9261L), anti-c-Jun (Santa Cruz; Catalog SC-1694), anti-

pCREB (Cell Signaling, Billerica, MA; Catalog 9198S), and anti-CREB (Cell Signaling, Billerica, MA; Catalog 9197). Recombinant human EGF was commercially obtained (Sigma-Aldrich). All the molecules tested *in vitro* were purchased from eMolecules (La Jolla, CA) or other registered vendors on the ZINC database. Molecules from other chemical libraries were provided by the University Of Kentucky College Of Pharmacy. Dimethyl sulfoxide (DMSO) was purchased from Alfa Aesar (Ward Hill, Massachusetts).

#### **4.3.2 Virtual screening to identify the Srx-Prx interaction inhibitor**

Binding pockets were predicted based on previous experiments mentioned in this dissertation as well as existing literature [54, 55]. Those binding pockets were further confirmed using ConCavity and MetaPocket 2.0 software. We screened approximately 8.8 million compounds from the ZINC database [170] using DOCK Blaster (an online server) [171] against Srx. Out of these compounds we identified approximately 1,400 that can bind to Srx in different orientations. We used iGEMDOCK as a second virtual screening software for confirming the output of DOCK Blaster [172]. We selected these molecules and further predicted their metabolic profile using MetaPrint2D-React (online server) [173]. We used multiple filters to further minimize the number of compounds to be tested. The filters are listed in Table 4-1 with their significance in the drug discovery process. After incorporating these filters, we still had approximately 100 compounds that could be tested *in vitro*; however, we tested 7 of them based on chemical class and individual filters.

**Table 4-1: Filters applied to shortlist virtually screened hits and their significance**

<b>Filter</b>	<b>Significance in Drug Discovery Process</b>
Binding site	Overall probability of inhibition
Binding energy	Probability of competitive inhibition
Number of contacts	Increases the probability that the aforementioned parameters will be fulfilled
Lipinski's Rule of Five	Drug-likeness
Metabolites	Pharmacokinetics as well as pharmacodynamics
Chemical class	Rough idea about other difficulties that may arise during testing of molecules
Toxicity	May limit pre-clinical/clinical outcomes



#### **4.3.3 Small molecule assay for Srx inhibitory activity**

A549 cells were pre-treated with 20  $\mu$ M of the individual compounds being tested for 45 min followed by treatment with H<sub>2</sub>O<sub>2</sub> for 10 min. The treatment groups were incubated with 20  $\mu$ M individual Srx inhibitor for another 4-6 hour. The DMSO treated group was used as recovery control, a 0-hour H<sub>2</sub>O<sub>2</sub> treated group was used as oxidation control, while a non-treated group was used as basal level oxidation control.

#### **4.3.4 Western blotting, IP, and phosphokinase profiling**

Earlier data from our group has shown that Srx enhances phosphokinase signaling [32]. Western blotting and IP were performed using standard protocols. Whole cell lysate as well as purified recombinant proteins (purified as per protocol in Chapter 3) were used for IP. According to affinity of the antibodies and protein molecular weight, membranes were cut and stripped for multiple western blots to minimize variation. All cells were cultured in T75 flasks, cells were collected by trypsinization, and cell numbers were counted in a Coulter cell counter. Cells were then lysed in RIPA buffer at a concentration of  $2 \times 10^7$  cells/mL. For phosphokinase profiling, cells were serum starved for 18-20 hours along with 20  $\mu$ M chemical inhibitor. After serum starvation, we added serum-containing medium along with 100 ng/mL EGF. The cells were incubated with EGF containing media for multiple different time-points. Cells were then lysed in RIPA buffer and western blot was performed to study phosphokinase signaling.

#### **4.3.5 Colony formation, cell proliferation assay and cell cycle analysis**

For the colony formation experiment, cells were suspended in 0.3% agar and 2,000 cells/well were seeded into a 24-well plate pre-coated with 0.5 ml of 0.6% agar. Culture medium was changed every 5 days for 4 weeks. The number and size of colonies were examined and data were obtained by analyzing with OpenCFU software. For the cell proliferation assay, 2,000 cells were plated per well of a 24-well plate. The chemicals were added the next day. The medium was changed every 24 hours with fresh media and inhibitor added at each time-point. After 72 hours, cells from each well were trypsinized and suspended in 1 mL media. The number of cells was counted 3 times with Coulter counter. To study the effect of Srx inhibition on cell cycle, we used flow cytometry analysis. An equal number of A549 (lung adenocarcinoma) cells were plated in 100 mm dishes. The next day, we started serum starvation with media free of any serum. After 24 hours serum starvation, we added fresh media containing 10% serum and 20  $\mu$ M ISO1. The cells were incubated for another 24 hours with inhibitor and serum containing media. Finally, cells were trypsinized and stained using propidium iodide. Cell cycle analysis was carried out using standard protocol at the University of Kentucky College of Medicine facility for Flow Cytometry. 10,000 cells were counted for each treatment group.

#### **4.3.6 Surface plasmon resonance study of Srx-Prx interaction kinetics**

The interaction kinetics of Srx (ligand) with chemical inhibitors was measured by SPR technique using ProteOn<sup>TM</sup> XPR36 instrument (Bio-Rad). Srx was immobilized on GLH sensor chips (Bio-Rad) using the amine coupling method.

Ligand capturing on the GLH chip was performed as per the manufacturer's protocol. Several different concentrations of pure chemical inhibitors were used to evaluate the ligand-analyte binding. The data were acquired and processed by ProteOn manager software and Langmuir 1:1 evaluation model was used for kinetic analysis.

#### **4.3.7 Wound healing assay**

To test the effect of ISO1 on wound healing, cells were seeded in 6-well plates at a density of  $1 \times 10^6$  cells per well to reach faster confluence. Wounds were made by scratching with a sterile 1000  $\mu$ L pipette tip. Floating cells were removed by rinsing three times with PBS. Images of cell migration at different time points were recorded using the microscopic camera and AmScope 3.7 software.

#### **4.3.8 Statistical analysis**

SPR data was analyzed using the Langmuir 1:1 evaluation model. Quantitative data were presented as mean  $\pm$  standard deviation ( $\bar{x} \pm SD$ ). Data were analyzed with indicated statistical methods by using SigmaPlot (version 13.0). For calculation of the p-value, parameters of two-tailed 95% confidence interval were used for all analyses.  $P \leq 0.05$  was considered statistically significant.

### **4.4 Results**

#### **4.4.1 Srx contains a good druggable pocket suitable for virtual screening**

Identifying a drug target site is a cumbersome step in the drug discovery process. We predicted a prospective target site in Srx and Prx using data from Chapter 3 of this dissertation as well as from existing literature [54, 55]. However,

druggability of these sites needed to be confirmed. First, we predicted possible small molecule binding sites in Srx and Prx1 homodimers (as a representative of typical 2-Cys Prx subfamily) using MetaPocket 2.0 open access software (Figure 4-1A&B), which predicts 3 possible target sites in each protein. The target sites that were predicted based on experimental data were confirmed by MetaPocket 2.0 prediction. To further confirm druggability of these target sites, we predicted druggable pocket(s) using ConCavity open access software (Figure 4-1C&D). ConCavity predicted a druggable pocket in sulfiredoxin that covers the target sites predicted based on experimental studies as well as one of the target sites predicted by MetaPocket 2.0 software. However, ConCavity failed to predict a druggable pocket in the Prx1 homodimer. Confirmation of the druggability of the Srx pocket by multiple approaches increased the chances of accurate prediction as a target site; hence we further pursued this target site during *in silico* screening.

#### **4.4.2 *In silico* studies led to selection of four chemicals for *in vitro* testing**

Based on earlier experimental results and *in silico* predictions, we defined multiple target sites of Srx and carried out virtual screening using DOCK Blaster. The output of DOCK Blaster was confirmed by iGEMDOCK. Based on two virtual screening methods we identified 1,400 hits. To further refine the list of molecules, we used multiple filters defined in Table 4-1. We shortlisted 100 molecules based on advanced filtration. Due to economic constraints, we could not test many molecules. Hence, we first selected 4 molecules from 4 different chemical classes with the best predicted results on the basis of individual filters.

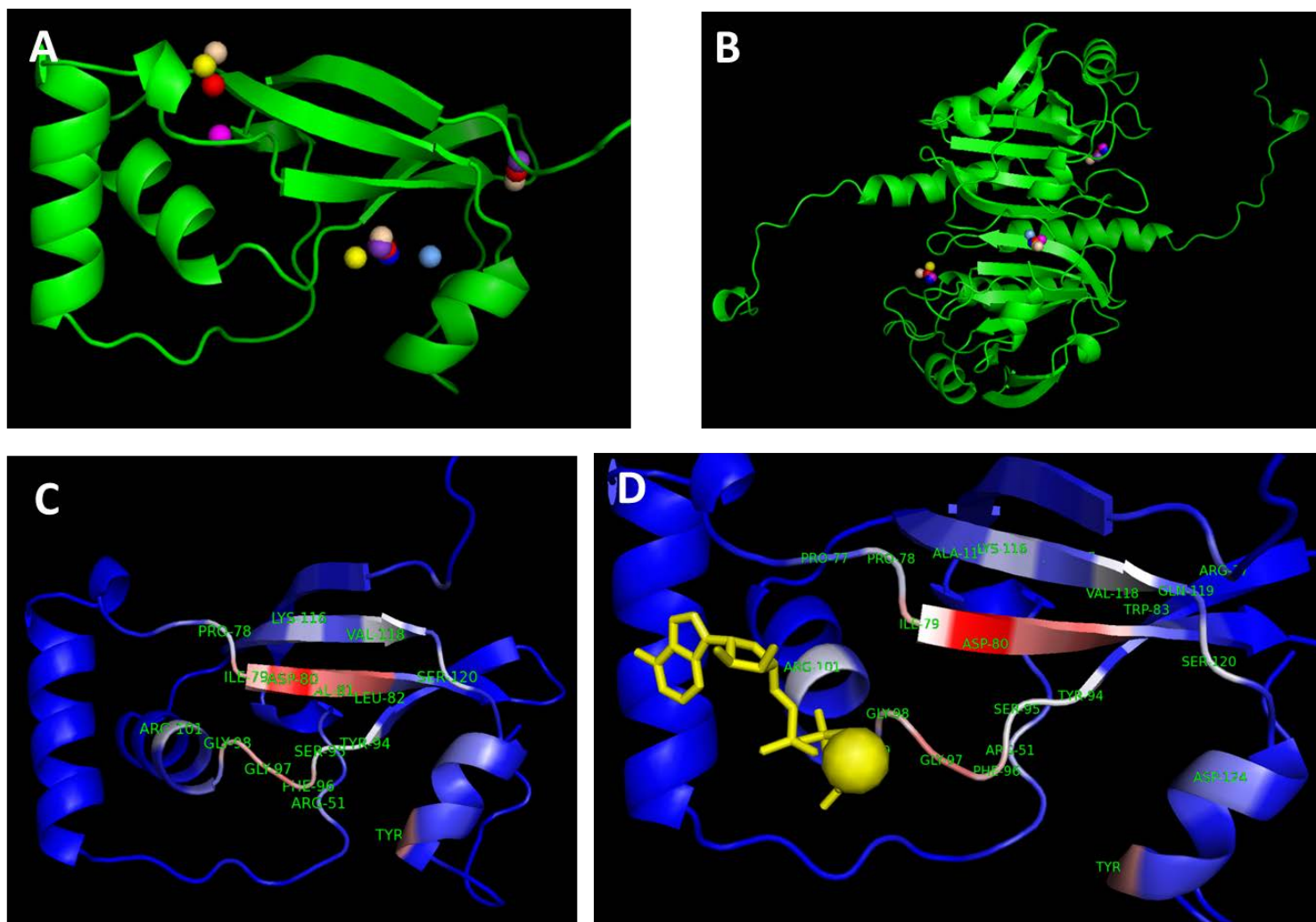


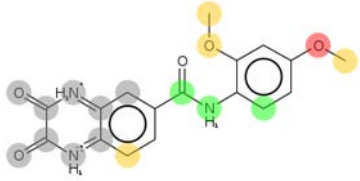
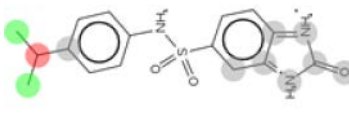
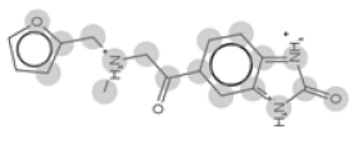
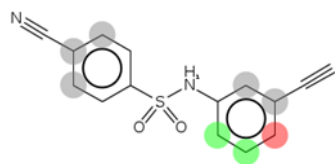
**Figure 4-1: Predicted pockets in Srx and Prx1:** MetaPocket 2.0 predicted 3 probable binding pockets in Srx (A) and Prx1 (B); ConCavity predicted one pocket in Srx (C & D) as a druggable target but it could not confirm the presence of a druggable pocket in Prx1.

The 4 chemicals with selected parameters are listed in Table 4-2, and representative images of the Srx-binding site are shown in Figure 4-2. Based on *in vitro* results, we carried out quantitative structure-activity relationship (QSAR) predictions to identify more molecules related to ISO1 while trying to identify an inhibitor with better pharmacokinetic profile. We tested 3 more chemicals related to ISO1 but none of them produced better effect. Hence, the majority of *in vitro* results reported in this chapter belong to ISO1.

#### **4.4.3 Two molecules showed inhibition of Srx activity**

First we tested all small molecules for Srx inhibitory activity. We over-oxidized the Prx in A549 cells and replenished the media with fresh media containing inhibitor. We allowed the cells to recover for 4-6 hours in the presence of inhibitor. ZINC64002748 (Mol3) and ISO1 showed inhibition of Prx reduction (Figure 4-3). We tested these two chemicals for the rest of the *in vitro* studies. We tested small molecules for their potential to inhibit Srx-Prx1 interaction using recombinant proteins and IP assay. Both chemicals inhibited pull-down of Prx1 with Srx at 100  $\mu$ M concentration (Figure 4-4A & B). However, at lower concentrations, ISO1 showed better effect compared to ZINC64002748. To compare the intracellular efficacy of these two molecules, we used HEK293T cells over-expressing FLAG-Srx. On treatment with H<sub>2</sub>O<sub>2</sub>, followed by cell lysis using IP buffer containing 20  $\mu$ M of small molecules, ISO1 successfully inhibited pull-down of Prx-SO<sub>3</sub> (i.e. over-oxidized form of Prx) with Srx (Figure 4-4 C & D). Hence, ISO1 can inhibit Srx interaction with Prx in both reduced as well as oxidized state.

**Table 4-2: List of 4 chemicals selected on the basis of virtual screening**

Parameter	ZINC38768782	ZINC39975876	ZINC 64002748	ZINC 142037 (ISO1)
	N-(4-isopropylphenyl)-2-oxo-benzimidazole-5-sulfonamide	N-(2,4-dimethoxyphenyl)-2,3-dioxo-quinoxaline-6-carboxamide	5-[2-[2-furylmethyl(methyl)amino]acetyl]benzimidazol-2-one	4-cyano-N-(3-ethynylphenyl)benzene-1-sulfonamide
Binding energy	-49.82 kcal/mol	-81.76 kcal/mol	-103.22 kcal/mol	-70.13 kcal/mol
Number of contacts	4	3	2	5
Sites of metabolic modifications				
xLogP	1.51	3.3	1.23	2.20
H-bond donors	3	3	3	1
H-bond acceptors	8	6	6	4
Alternative names used in this dissertation	Mol1	Mol2	<b>Mol3</b>	<b>ISO1</b>

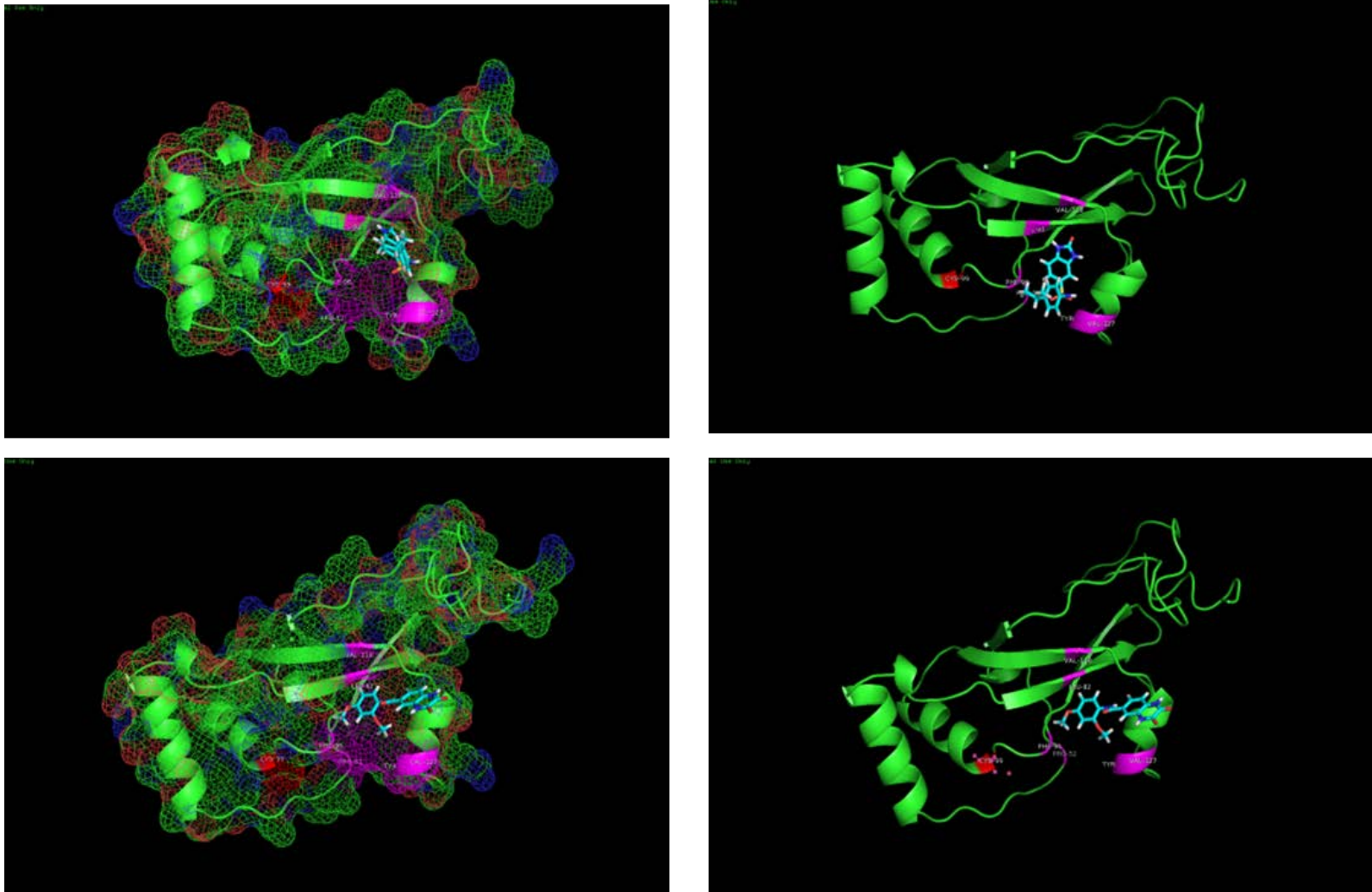
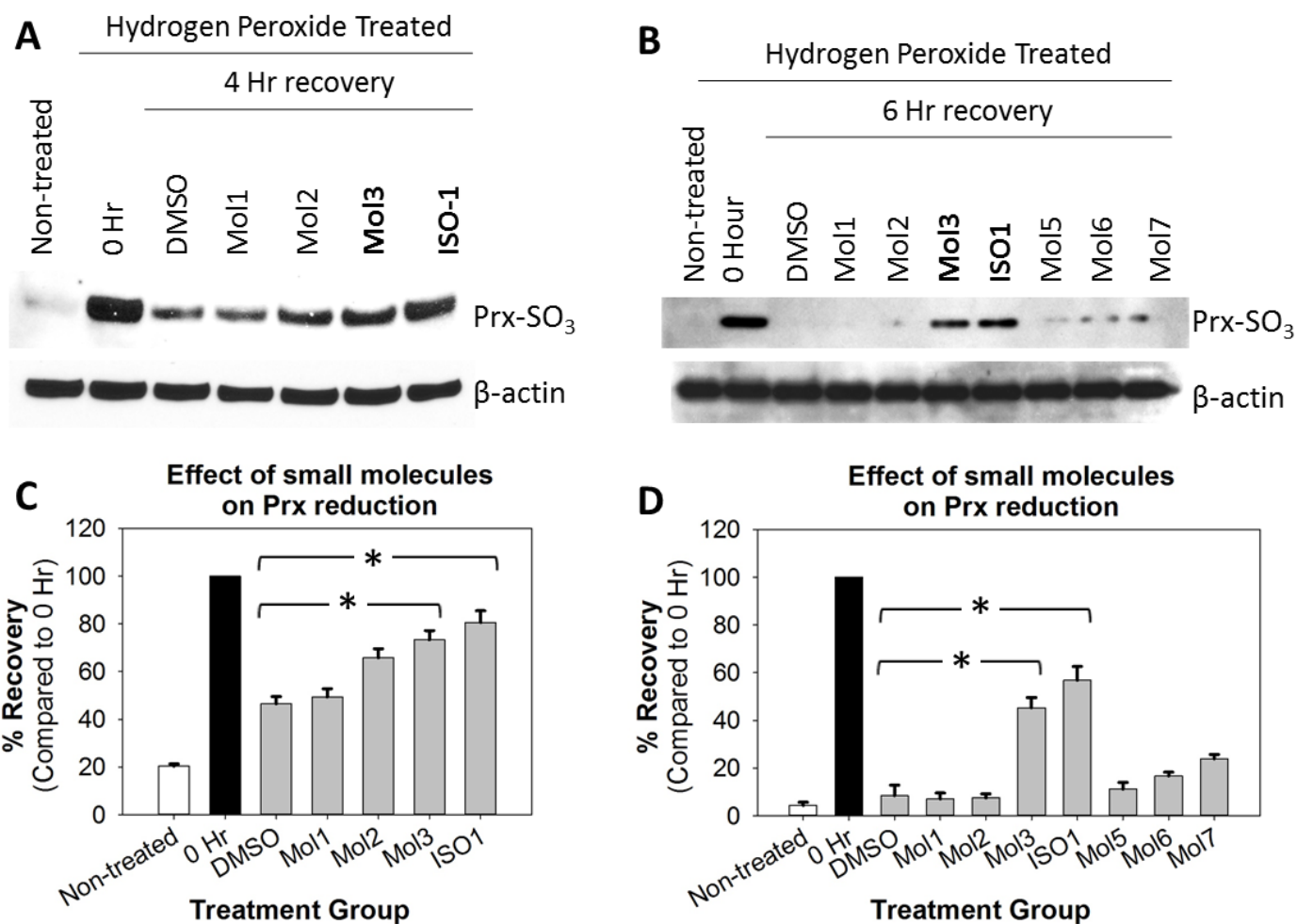
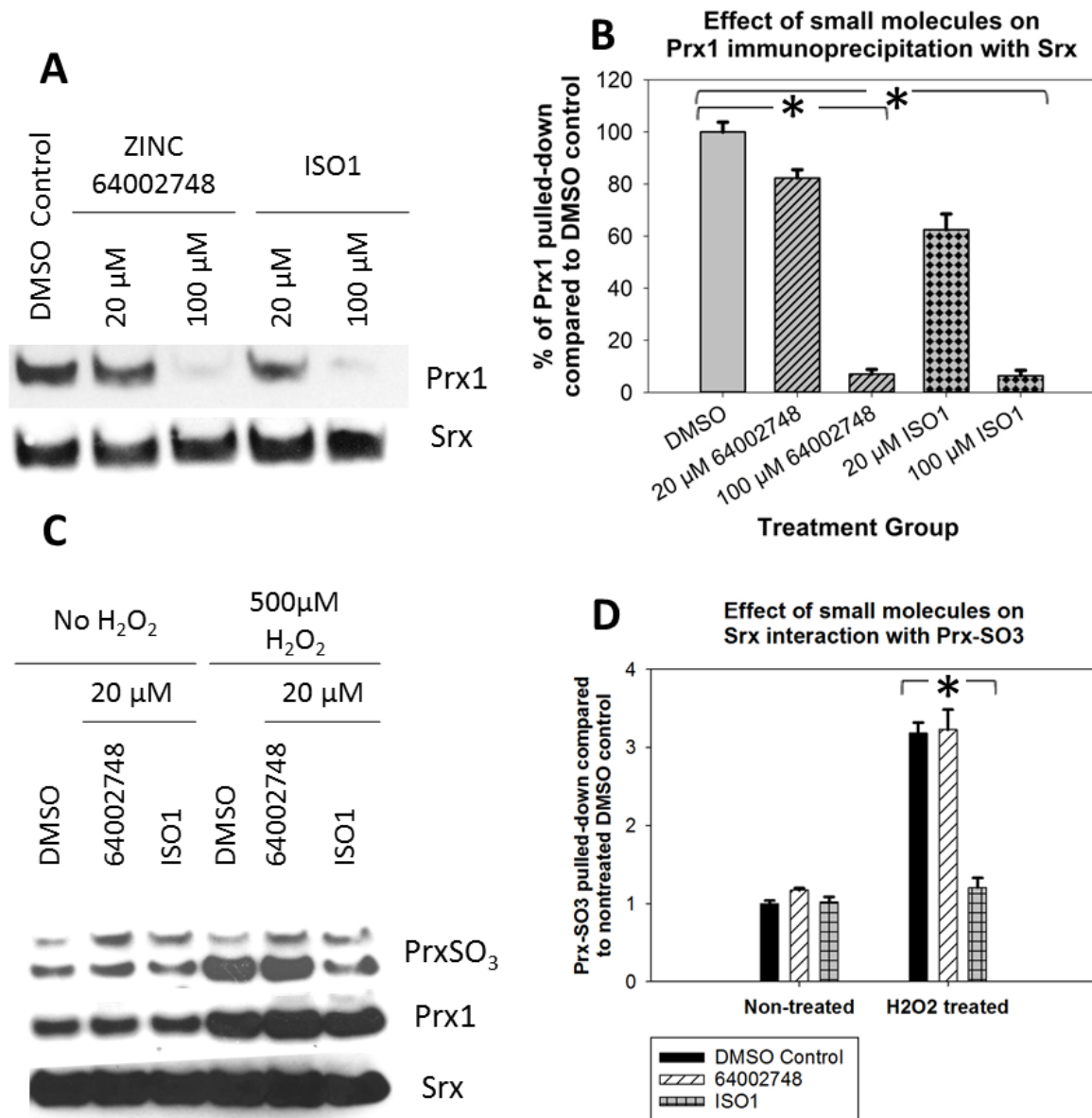


Figure 4-2: Representative images of docked small molecules in Srx-binding pocket.





**Figure 4-3: Effect of individual small molecules on Prx-SO<sub>3</sub> reduction:** ZINC64002748 and ISO1 inhibit Prx-SO<sub>3</sub> reduction in A549 cells as evident from western blot and quantitative values of band in 4-hour (A & C) and 6-hour (B & D) recovery.



**Figure 4-4: Effect of ZINC64002748 and ISO1 on pull-down of Prx1 and Prx-SO<sub>3</sub> along with Srx:** (A-B) Inhibition of Prx1 recombinant protein immunoprecipitation with Srx recombinant protein; (C-D) Prx-SO<sub>3</sub> IP along with Srx in FLAG-Srx overexpressing HEK293T cells. Statistical method applied was one-way ANOVA followed by Holm-Sidak post-hoc analysis (\*p $\leq$ 0.05). Upper band in Prx-SO<sub>3</sub> band represent Prx4-SO<sub>3</sub> while other 3 Prx are part of lower band.

#### **4.4.4 Two molecules inhibit cell growth and colony formation in lung and colon cancer cells**

On testing the effect of ZINC64002748 and ISO1 in lung cancer cell lines, we found successful inhibition of non-small cell lung cancer (NSCLC) cell growth at concentrations which showed minimal toxicity in non-cancer BEAS2B cell lines from lungs (Figure 4-5 A & B). The effect was more selective for NSCLC cells compared to small cell lung cancer (SCLC) cell lines i.e. H69 and H82 cells. ZINC64002748 showed higher potency in A549 cells compared to ISO1. Similar results were observed in the anchorage-independent cell growth (colony formation) assay. Both ISO1 and ZINC64002748 inhibited anchorage-independent colony formation in the A549 NSCLC cell line. ZINC64002748 showed more potent inhibition of colony formation in A549 cells compared to ISO1 treatment (Figure 4-6).

#### **4.4.5 Surface plasmon resonance studies indicate higher affinity of Srx for ZINC64002748 and ISO1 compared to Prx1**

GLH chips were utilized to study the affinity of Srx for individual chemicals. Srx was used as ligand while ZINC64002748 and ISO1 were used as analytes. On calculation of kinetic parameters, we found both the chemicals showed higher association rate constant ( $k_a$ ) for Srx compared to  $k_a$  of Prx1 for Srx (Table 4-3; Figure 4-7). On comparison of dissociation rate constant ( $k_d$ ), we found both the chemicals have higher  $k_d$  compared to Prx1. On comparison of equilibrium dissociation rate constant ( $K_D$ ), we found that both the chemicals have lower  $K_D$  compared to Prx1 (Table 4-3). The kinetic parameters of Prx1 are calculated and discussed in Chapter 3 of this dissertation.

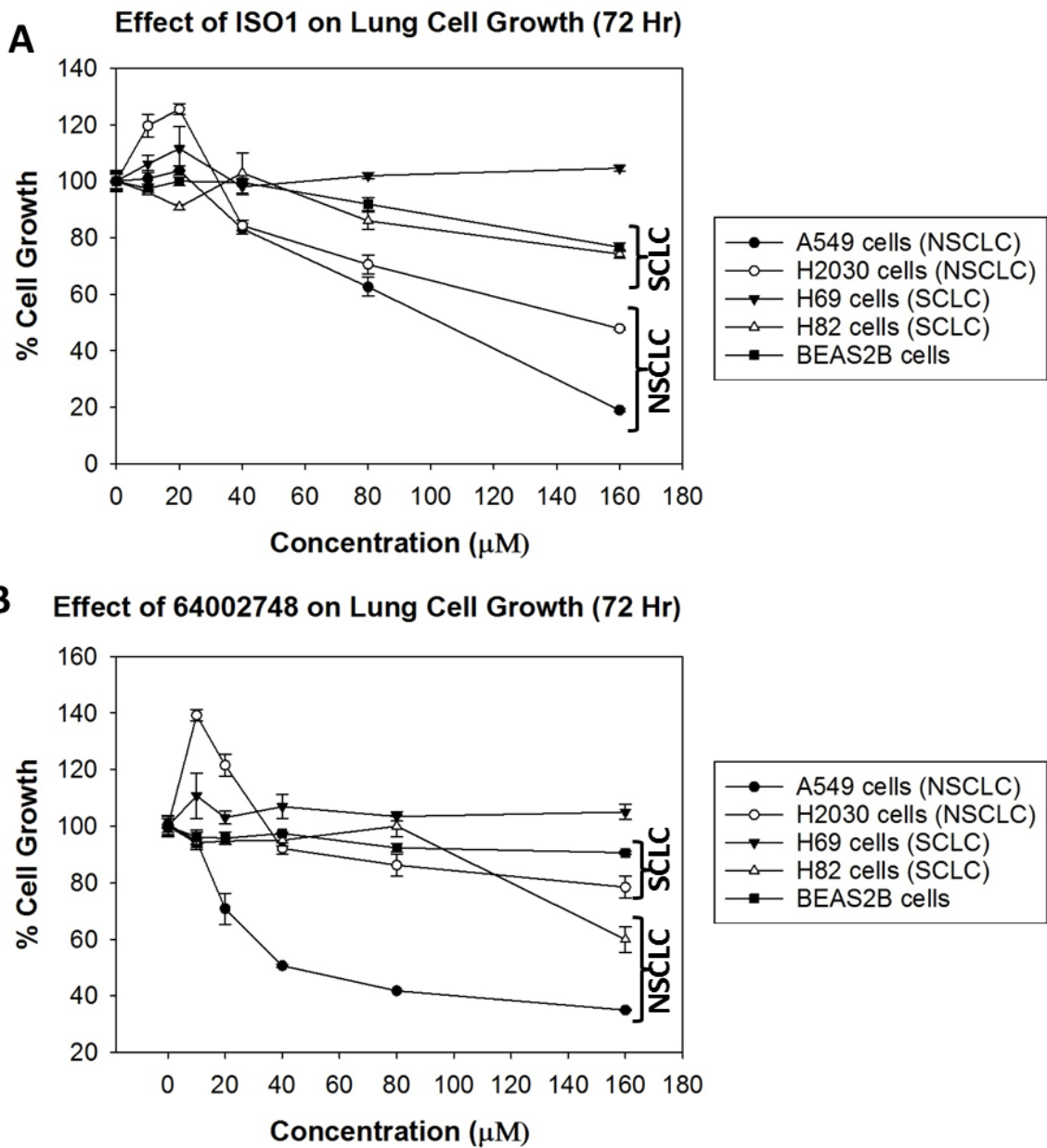


**Figure 4-5: Effect of ZINC64002748 and ISO1 on cell growth:** Small molecules that inhibit Srx-expressing cell growth in lung cancer cells: (A) ISO1 and (B) ZINC64002748. Each treatment was carried out in triplicates (n = 3).

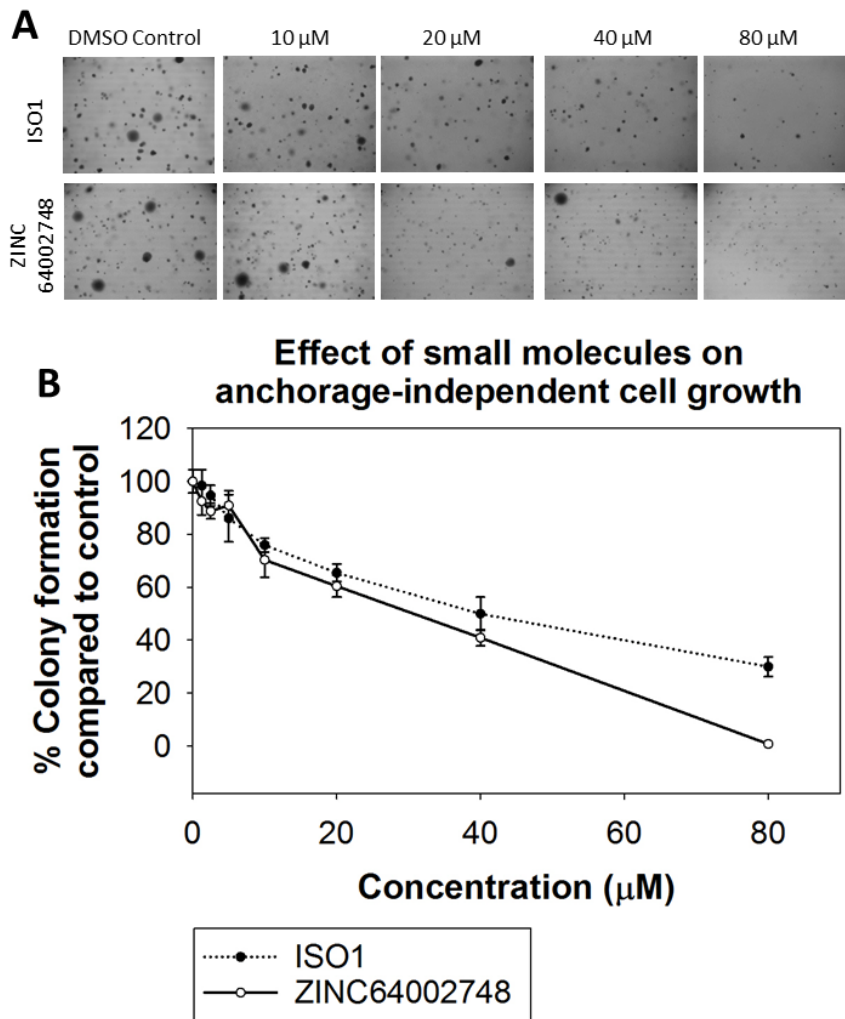


**Figure 4-6: Small molecules inhibit anchorage-independent cell growth:** (A) Representative images of colonies; (B) concentration-dependent effect of ISO1 and ZINC64002748 on colony formation. Each treatment represents the triplicates (n = 3).

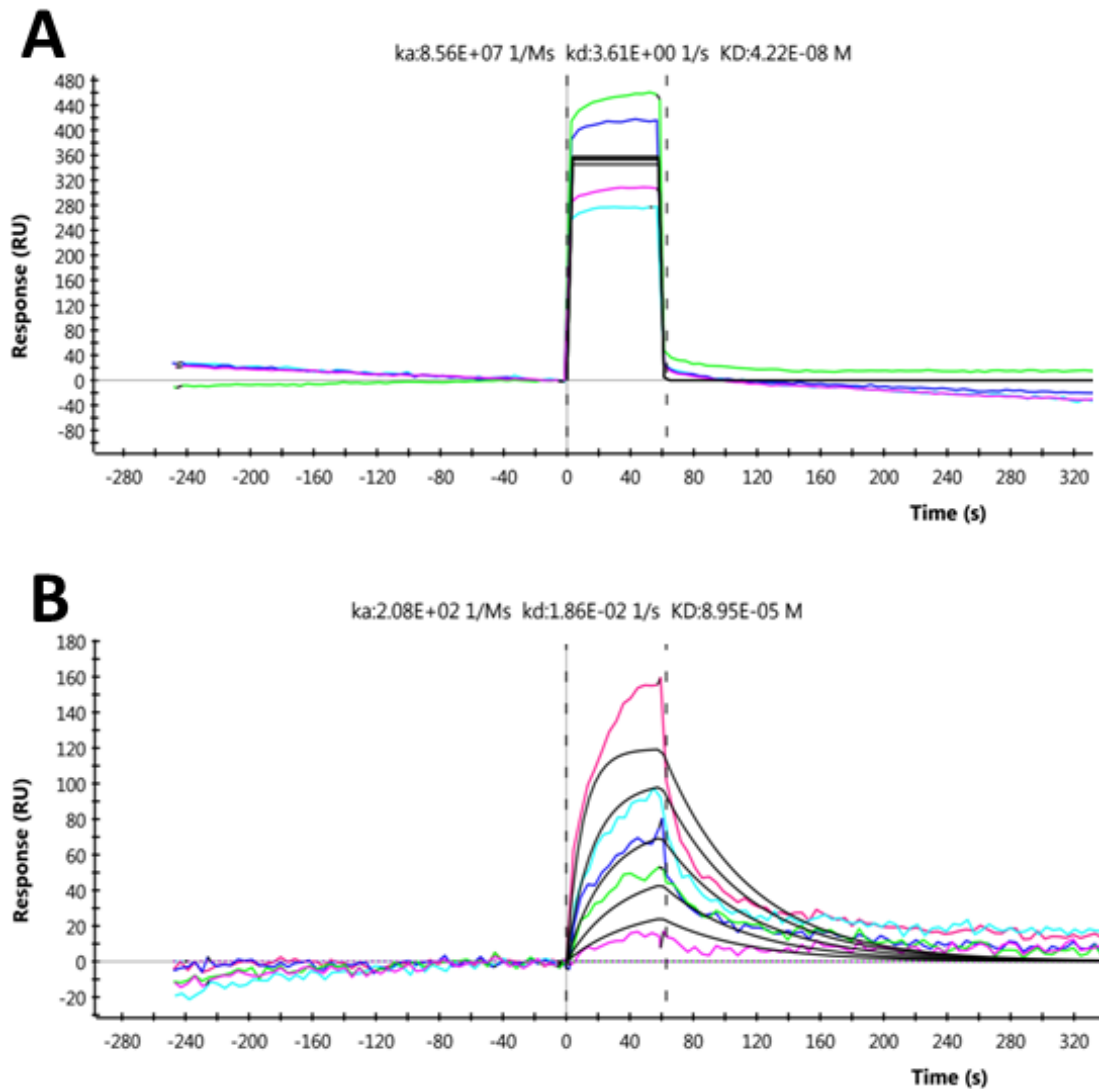


**Figure 4-7: Surface plasmon resonance curves of Srx interaction with small molecules:** (A) ISO1 and (B) ZINC64002748. The faster on and off rate represents micelle formation in case of ISO1 as shown in panel (A). It can also occur due to multi-molecular binding to same protein molecule.

**Table 4-3: Srx has higher binding affinity for chemical inhibitors than Prx1 (SPR analysis):** Srx-Prx1 kinetic parameters were taken from Chapter 3 of this dissertation. The data represents a calculation carried out using 5 different concentrations of analyte (small molecules).

Parameters (Unit)	Ka (1/Ms)	Kd (1/s)	K <sub>D</sub> (M)	Comments
ISO1	8.65 E <sup>+07</sup>	3.61 E <sup>00</sup>	4.22 E <sup>-08</sup>	Srx has much higher affinity for ISO1 compared to Srx affinity for Prx1 or ZINC64002748
ZINC64002748	2.08 E <sup>+02</sup>	1.86 E <sup>-02</sup>	8.95 E <sup>-05</sup>	Srx has slightly higher affinity for ZINC64002748 compared to Srx affinity for Prx1
Prx1	6.93 E <sup>-01</sup>	5.32 E <sup>-04</sup>	7.69 E <sup>-04</sup>	

On comparison of  $K_D$  values between the chemicals, we found ISO1 has a lower  $K_D$  (hence, higher affinity) for its interaction with Srx compared to ZINC64002748-Srx interaction. The  $K_D$  value for Srx-ISO1 interaction was  $4.22 \text{ E}^{-08} \text{ M}$  (i.e. 42.2 nM) while that for Srx-ZINC64002748 interaction was  $8.95 \text{ E}^{-05} \text{ M}$  (i.e. 89.5  $\mu\text{M}$ ). These values are inversely proportional to the affinity of these molecules for Srx. However, the  $\text{EC}_{50}$  in cell culture depends on variety of parameters including uptake of these molecules by cells. As ISO1 is amphoteric in nature, it forms micelles leading to hindered uptake into the cells. Hence, effect of ZIN64002748 is better in terms of  $\text{EC}_{50}$  compared to effect of ISO1.

#### **4.4.6 ISO1 inhibits Srx-mediated phosphokinase signaling**

Previous data from our lab indicates that Srx enhances phosphokinase signaling. Knockdown of Srx results in reduced phosphokinase signaling. Hence, any Srx inhibitor should produce effect similar to Srx knockdown on phosphokinase signaling. To further confirm specificity of effects produced by two small molecules, we tested their effects on phosphokinase signaling. ZINC64002748 indicated a slight stimulatory effect on phosphokinase signaling. However, Srx inhibition should reduce the phosphokinase signaling. For individual time points, ISO1 reduced the phosphokinase signaling at 20  $\mu\text{M}$  concentrations (Figure 4-8). The effect of ISO1 was similar to the one produced as a result of Srx knockdown. Hence, all the effects produced by ISO1 add up to show its efficacy as a specific Srx inhibitor. Even though ZINC64002748 showed higher potency against lung and colon cancer cells, its effect may not be specific to Srx inhibition as it could not consistently inhibit phosphokinase signaling as expected from a Srx inhibitor.



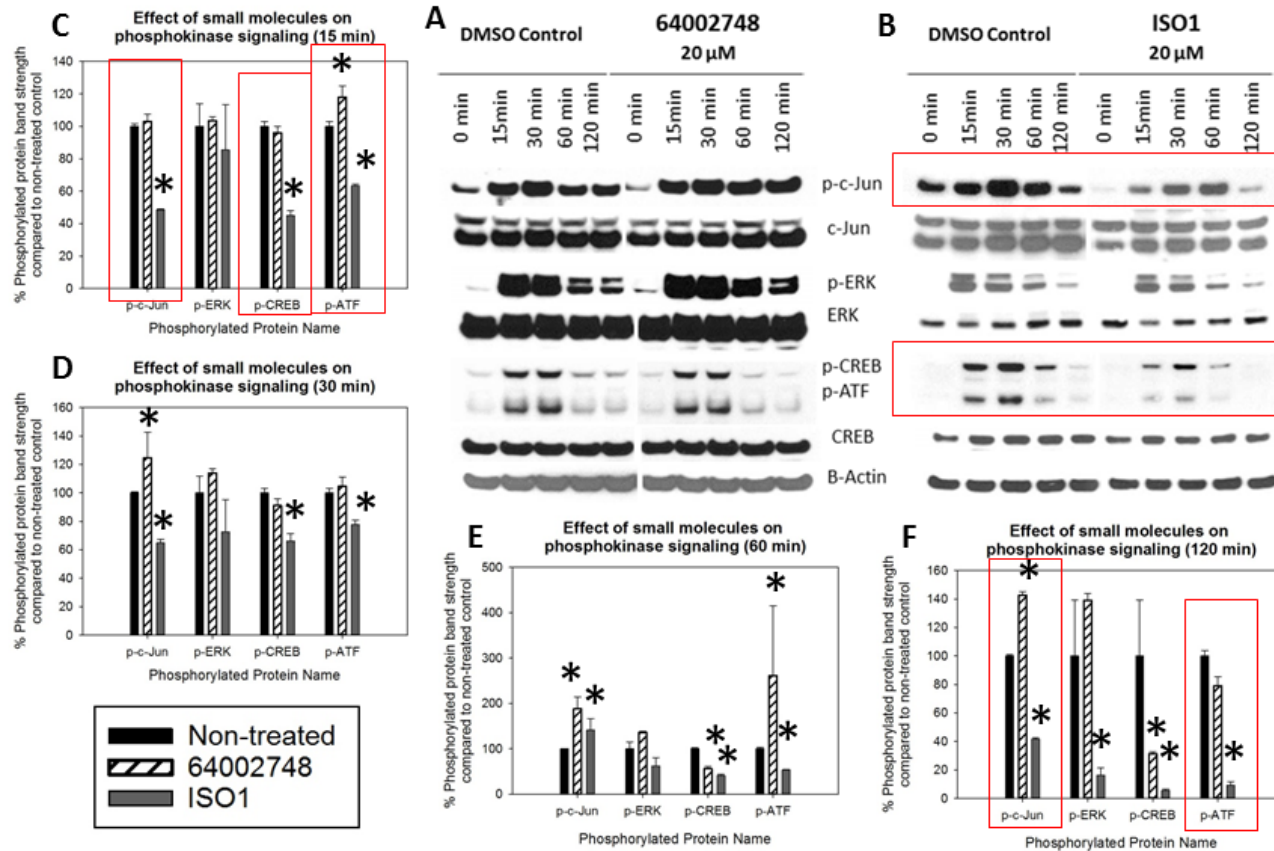


**Figure 4-8: ISO1 inhibits phosphokinase signaling:** The western blot showing EGF-induced phosphokinase signaling after (A) ZINC64002748 and (B) ISO1 treatment; the bands for individual time-points were quantitated using ImageJ software and plotted as shown (C) 15 min, (D) 30 min, (E) 60 min, and (F) 120 min.

Hence, ZINC64002748 may not be a specific inhibitor of Srx. Considering specificity of ISO1; we carried out the rest of the *in vitro* studies with ISO1.

#### **4.4.7 ISO1 arrests cell growth in G<sub>2</sub> phase**

To confirm the effect of Srx inhibitor ISO1 on cell cycle phase, we used flow cytometry. On testing the effect of ISO1 in lung cancer cells (A549), we found substantial reduction in number of cells in the S-phase of cell growth (Figure 4-9A). The number of cells in G<sub>2</sub> phase was higher compared to non-treated control.

#### **4.4.8 ISO1 inhibits cell-migration in wound healing assay**

Earlier research from our lab shows that Srx enhances cell-migration in wound healing assay [32]. To further confirm the specificity of ISO1, we tested its effect on A549 cell-migration using wound healing assay. The wound was made by scratching with a micropipette tip and cells were incubated with multiple concentrations of ISO1. The ISO1 inhibited wound healing in a dose-dependent manner (Figure 4-9B) with statistically significant inhibition obtained at concentrations above 20  $\mu$ M ( $p \leq 0.05$ ).

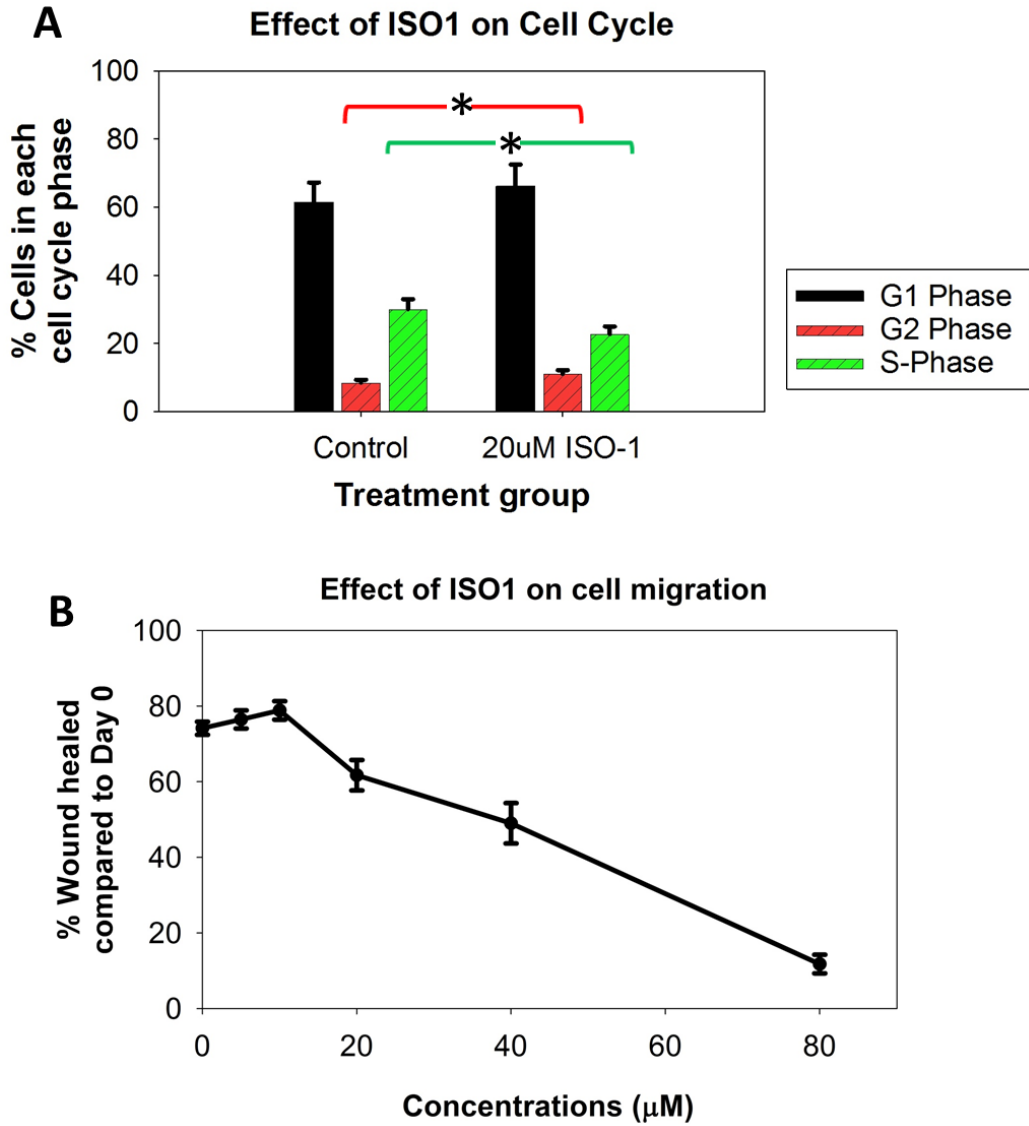


**Figure 4-9: ISO1 inhibits lung cancer cell growth and migration: ISO1 (A) inhibits cell cycle progression to S-phase; (B) inhibits cell migration in wound healing assay.**

## 4.5 Discussion

Homology modeling and protein-protein docking studies reported in Chapter 3 along with existing literature helped us to identify the Srx-Prx interaction interface. This interface could be targeted via amino acids in the Srx or Prx chain that are present at interface or via dual binders that can act on amino acids at both the Srx and Prx interfaces. Srx has three different sites that can be targeted for inhibition of its enzymatic activity. Those sites include: (1) hydrophobic pocket (i.e. a groove with multiple hydrophobic amino acids); (2) the ATP and  $Mg^{2+}$  cofactor binding site; and (3) Cys<sup>99</sup> and neighboring amino acids [54, 55, 163]. The hydrophobic pocket is involved in Srx-Prx binding. ATP hydrolysis is necessary for reduction of Prx-SO<sub>3</sub> and  $Mg^{2+}$  acts as a cofactor in this process. Cys<sup>99</sup> is involved in formation of thiosulfinate intermediate, which is required for reduction of Prx-SO<sub>3</sub> but it is not important for the Srx-Prx binding [24]. Targeting the ATP binding site has good potential to inhibit Srx and this site is easily accessible to small molecules. However, the probability of toxicity was predicted to be very high for any molecule that could bind at the ATP binding site. Therefore, we did not test any of these molecules. Cys<sup>99</sup> is also easily accessible for small molecules. However, an effort to define Cys<sup>99</sup> and only its adjacent amino acids led to a huge number of hits during virtual screening. The chances of non-specificity of interaction were very high in those molecules. The hydrophobic pocket is an easily accessible groove with well-defined 3-dimensional structure. This groove is responsible for Srx-Prx binding. Cys<sup>99</sup> is also present in proximity (but not inside) of this pocket. Hence, it may be a site of interaction for a specific inhibitor. To reduce the number of false positive

molecules in virtual screening, we defined a complex 3-dimensional target site that included all important amino acid components of the hydrophobic pocket (Pro<sup>52</sup>, Leu<sup>82</sup>, Phe<sup>96</sup>, Val<sup>118</sup>, Val<sup>127</sup> and Tyr<sup>128</sup>) along with Cys<sup>99</sup>. Proximity of these amino acids to each other made me believe that it would be a druggable target site. However, druggability of a protein intramolecular target site can be affected by myriad biochemical and structural factors. Therefore, I decided to confirm it with two existing druggable pocket prediction tools: MetaPocket 2.0 and ConCavity. The druggability of the pocket defined in this study was confirmed by both *in silico* prediction methods. Based on existing literature and earlier experiments, we had defined a pocket in the Prx dimer as a target site. However, the Prx binding pocket druggability could not be confirmed using all methods. Considering the narrower Prx pocket and inability to confirm its druggability by prediction method, the chances of false positive in virtual screening was predicted to be high.

Virtual screening is not a 100% accurate method and human judgment must be used to improve the chances of success and minimize the numbers of false positive as well as false negative. To reduce the chances of failure, we decided to confine ourselves to virtual screening against the Srx pocket and use Prx interface only for guidance. Virtual screening using DOCK Blaster and iGEMDOCK helped us select 1,400 hits out of 8,836,468 molecules that were originally screened against Srx. To minimize the number of false positives, we utilized multiple filters related to pharmacokinetic and pharmacodynamic descriptors. The filters allowed us to reduce the number to 100 chemicals. I

refined the methodology and filters to select 4 compounds from 4 different chemical classes. These molecules had the highest predicted probability of success based on docking and molecular descriptors. The 4 chemicals were first tested for their ability to inhibit the reduction of over-oxidized Prx. ZINC64002748 and ISO1 showed acceptable inhibition at 20  $\mu$ M concentrations. Hence, both were selected for further *in vitro* testing in cell culture. We later carried out a QSAR study to improve the pharmacokinetic profile of ISO1 and selected 3 molecules for further testing. However, changes in structure that led to better pharmacokinetic profile resulted in loss of anti-Srx activity. Hence, the majority of data reported here are results of ISO1 testing in cell culture.

The chemicals were first tested for their ability to inhibit Srx by testing inhibition of Prx-SO<sub>3</sub> reduction. Oxidative stress resulted in hyperoxidation of Prxs. A 5-hour recovery after induction of oxidation is sufficient for reduction of the majority of Prx-SO<sub>3</sub>. Hence, the A549 cells were first treated for 10 minutes with H<sub>2</sub>O<sub>2</sub>, and then were allowed to recover for 5 hours with fresh media containing different concentrations of small molecules. The 0-hour oxidation control and DMSO (vehicle) reduction control groups were used as controls for induction of oxidation and recovery. Both ZINC64002748 and ISO1 showed successful inhibition of Prx-SO<sub>3</sub> reduction; however, the effect was more promising for ISO1. We next tested the ability of these chemicals to inhibit the Srx-Prx and Srx-PrxSO<sub>3</sub> interaction using pull-down assay. Both molecules inhibited the Srx-Prx interaction at higher concentrations. However, at lower concentrations only ISO1 could significantly reduce the Prx pull-down along with Srx. Similarly, ISO1

successfully inhibited Prx-SO<sub>3</sub> pull-down along with Srx at 20 μM concentration while ZINC64002748 could not produce significant effect on Prx-SO<sub>3</sub> pull-down. As mentioned earlier, the hydrophobic pocket of Srx is responsible for Srx-Prx binding while Cys<sup>99</sup> (amino acid outside hydrophobic pocket) is responsible for enzymatic activity. Hence, Srx enzymatic activity can still be inhibited even if the Srx-Prx binding is not affected. Therefore, we decided to further test both the molecules to select one with specific activity.

Earlier publications from our group reported the role of Srx in promoting cell growth and colony formation in NSCLC cell lines [32, 70]. Therefore, we decided to test the effect of these chemicals on cell growth in lung cancer cell lines. For confirming the specificity of effect, we simultaneously tested NSCLC cell lines, SCLC lines, and a lung normal immortalized cell line (i.e. BEAS2B cells). Both the chemicals inhibited lung cancer cell growth. The effect was more selective towards inhibition of NSCLC cell lines compared to SCLC or non-cancer lung cell lines. ZINC64002748 showed more potent inhibition of cell growth compared to ISO1. Similarly, on testing in colony formation, both small molecules inhibited the anchorage-independent colony formation in A549 cells.

An ideal inhibitor should have a higher affinity for the target enzyme compared to its physiological substrate. We tested Srx-Prx affinity using SPR as reported in Chapter 3 of this dissertation. To compare the affinities, we carried out SPR analysis for individual chemicals. Both the chemicals showed higher affinity (i.e. lower K<sub>D</sub>) for Srx compared to the Srx affinity for Prx. The affinity of ISO1 was higher for Srx compared to that of ZINC64002748.

Another report from our group indicates that the Srx-Prx axis promotes phosphokinase signaling in lung cancer cells [32]. Therefore, we expected Srx inhibitors to reduce phosphokinase signaling in a manner similar to that observed in the Srx-knockdown cell lines. The A549 cells were serum starved for 16-18 hours in the presence of 20  $\mu$ M chemical inhibitor followed by stimulation of phosphokinase signaling with media containing 10% serum and 100 ng/mL EGF. The phosphokinase signaling was studied using western blot analysis and specific antibody against phosphorylated proteins. On comparison of phosphokinase signal (especially p-c-Jun, p-CREB and p-ATF) at individual time-points, we observed significant reduction in phosphokinase signaling in the ISO1 treatment group compared to DMSO (vehicle) treated control group. ZINC64002748 failed to inhibit phosphokinase signaling in the expected manner.

The results of all experiments discussed so far led us to conclude that ISO1 may be a more specific inhibitor of Srx compared to ZINC64002748. Even though the latter showed more potent effect in inhibition of cell growth and colony formation, it may be partially mediated through a mechanism other than inhibition of Srx-Prx interaction. Considering the effect of ISO1 in all tests, we decided to further study its effect on cancer cells. On testing its effect on cell cycle, we found that ISO1 inhibits the progression of cells to S-phase by blocking the majority of cells in G<sub>1</sub>/G<sub>2</sub> phase (mainly G<sub>2</sub> phase). On comparing this effect to Srx knockdown, we found that this effect is similar to the one observed in Srx-knockdown cells [32]. Similar to Srx-knockdown cells, ISO1 also inhibited tumor cell migration in the wound healing assay. Taken together, ISO1 is a promising molecule that can



inhibit Srx. All the tests performed in this study have confirmed specificity of ISO1 mechanism. Further QSAR studies can help to identify a Srx inhibitor with better efficacy and pharmacokinetic profile.

#### **4.6 Summary**

The Srx hydrophobic pocket is directly involved in Srx-Prx binding. The hydrophobic pocket is a well-defined druggable target site for inhibition of Srx-Prx interaction. Virtual screening led to a list of multiple molecules that have potential to bind with Srx. Careful selection of filters led to minimization of the number of molecules to be tested *in vitro*. Seven molecules were tested *in vitro* for their ability to inhibit the reduction of over-oxidized Prx by Srx. Two molecules (ZINC64002748 and ZINC142037) out of 7 successfully inhibited reduction of over-oxidized Prx. Further *in vitro* testing confirmed that ZINC142037 can inhibit Srx specifically. ZINC142037 was named inhibitor of sulfiredoxin oxidoreductase 1 (ISO1). In the future, more QSAR studies can help identify a molecule related to ISO1 that has better efficacy of Srx inhibition and a better pharmacokinetic profile. ISO1 and other molecules identified using QSAR can be further explored for their efficacy as chemotherapeutic molecules in lung cancer.

## CHAPTER 5 OVERALL DISCUSSION

### 5.1 Summary of dissertation

Srx is an exclusive molecule that can reduce over-oxidized Prx. The Srx-Prx axis plays a critical role in a variety of physiological as well as pathological conditions involving redox signaling. Some information is available about the cross-talk of the Srx-Prx axis in several signaling pathways, but the factors that affect these are largely unknown. Prx has clearly been shown to play a protective role in cardiovascular and neurological diseases. However, its role in cancer is still controversial due to both tumor-suppressor and oncogenic roles played by Prx-isoforms in different cancer types. More in-depth mechanistic studies in the future will help to unravel interweaved behavior of Prx and will lead to development of better therapeutic strategies for cancer prevention or treatment. Srx itself plays an oncogenic role in multiple types of cancer, including cancers of the skin, colon, and lung. The biochemistry of Srx function has been studied in great detail. However, the role of Srx in carcinogenesis needs a deeper understanding, which can be fulfilled by future research. Considering the oncogenic roles of Srx, it will be worth exploring Srx inhibitors as a molecule of choice for chemoprevention and/or chemotherapy.

The majority of Srx functions are mediated through Srx-Prx interaction. Previous publications from our research group have demonstrated the role of Srx-Prx interaction in tumor promotion and metastasis. Based on existing information available about the Srx-Prx interaction, we designed a general hypothesis that Srx plays a critical role in lung carcinogenesis, and targeting the Srx-Prx axis or

Srx alone may facilitate future development of targeted therapeutics for prevention and treatment of lung cancer.

To test this hypothesis, we first demonstrated that Srx enhances urethane-induced lung carcinogenesis (**Specific Aim 1**). Urethane is a well-known lung carcinogen in mice [138]. Urethane is metabolized to vinyl carbamate epoxide, which later causes the majority of urethane toxicity [143]. Humans are mainly exposed to urethane from alcoholic beverages and cigarette smoke. Alcohol increases the expression of CYP2E1 [145], which along with esterase are two enzymes that play a main role in metabolism of urethane [146]. CYP2E1 converts urethane to vinyl carbamate epoxide, whereas esterase converts it to ethanol [146]. Considering the stoichiometry of reaction, the presence of alcohol has potential to slow down the metabolism of urethane by esterase. Hence, the metabolism of urethane to vinyl carbamate epoxide becomes the predominant mechanism of metabolism partially due to increased CYP2E1 expression and partially due to reduced rate of metabolism by esterase. Many individuals consume alcohol and smoke cigarettes at the same time [147]. Hence, the risk of urethane toxicity and urethane-induced lung cancer may be higher in these individuals. Human lungs have lower expression of urethane metabolizing enzymes (i.e. CYP2E1) and esterase [148, 149], which multiplies the risk of stoichiometric inhibition of esterase in human lungs. Hence, the risk of urethane conversion to carcinogenic metabolite increases under regular exposure conditions where lungs are simultaneously exposed to alcohol and cigarette smoke.

To study the role of Srx in lung carcinogenesis, we used the urethane model to mimic lung cancer development in humans. Srx knockout mice were established on an FVB background. Srx knockout mice were completely normal under standard laboratory conditions. We demonstrated that depletion of Srx rendered mice resistant to the urethane-induced lung cancer as Srx null mice showed reduced tumor multiplicity as well as tumor diameter compared to wild type mice. In mechanistic studies, we found that depletion of Srx led to reduction in cell proliferation and increased the rate of intra-tumoral apoptosis. Reduced cell proliferation and increased intra-tumoral apoptosis may contribute to tumor-resistant phenotype of Srx knockout mice. Our findings of the tumor-resistant phenotype of Srx knockout mice may reflect a long-term accumulative effect of urethane exposure. Our findings suggest that Srx is one of the critical components that contribute to mouse lung tumorigenesis *in vivo*. Targeting Srx may thus be used as a novel strategy for lung cancer prevention and/or treatment in the future.

Molecular interaction of individual proteins can regulate a variety of cell signaling processes leading to their role in physiological homeostasis as well as pathological conditions. We used computation methods of homology modeling and protein-protein docking to study the characteristics of Srx-Prx interaction. A great amount of biochemical data related to Srx-Prx interaction is already available. We utilized both experimental and computational prediction data to make a hypothesis that the C-terminal arm of typical 2-Cys Prxs may cause steric hindrance for the Srx access to Prx. The experimental proofs of

demonstrated that the C-terminal arm of Prx is not essential for Srx-Prx binding (**Specific Aim 2**). Experimental evidence from existing literature suggests the similarity in interaction of Srx with all four typical 2-Cys Prxs. However, by virtue of being different proteins of same subfamily, they also have minor differences in their characteristics. Our computational prediction indicated that those minor differences in interaction could be due to different orientation of the C-terminal arm in individual Prxs. To confirm our prediction on steric hindrance and role of Prx C-terminal arm in Srx-Prx interaction, we carried out deletion mutation and tested our hypothesis.

Due to similarities in typical 2-Cys Prx and accepted conventions in the field, we decided to first study the effect of the C-terminal arm of Prx1 on its interaction with Srx. Research in this field clearly establishes that differences in biochemistry of Srx interaction with individual typical 2-Cys Prxs are small and it can be safely assumed to be quite close to interaction characteristics of any other typical 2-Cys Prx. The major differences among the four typical 2-Cys Prxs comes from their subcellular localization rather than their molecular characteristics [30]. The Prx C-terminal arm contains 26 amino acids. Out of those, the initial four are critical for Prx antioxidant function. However, the last 22 amino acids do not affect Prx antioxidant function. Hence, we deleted the last 22 amino acids of the Prx1 C-terminal and studied the effect on Srx-Prx interaction.

The effect of deletion mutation was studied on both the steady-state Srx-Prx interaction as well as kinetics of the Srx-Prx interaction. IP experiments indicated that deletion mutation enhances the steady-state Srx-Prx interaction. However, it

was not clear whether the effect on steady state interaction was due to changes in rate of association or rate of dissociation or both. The SPR results indicated a more than 1,000-fold increase in the association rate constant ( $k_a$ ) after deletion of the C-terminal arm. Higher  $k_a$  is a direct indicator of faster rate of association. Hence, C-terminal arm deletion leads to approximately 1000-fold faster rate of association than Prx1<sup>wildtype</sup>. The deletion mutation resulted in a slight change in dissociation rate constant ( $k_d$ ). The ratio of  $k_d/k_a$  is equal to the equilibrium dissociation rate constant ( $K_D$ ) in SPR. The reciprocal of  $K_D$  is an indicator of affinity of interaction. Hence, lower  $K_D$  indicates better affinity of the Srx-Prx interaction. The deletion mutation reduces the value of  $K_D$  by more than 1000-fold. Hence, Prx1 C-terminal arm deletion results in more than 1000-fold increase in affinity of the Srx-Prx1 interaction.

To further confirm the applicability of these results to other typical 2-Cys Prxs, the effect of the same deletion mutation was studied in Prx4. Considering differences in C-terminal arm orientation (as predicted from homology modeling), we expected that the extent of steric hindrance may be different than what we saw in Prx1. This prediction was confirmed by SPR analysis of Srx interaction with Prx4<sup>wildtype</sup> and Prx4<sup>mutant</sup>. The deletion mutation in Prx4 resulted in roughly 100-fold increase in  $k_a$  with minimal effect on  $k_d$ . Again, the equilibrium dissociation constant ( $K_D$ ) for the Srx-Prx4<sup>mutant</sup> interaction was calculated to be approximately 100 times lower than the  $K_D$  for the Srx-Prx4<sup>wildtype</sup> interaction. Hence, the deletion of the C-terminal arm of Prx affects the rate of the Srx-Prx association and these results can be extrapolated to other typical 2-Cys Prxs. However, the

extent of the effect may be different in different typical 2-Cys Prxs. This data confirms that the C-terminal arm of Prx is present at the Srx-Prx interface and it can cause some steric hindrance for Srx access to Prxs. The crystal structure of Prx show slight conformational change in oxidized state. Srx access to Prx further promotes a conformation change so that Srx can fit in Prx binding site. Taken together, these results give us some insight about molecular characteristics of the Srx-Prx interaction. Hence, this information about the Srx-Prx interaction interface can help in successful designing of targeting strategies to inhibit the Srx-Prx interaction.

Our experimental data along with existing literature helped us to identify the Srx-Prx interaction interface. This interface could be targeted either by targeting the amino acids in Srx chain that are present at interface, or amino acids in Prx chain that are present at interface or dual binders that can bind both amino acids in Srx interface as well as amino acids in Prx interface. Srx has three different sites that can be targeted for inhibition of its enzymatic activity. Those sites include (1) hydrophobic pocket; (2) the ATP and  $Mg^{2+}$  cofactor binding site; and (3) Cys<sup>99</sup> and neighboring amino acids [54, 55, 163]. Considering the factors determining specificity, we defined a complex 3-dimensional target site that included all important amino acid components of hydrophobic pocket (Pro<sup>52</sup>, Leu<sup>82</sup>, Phe<sup>96</sup>, Val<sup>118</sup>, Val<sup>127</sup> and Tyr<sup>128</sup>) along with Cys<sup>99</sup>. Proximity of these amino acids to each other made me believe that it would be a druggable target site. However, druggability of a protein intramolecular target site can be affected by multiple biochemical and structural factors. Therefore, I decided to confirm it with existing

druggable pocket prediction tools, i.e. MetaPocket 2.0 and ConCavity. The druggability of the pocket defined in this study was confirmed by both *in silico* prediction methods. Based on existing literature and earlier experiments, we defined a pocket in the Prx dimer as a target site. However, the Prx binding pocket druggability could not be confirmed using all methods. Considering the narrower Prx pocket and inability to confirm its druggability by prediction method, the chances of false positive in virtual screening was predicted to be high. Virtual screening is not a 100% accurate method and human judgment must be used to improve the chances of success. Both false positive as well as false –ve are high in virtual screening if human judgment is not used. Due to minimal funding available for this study, we decided to confine ourselves to virtual screening against the Srx pocket and use Prx interface only for guidance for inhibition of interaction. The virtual screening using DOCK Blaster and iGEMDOCK helped us in selection of 1,400 hits out of 8,836,468 molecules that were originally screened against Srx. To minimize the number of false positives, we utilized multiple filters related to pharmacokinetic and pharmacodynamic parameters. These filters helped us in minimizing the number to 100 chemicals. However, due to economic constraints and lack of funding we could test only 7 chemicals.

Two of these chemicals (i.e. ZINC64002748 and ISO1) showed acceptable inhibition of Prx-SO<sub>3</sub> reduction at 20 µM concentrations (**Specific Aim 3**). Hence, ZINC64002748 and ISO1 were selected for further *in vitro* testing in cell culture. We next tested the ability of these chemicals to inhibit Srx-Prx and Srx-PrxSO<sub>3</sub> interaction using pull-down assay. Compared to ZINC64002748, ISO1 showed



more significant inhibition of the Prx and Prx-SO<sub>3</sub> pull-down along with Srx. As mentioned earlier, the hydrophobic pocket of Srx is responsible for Srx-Prx binding while Cys<sup>99</sup> (an amino acid outside the hydrophobic pocket) is responsible for enzymatic activity. Hence, Srx enzymatic activity can still be inhibited even if Srx-Prx binding is not affected. Therefore, we decided to further test both the molecules to select one with specific activity.

Earlier publications from our group reported the role of Srx in promoting cell growth and colony formation in NSCLC cell lines [32, 70]. Therefore, we decided to test the effect of these chemicals on cell growth in lung cancer cell lines. For confirming the specificity of effect, we simultaneously tested NSCLC cell lines, SCLC lines, and a lung normal immortalized cell line (BEAS2B cells). Both the chemicals inhibited lung cancer cell growth. The effect was more selective towards inhibition of NSCLC cell lines compared to SCLC or non-cancer lung cell lines. ZINC64002748 showed more potent inhibition of cell growth compared to ISO1. However, the effect of ISO1 was more selective towards NSCLC cell lines. Similarly, on testing in colony formation, both small molecules inhibited anchorage-independent colony formation in A549 cells.

An ideal inhibitor should have higher affinity for the target enzyme compared to its physiological substrate. To compare the affinities, we carried out SPR analyses for the individual chemicals. Both the chemicals showed higher affinity (i.e. lower K<sub>D</sub>) for Srx compared to the Srx affinity for Prx. The affinity of ISO1 was higher for Srx compared to that of ZINC64002748. Another report from our group indicates that the Srx-Prx axis promotes phosphokinase signaling in lung

cancer cells [32]. Therefore, we expected a Srx inhibitor to reduce phosphokinase signaling in a manner similar to that observed in Srx-knockdown cell lines. On comparison of phosphokinase signal (especially p-c-Jun, p-CREB and p-ATF) at individual time-points, we observed significant reduction in phosphokinase signaling in the ISO1 treatment group compared to DMSO (vehicle)-treated control group. ZINC64002748 failed to inhibit phosphokinase signaling in the expected manner.

The results of all experiments discussed so far led us to a conclusion that ISO1 may be a more specific inhibitor of Srx compared to ZINC64002748. Further testing of ISO1 demonstrated its ability to inhibit cell cycle progression. ISO1 reduced the ability of cells to progress to S-phase by slowing down G1 and G2 phases. Similar to Srx-knockdown cells, ISO1 also inhibited tumor cell migration in a wound healing assay. Taken together; ISO1 is a promising molecule that can inhibit Srx. All the tests performed in this study have confirmed specificity of ISO1 mechanism. However, further QSAR studies can help to identify a Srx inhibitor with better efficacy. In the future, more QSAR studies can help to identify a molecule related to ISO1 that has better efficacy of Srx inhibition and better pharmacokinetic profile. ISO1 and other molecules identified using QSAR study can be further explored for their efficacy as a chemotherapeutic molecule in lung cancer.

## 5.2 Conclusions and future directions

Srx plays a critical role in lung carcinogenesis. Hence, it can be explored as a potential target for chemoprevention as well as chemotherapy. The majority of Srx actions are mediated through its interaction with Prx, which is a class of thiol-based antioxidant proteins. Hence, understanding the molecular characteristics of Srx-Prx interaction can help in designing better targeting strategies against the Srx-Prx axis. Our study first demonstrated the oncogenic role of Srx in urethane-induced lung carcinogenesis (**Specific Aim 1**). Next we demonstrated the effect of Prx C-terminal arm on Srx-Prx interaction. This study demonstrated that the Prx C-terminal arm is present at Srx-Prx interface and it can cause steric hindrance for Srx access to Prx (**Specific Aim 2**). Finally, we used *in silico* methods to screen chemical databases and selected a few potential hits that can act as inhibitors of Srx. On testing these molecules *in vitro*, we identified ISO1 as a specific inhibitor of Srx (**Specific Aim 3**). ISO1 showed *in vitro* inhibition of lung cancer cell growth as well as colony formation. However, its *in vivo* efficacy needs to be tested in the future.

In the future, our lab can utilize QSAR approaches to identify a molecule that has better efficacy of Srx-inhibition with better pharmacokinetic profile. These molecules can be tested for their *in vivo* efficacy in chemoprevention and/or chemotherapy.

## APPENDIX 1

### Abbreviations

AP-1	activator protein-1
ATP	adenosine triphosphate
C <sub>P</sub>	peroxidatic cysteine (N-terminal cysteine)
C <sub>R</sub>	resolving cysteine (C-terminal cysteine)
CSC	cigarette smoke condensate
Cys	cysteine
DMSO	dimethyl sulfoxide
EGF	epidermal growth factor
EMT	epithelial-mesenchymal transition
GLC	general ligand coupling chip with compact capacity
GLH	general ligand coupling chip with high capacity
Het	Heterozygous i.e. Srx (+/-)
H&E	hematoxylin and eosin
IP	immunoprecipitation
ISO1	inhibitor of sulfiredoxin oxidoreductase 1
KO	Knockout i.e. Srx (-/-)
Nrf2	Nuclear factor erythroid 2 [NF-E2]-related factor 2
PBS	phosphate buffer saline
PCR	polymerase chain reaction
Prx	peroxiredoxin
PTEN	phosphatase and tensin homolog
PTP1B	protein-tyrosine phosphatase 1B
QSAR	quantitative structure-activity relationship

RIPA	radioimmunoprecipitation assay buffer
RNS	reactive nitrogen species
ROS	reactive oxygen species
RT-PCR	reverse transcription - polymerase chain reaction
SCLC	small cell lung cancer
SPR	surface plasmon resonance
Srx	sulfiredoxin
TGF- $\beta$ 1	transforming growth factor- $\beta$ 1
TPA	12-O-tetradecanoyl-phorbol-13-acetate
TRAIL	tumor necrosis factor-related apoptosis-inducing ligand
Trx	thioredoxin
TUNEL	terminal deoxynucleotidyl transferase-mediated dUTP nick end labeling
Wt	wild type i.e. Srx (+/+)

## APPENDIX 2

### Copyrights

Parts of content (text as well as images) in this dissertation are reproduced from our group publication:

### **The sulfiredoxin-peroxiredoxin (Srx-Prx) axis in cell signal transduction and cancer development**

Mishra M, Jiang H, Wu L, Chawsheen HA, Wei Q.

Cancer Lett. 2015 Oct 1;366(2):150-9. doi: 10.1016/j.canlet.2015.07.002

PMID: 26170166

The journal allows authors to use their work for scholarly sharing (applicable in this case). More details of authors rights can be found on following website:

<https://www.elsevier.com/about/company-information/policies/copyright>

## REFERENCES

- [1] K. Palanivel, V. Kanimozhi, B. Kadalmani, M.A. Akbarsha, Verrucaric acid induces apoptosis through ROS-mediated EGFR/MAPK/Akt signaling pathways in MDA-MB-231 breast cancer cells, *Journal of cellular biochemistry*, (2014).
- [2] Y.I. Oh, J.H. Kim, C.W. Kang, Protective effect of short-term treatment with parathyroid hormone 1-34 on oxidative stress is involved in insulin-like growth factor-I and nuclear factor erythroid 2-related factor 2 in rat bone marrow derived mesenchymal stem cells, *Regulatory peptides*, 189 (2014) 1-10.
- [3] S. Diano, Role of reactive oxygen species in hypothalamic regulation of energy metabolism, *Endocrinology and metabolism*, 28 (2013) 3-5.
- [4] T. Nakamura, D.H. Cho, S.A. Lipton, Redox regulation of protein misfolding, mitochondrial dysfunction, synaptic damage, and cell death in neurodegenerative diseases, *Experimental neurology*, 238 (2012) 12-21.
- [5] L. Rochette, M. Zeller, Y. Cottin, C. Vergely, Diabetes, oxidative stress and therapeutic strategies, *Biochimica et biophysica acta*, 1840 (2014) 2709-2729.
- [6] B. Groitl, U. Jakob, Thiol-based redox switches, *Biochimica et biophysica acta*, 1844 (2014) 1335-1343.
- [7] K. Kim, I.H. Kim, K.Y. Lee, S.G. Rhee, E.R. Stadtman, The isolation and purification of a specific "protector" protein which inhibits enzyme inactivation by a thiol/Fe(III)/O<sub>2</sub> mixed-function oxidation system, *The Journal of biological chemistry*, 263 (1988) 4704-4711.
- [8] Y.S. Lim, M.K. Cha, H.K. Kim, T.B. Uhm, J.W. Park, K. Kim, I.H. Kim, Removals of hydrogen peroxide and hydroxyl radical by thiol-specific antioxidant protein as a possible role in vivo, *Biochemical and biophysical research communications*, 192 (1993) 273-280.
- [9] M.K. Cha, H.K. Kim, I.H. Kim, Thioredoxin-linked "thiol peroxidase" from periplasmic space of *Escherichia coli*, *The Journal of biological chemistry*, 270 (1995) 28635-28641.
- [10] S. Ichimiya, J.G. Davis, D.M. O'Rourke, M. Katsumata, M.I. Greene, Murine thioredoxin peroxidase delays neuronal apoptosis and is expressed in areas of the brain most susceptible to hypoxic and ischemic injury, *DNA and cell biology*, 16 (1997) 311-321.
- [11] R.A. Stacy, E. Munthe, T. Steinum, B. Sharma, R.B. Aalen, A peroxiredoxin antioxidant is encoded by a dormancy-related gene, *Per1*, expressed during late development in the aleurone and embryo of barley grains, *Plant molecular biology*, 31 (1996) 1205-1216.
- [12] Y. Zhou, X.Y. Wan, H.L. Wang, Z.Y. Yan, Y.D. Hou, D.Y. Jin, Bacterial scavengase p20 is structurally and functionally related to peroxiredoxins, *Biochemical and biophysical research communications*, 233 (1997) 848-852.
- [13] P. Dammeyer, E.S. Arner, Human Protein Atlas of redox systems - what can be learnt?, *Biochimica et biophysica acta*, 1810 (2011) 111-138.
- [14] E.M. Hanschmann, J.R. Godoy, C. Berndt, C. Hudemann, C.H. Lillig, Thioredoxins, glutaredoxins, and peroxiredoxins--molecular mechanisms and

health significance: from cofactors to antioxidants to redox signaling, *Antioxidants & redox signaling*, 19 (2013) 1539-1605.

[15] S.G. Rhee, S.W. Kang, T.S. Chang, W. Jeong, K. Kim, Peroxiredoxin, a novel family of peroxidases, *IUBMB life*, 52 (2001) 35-41.

[16] E.S. Arner, A. Holmgren, Physiological functions of thioredoxin and thioredoxin reductase, *European journal of biochemistry / FEBS*, 267 (2000) 6102-6109.

[17] K.J. Dietz, Plant peroxiredoxins, *Annual review of plant biology*, 54 (2003) 93-107.

[18] A. Zeida, A.M. Reyes, M.C. Lebrero, R. Radi, M. Trujillo, D.A. Estrin, The extraordinary catalytic ability of peroxiredoxins: a combined experimental and QM/MM study on the fast thiol oxidation step, *Chemical communications*, 50 (2014) 10070-10073.

[19] C.C. Winterbourn, The biological chemistry of hydrogen peroxide, *Methods in enzymology*, 528 (2013) 3-25.

[20] T. Rabilloud, M. Heller, F. Gasnier, S. Luche, C. Rey, R. Aebersold, M. Benahmed, P. Louisot, J. Lunardi, Proteomics analysis of cellular response to oxidative stress. Evidence for in vivo overoxidation of peroxiredoxins at their active site, *The Journal of biological chemistry*, 277 (2002) 19396-19401.

[21] M.B. Pascual, A. Mata-Cabana, F.J. Florencio, M. Lindahl, F.J. Cejudo, Overoxidation of 2-Cys peroxiredoxin in prokaryotes: cyanobacterial 2-Cys peroxiredoxins sensitive to oxidative stress, *The Journal of biological chemistry*, 285 (2010) 34485-34492.

[22] H.H. Jang, K.O. Lee, Y.H. Chi, B.G. Jung, S.K. Park, J.H. Park, J.R. Lee, S.S. Lee, J.C. Moon, J.W. Yun, Y.O. Choi, W.Y. Kim, J.S. Kang, G.W. Cheong, D.J. Yun, S.G. Rhee, M.J. Cho, S.Y. Lee, Two enzymes in one; two yeast peroxiredoxins display oxidative stress-dependent switching from a peroxidase to a molecular chaperone function, *Cell*, 117 (2004) 625-635.

[23] M.H. Chuang, M.S. Wu, W.L. Lo, J.T. Lin, C.H. Wong, S.H. Chiou, The antioxidant protein alkylhydroperoxide reductase of *Helicobacter pylori* switches from a peroxide reductase to a molecular chaperone function, *Proceedings of the National Academy of Sciences of the United States of America*, 103 (2006) 2552-2557.

[24] B. Biteau, J. Labarre, M.B. Toledano, ATP-dependent reduction of cysteine-sulphinic acid by *S. cerevisiae* sulphiredoxin, *Nature*, 425 (2003) 980-984.

[25] C.A. Tairum, Jr., M.A. de Oliveira, B.B. Horta, F.J. Zara, L.E. Netto, Disulfide biochemistry in 2-cys peroxiredoxin: requirement of Glu50 and Arg146 for the reduction of yeast Tsa1 by thioredoxin, *Journal of molecular biology*, 424 (2012) 28-41.

[26] X. Roussel, G. Bechade, A. Kriznik, A. Van Dorselaer, S. Sanglier-Cianferani, G. Branlant, S. Rahuel-Clermont, Evidence for the formation of a covalent thiosulfinate intermediate with peroxiredoxin in the catalytic mechanism of sulfiredoxin, *J Biol Chem*, 283 (2008) 22371-22382.

[27] M.K. Basu, E.V. Koonin, Evolution of eukaryotic cysteine sulfinic acid reductase, sulfiredoxin (Srx), from bacterial chromosome partitioning protein ParB, *Cell cycle*, 4 (2005) 947-952.



- [28] P. Maindola, R. Raina, P. Goyal, K. Atmakuri, A. Ojha, S. Gupta, P.J. Christie, L.M. Iyer, L. Aravind, A. Arockiasamy, Multiple enzymatic activities of ParB/Srx superfamily mediate sexual conflict among conjugative plasmids, *Nature communications*, 5 (2014) 5322.
- [29] T.S. Chang, W. Jeong, H.A. Woo, S.M. Lee, S. Park, S.G. Rhee, Characterization of mammalian sulfiredoxin and its reactivation of hyperoxidized peroxiredoxin through reduction of cysteine sulfinic acid in the active site to cysteine, *The Journal of biological chemistry*, 279 (2004) 50994-51001.
- [30] Y.H. Noh, J.Y. Baek, W. Jeong, S.G. Rhee, T.S. Chang, Sulfiredoxin Translocation into Mitochondria Plays a Crucial Role in Reducing Hyperoxidized Peroxiredoxin III, *The Journal of biological chemistry*, 284 (2009) 8470-8477.
- [31] I.S. Kil, K.W. Ryu, S.K. Lee, J.Y. Kim, S.Y. Chu, J.H. Kim, S. Park, S.G. Rhee, Circadian Oscillation of Sulfiredoxin in the Mitochondria, *Molecular cell*, 59 (2015) 651-663.
- [32] Q. Wei, H. Jiang, Z. Xiao, A. Baker, M.R. Young, T.D. Veenstra, N.H. Colburn, Sulfiredoxin-Peroxiredoxin IV axis promotes human lung cancer progression through modulation of specific phosphokinase signaling, *Proceedings of the National Academy of Sciences of the United States of America*, 108 (2011) 7004-7009.
- [33] T.H. Kim, J. Song, S.R. Alcantara Llaguno, E. Murnan, S. Liyanarachchi, K. Palanichamy, J.Y. Yi, M.S. Viapiano, I. Nakano, S.O. Yoon, H. Wu, L.F. Parada, C.H. Kwon, Suppression of peroxiredoxin 4 in glioblastoma cells increases apoptosis and reduces tumor growth, *PloS one*, 7 (2012) e42818.
- [34] Q. Wei, H. Jiang, A. Baker, L.K. Dodge, M. Gerard, M.R. Young, M.B. Toledano, N.H. Colburn, Loss of sulfiredoxin renders mice resistant to azoxymethane/dextran sulfate sodium-induced colon carcinogenesis, *Carcinogenesis*, 34 (2013) 1403-1410.
- [35] R. Ummanni, F. Barreto, S. Venz, C. Scharf, C. Barrett, H.A. Mannsperger, J.C. Brase, R. Kuner, T. Schlomm, G. Sauter, H. Sultmann, U. Korf, C. Bokemeyer, R. Walther, T.H. Brummendorf, S. Balabanov, Peroxiredoxins 3 and 4 are overexpressed in prostate cancer tissue and affect the proliferation of prostate cancer cells in vitro, *Journal of proteome research*, 11 (2012) 2452-2466.
- [36] L. Li, W. Shoji, H. Takano, N. Nishimura, Y. Aoki, R. Takahashi, S. Goto, T. Kaifu, T. Takai, M. Obinata, Increased susceptibility of MER5 (peroxiredoxin III) knockout mice to LPS-induced oxidative stress, *Biochemical and biophysical research communications*, 355 (2007) 715-721.
- [37] Y. Iuchi, F. Okada, S. Tsunoda, N. Kibe, N. Shirasawa, M. Ikawa, M. Okabe, Y. Ikeda, J. Fujii, Peroxiredoxin 4 knockout results in elevated spermatogenic cell death via oxidative stress, *The Biochemical journal*, 419 (2009) 149-158.
- [38] C.A. Neumann, D.S. Krause, C.V. Carman, S. Das, D.P. Dubey, J.L. Abraham, R.T. Bronson, Y. Fujiwara, S.H. Orkin, R.A. Van Etten, Essential role for the peroxiredoxin Prdx1 in erythrocyte antioxidant defence and tumour suppression, *Nature*, 424 (2003) 561-565.
- [39] T.H. Lee, S.U. Kim, S.L. Yu, S.H. Kim, D.S. Park, H.B. Moon, S.H. Dho, K.S. Kwon, H.J. Kwon, Y.H. Han, S. Jeong, S.W. Kang, H.S. Shin, K.K. Lee, S.G.

- Rhee, D.Y. Yu, Peroxiredoxin II is essential for sustaining life span of erythrocytes in mice, *Blood*, 101 (2003) 5033-5038.
- [40] X. Hu, Z. Weng, C.T. Chu, L. Zhang, G. Cao, Y. Gao, A. Signore, J. Zhu, T. Hastings, J.T. Greenamyre, J. Chen, Peroxiredoxin-2 protects against 6-hydroxydopamine-induced dopaminergic neurodegeneration via attenuation of the apoptosis signal-regulating kinase (ASK1) signaling cascade, *The Journal of neuroscience : the official journal of the Society for Neuroscience*, 31 (2011) 247-261.
- [41] Y. Yoshida, A. Yoshikawa, T. Kinumi, Y. Ogawa, Y. Saito, K. Ohara, H. Yamamoto, Y. Imai, E. Niki, Hydroxyoctadecadienoic acid and oxidatively modified peroxiredoxins in the blood of Alzheimer's disease patients and their potential as biomarkers, *Neurobiology of aging*, 30 (2009) 174-185.
- [42] L. Chen, R. Na, M. Gu, A.B. Salmon, Y. Liu, H. Liang, W. Qi, H. Van Remmen, A. Richardson, Q. Ran, Reduction of mitochondrial H<sub>2</sub>O<sub>2</sub> by overexpressing peroxiredoxin 3 improves glucose tolerance in mice, *Aging cell*, 7 (2008) 866-878.
- [43] E. Zeldich, C.D. Chen, T.A. Colvin, E.A. Bove-Fenderson, J. Liang, T.B. Tucker Zhou, D.A. Harris, C.R. Abraham, The neuroprotective effect of Klotho is mediated via regulation of members of the redox system, *The Journal of biological chemistry*, 289 (2014) 24700-24715.
- [44] V.J. Findlay, H. Tapiero, D.M. Townsend, Sulfiredoxin: a potential therapeutic agent?, *Biomedicine & pharmacotherapy = Biomedecine & pharmacotherapie*, 59 (2005) 374-379.
- [45] V.J. Findlay, D.M. Townsend, T.E. Morris, J.P. Fraser, L. He, K.D. Tew, A novel role for human sulfiredoxin in the reversal of glutathionylation, *Cancer research*, 66 (2006) 6800-6806.
- [46] A. Perkins, L.B. Poole, P.A. Karplus, Tuning of Peroxiredoxin Catalysis for Various Physiological Roles, *Biochemistry*, (2014).
- [47] H.A. Woo, W. Jeong, T.S. Chang, K.J. Park, S.J. Park, J.S. Yang, S.G. Rhee, Reduction of cysteine sulfinic acid by sulfiredoxin is specific to 2-cys peroxiredoxins, *The Journal of biological chemistry*, 280 (2005) 3125-3128.
- [48] X. Roussel, A. Kriznik, C. Richard, S. Rahuel-Clermont, G. Branlant, Catalytic mechanism of Sulfiredoxin from *Saccharomyces cerevisiae* passes through an oxidized disulfide sulfiredoxin intermediate that is reduced by thioredoxin, *The Journal of biological chemistry*, 284 (2009) 33048-33055.
- [49] S. Boukhenouna, H. Mazon, G. Branlant, C. Jacob, M.B. Toledano, S. Rahuel-Clermont, Evidence that glutathione and the glutathione system efficiently recycle 1-cys sulfiredoxin in vivo, *Antioxidants & redox signaling*, 22 (2015) 731-743.
- [50] J.C. Moon, G.M. Kim, E.K. Kim, H.N. Lee, B. Ha, S.Y. Lee, H.H. Jang, Reversal of 2-Cys peroxiredoxin oligomerization by sulfiredoxin, *Biochemical and biophysical research communications*, 432 (2013) 291-295.
- [51] H.Z. Chae, H. Oubrahim, J.W. Park, S.G. Rhee, P.B. Chock, Protein glutathionylation in the regulation of peroxiredoxins: a family of thiol-specific peroxidases that function as antioxidants, molecular chaperones, and signal modulators, *Antioxidants & redox signaling*, 16 (2012) 506-523.

- [52] R.R. Bowers, Y. Manevich, D.M. Townsend, K.D. Tew, Sulfiredoxin redox-sensitive interaction with S100A4 and non-muscle myosin IIA regulates cancer cell motility, *Biochemistry*, 51 (2012) 7740-7754.
- [53] J.W. Park, J.J. Mieyal, S.G. Rhee, P.B. Chock, Deglutathionylation of 2-Cys peroxiredoxin is specifically catalyzed by sulfiredoxin, *The Journal of biological chemistry*, 284 (2009) 23364-23374.
- [54] T.J. Jonsson, M.S. Murray, L.C. Johnson, L.B. Poole, W.T. Lowther, Structural basis for the retroreduction of inactivated peroxiredoxins by human sulfiredoxin, *Biochemistry*, 44 (2005) 8634-8642.
- [55] T.J. Jonsson, L.C. Johnson, W.T. Lowther, Protein engineering of the quaternary sulfiredoxin.peroxiredoxin enzyme.substrate complex reveals the molecular basis for cysteine sulfinic acid phosphorylation, *The Journal of biological chemistry*, 284 (2009) 33305-33310.
- [56] W. Lee, K.S. Choi, J. Riddell, C. Ip, D. Ghosh, J.H. Park, Y.M. Park, Human peroxiredoxin 1 and 2 are not duplicate proteins: the unique presence of CYS83 in Prx1 underscores the structural and functional differences between Prx1 and Prx2, *The Journal of biological chemistry*, 282 (2007) 22011-22022.
- [57] T. Matsumura, K. Okamoto, S. Iwahara, H. Hori, Y. Takahashi, T. Nishino, Y. Abe, Dimer-oligomer interconversion of wild-type and mutant rat 2-Cys peroxiredoxin: disulfide formation at dimer-dimer interfaces is not essential for decamerization, *The Journal of biological chemistry*, 283 (2008) 284-293.
- [58] A. Echalié, X. Trivelli, C. Corbier, N. Rouhier, O. Walker, P. Tsan, J.P. Jacquot, A. Aubry, I. Krimm, J.M. Lancelin, Crystal structure and solution NMR dynamics of a D (type II) peroxiredoxin glutaredoxin and thioredoxin dependent: a new insight into the peroxiredoxin oligomerism, *Biochemistry*, 44 (2005) 1755-1767.
- [59] Z.A. Wood, L.B. Poole, P.A. Karplus, Peroxiredoxin evolution and the regulation of hydrogen peroxide signaling, *Science*, 300 (2003) 650-653.
- [60] A. Hall, P.A. Karplus, L.B. Poole, Typical 2-Cys peroxiredoxins--structures, mechanisms and functions, *The FEBS journal*, 276 (2009) 2469-2477.
- [61] J.R. Harris, E. Schroder, M.N. Isupov, D. Scheffler, P. Kristensen, J.A. Littlechild, A.A. Vagin, U. Meissner, Comparison of the decameric structure of peroxiredoxin-II by transmission electron microscopy and X-ray crystallography, *Biochimica et biophysica acta*, 1547 (2001) 221-234.
- [62] F. Angelucci, F. Saccoccia, M. Ardini, G. Boumis, M. Brunori, L. Di Leandro, R. Ippoliti, A.E. Miele, G. Natoli, S. Scotti, A. Bellelli, Switching between the alternative structures and functions of a 2-Cys peroxiredoxin, by site-directed mutagenesis, *Journal of molecular biology*, 425 (2013) 4556-4568.
- [63] A.C. Haynes, J. Qian, J.A. Reisz, C.M. Furdai, W.T. Lowther, Molecular basis for the resistance of human mitochondrial 2-Cys peroxiredoxin 3 to hyperoxidation, *The Journal of biological chemistry*, 288 (2013) 29714-29723.
- [64] A. Hall, D. Parsonage, L.B. Poole, P.A. Karplus, Structural evidence that peroxiredoxin catalytic power is based on transition-state stabilization, *Journal of molecular biology*, 402 (2010) 194-209.
- [65] Ensembl Genome Browser [www.ensembl.org/index.html](http://www.ensembl.org/index.html).

- [66] W.R. Pearson, BLAST and FASTA similarity searching for multiple sequence alignment, *Methods in molecular biology*, 1079 (2014) 75-101.
- [67] Oncomine [www.oncomine.org](http://www.oncomine.org).
- [68] F.X. Soriano, F. Leveille, S. Papadia, L.G. Higgins, J. Varley, P. Baxter, J.D. Hayes, G.E. Hardingham, Induction of sulfiredoxin expression and reduction of peroxiredoxin hyperoxidation by the neuroprotective Nrf2 activator 3H-1,2-dithiole-3-thione, *Journal of neurochemistry*, 107 (2008) 533-543.
- [69] F.X. Soriano, P. Baxter, L.M. Murray, M.B. Sporn, T.H. Gillingwater, G.E. Hardingham, Transcriptional regulation of the AP-1 and Nrf2 target gene sulfiredoxin, *Molecules and cells*, 27 (2009) 279-282.
- [70] Q. Wei, H. Jiang, C.P. Matthews, N.H. Colburn, Sulfiredoxin is an AP-1 target gene that is required for transformation and shows elevated expression in human skin malignancies, *Proceedings of the National Academy of Sciences of the United States of America*, 105 (2008) 19738-19743.
- [71] K. Abbas, S. Riquier, J.C. Drapier, Peroxiredoxins and sulfiredoxin at the crossroads of the NO and H<sub>2</sub>O<sub>2</sub> signaling pathways, *Methods in enzymology*, 527 (2013) 113-128.
- [72] H. Kim, Y. Jung, B.S. Shin, H. Kim, H. Song, S.H. Bae, S.G. Rhee, W. Jeong, Redox regulation of lipopolysaccharide-mediated sulfiredoxin induction, which depends on both AP-1 and Nrf2, *The Journal of biological chemistry*, 285 (2010) 34419-34428.
- [73] M. Molin, J. Yang, S. Hanzen, M.B. Toledano, J. Labarre, T. Nystrom, Life span extension and H<sub>2</sub>O<sub>2</sub> resistance elicited by caloric restriction require the peroxiredoxin Tsa1 in *Saccharomyces cerevisiae*, *Molecular cell*, 43 (2011) 823-833.
- [74] Y.S. Kim, H.L. Lee, K.B. Lee, J.H. Park, W.Y. Chung, K.S. Lee, S.S. Sheen, K.J. Park, S.C. Hwang, Nuclear factor E2-related factor 2 dependent overexpression of sulfiredoxin and peroxiredoxin III in human lung cancer, *The Korean journal of internal medicine*, 26 (2011) 304-313.
- [75] H. Merikallio, P. Paakko, V.L. Kinnula, T. Harju, Y. Soini, Nuclear factor erythroid-derived 2-like 2 (Nrf2) and DJ1 are prognostic factors in lung cancer, *Human pathology*, 43 (2012) 577-584.
- [76] Y. Soini, M. Eskelinen, P. Juvonen, V. Karja, K.M. Haapasaari, A. Saarela, P. Karihtala, Nuclear Nrf2 expression is related to a poor survival in pancreatic adenocarcinoma, *Pathology, research and practice*, 210 (2014) 35-39.
- [77] B. Seliger, S.P. Dressler, C. Massa, C.V. Recktenwald, F. Altenberend, J. Bukur, F.M. Marincola, E. Wang, S. Stevanovic, R. Lichtenfels, Identification and characterization of human leukocyte antigen class I ligands in renal cell carcinoma cells, *Proteomics*, 11 (2011) 2528-2541.
- [78] L. Wu, H. Jiang, H.A. Chawsheen, M. Mishra, M.R. Young, M. Gerard, M.B. Toledano, N.H. Colburn, Q. Wei, Tumor promoter-induced sulfiredoxin is required for mouse skin tumorigenesis, *Carcinogenesis*, 35 (2014) 1177-1184.
- [79] Z.A. Wood, E. Schroder, J. Robin Harris, L.B. Poole, Structure, mechanism and regulation of peroxiredoxins, *Trends Biochem Sci*, 28 (2003) 32-40.

- [80] Y.J. Kim, J.Y. Ahn, P. Liang, C. Ip, Y. Zhang, Y.M. Park, Human prx1 gene is a target of Nrf2 and is up-regulated by hypoxia/reoxygenation: implication to tumor biology, *Cancer research*, 67 (2007) 546-554.
- [81] D.M. McKean, L. Sisbarro, D. Ilic, N. Kaplan-Alburquerque, R. Nemenoff, M. Weiser-Evans, M.J. Kern, P.L. Jones, FAK induces expression of Prx1 to promote tenascin-C-dependent fibroblast migration, *The Journal of cell biology*, 161 (2003) 393-402.
- [82] J. Uwayama, A. Hirayama, T. Yanagawa, E. Warabi, R. Sugimoto, K. Itoh, M. Yamamoto, H. Yoshida, A. Koyama, T. Ishii, Tissue Prx I in the protection against Fe-NTA and the reduction of nitroxyl radicals, *Biochemical and biophysical research communications*, 339 (2006) 226-231.
- [83] J. Cao, J. Schulte, A. Knight, N.R. Leslie, A. Zagozdzon, R. Bronson, Y. Manevich, C. Beeson, C.A. Neumann, Prdx1 inhibits tumorigenesis via regulating PTEN/AKT activity, *The EMBO journal*, 28 (2009) 1505-1517.
- [84] Y.Y. Huo, G. Li, R.F. Duan, Q. Gou, C.L. Fu, Y.C. Hu, B.Q. Song, Z.H. Yang, D.C. Wu, P.K. Zhou, PTEN deletion leads to deregulation of antioxidants and increased oxidative damage in mouse embryonic fibroblasts, *Free radical biology & medicine*, 44 (2008) 1578-1591.
- [85] Y.H. Park, S.U. Kim, B.K. Lee, H.S. Kim, I.S. Song, H.J. Shin, Y.H. Han, K.T. Chang, J.M. Kim, D.S. Lee, Y.H. Kim, C.M. Choi, B.Y. Kim, D.Y. Yu, Prx I suppresses K-ras-driven lung tumorigenesis by opposing redox-sensitive ERK/cyclin D1 pathway, *Antioxidants & redox signaling*, 19 (2013) 482-496.
- [86] H. Jiang, L. Wu, M. Mishra, H.A. Chawsheen, Q. Wei, Expression of peroxiredoxin 1 and 4 promotes human lung cancer malignancy, *American journal of cancer research*, 4 (2014) 445-460.
- [87] I. Hoshino, H. Matsubara, N. Hanari, M. Mori, T. Nishimori, Y. Yoneyama, Y. Akutsu, H. Sakata, K. Matsushita, N. Seki, T. Ochiai, Histone deacetylase inhibitor FK228 activates tumor suppressor Prdx1 with apoptosis induction in esophageal cancer cells, *Clinical cancer research : an official journal of the American Association for Cancer Research*, 11 (2005) 7945-7952.
- [88] R. Godfrey, D. Arora, R. Bauer, S. Stopp, J.P. Muller, T. Heinrich, S.A. Bohmer, M. Dagnell, U. Schnetzke, S. Scholl, A. Ostman, F.D. Bohmer, Cell transformation by FLT3 ITD in acute myeloid leukemia involves oxidative inactivation of the tumor suppressor protein-tyrosine phosphatase DEP-1/PTPRJ, *Blood*, 119 (2012) 4499-4511.
- [89] J.R. Riddell, P. Maier, S.N. Sass, M.T. Moser, B.A. Foster, S.O. Gollnick, Peroxiredoxin 1 stimulates endothelial cell expression of VEGF via TLR4 dependent activation of HIF-1alpha, *PLoS one*, 7 (2012) e50394.
- [90] J.R. Riddell, W. Bshara, M.T. Moser, J.A. Spornyak, B.A. Foster, S.O. Gollnick, Peroxiredoxin 1 controls prostate cancer growth through Toll-like receptor 4-dependent regulation of tumor vasculature, *Cancer research*, 71 (2011) 1637-1646.
- [91] P. Ren, H. Ye, L. Dai, M. Liu, X. Liu, Y. Chai, Q. Shao, Y. Li, N. Lei, B. Peng, W. Yao, J. Zhang, Peroxiredoxin 1 is a tumor-associated antigen in esophageal squamous cell carcinoma, *Oncology reports*, 30 (2013) 2297-2303.

- [92] G.L. Maxwell, B.L. Hood, R. Day, U. Chandran, D. Kirchner, V.S. Kolli, N.W. Bateman, J. Allard, C. Miller, M. Sun, M.S. Flint, C. Zahn, J. Oliver, S. Banerjee, T. Litzi, A. Parwani, G. Sandburg, S. Rose, M.J. Becich, A. Berchuck, E. Kohn, J.I. Risinger, T.P. Conrads, Proteomic analysis of stage I endometrial cancer tissue: identification of proteins associated with oxidative processes and inflammation, *Gynecologic oncology*, 121 (2011) 586-594.
- [93] I.S. Song, S.U. Kim, N.S. Oh, J. Kim, D.Y. Yu, S.M. Huang, J.M. Kim, D.S. Lee, N.S. Kim, Peroxiredoxin I contributes to TRAIL resistance through suppression of redox-sensitive caspase activation in human hepatoma cells, *Carcinogenesis*, 30 (2009) 1106-1114.
- [94] G. Wu, Z. Ji, H. Li, Y. Lei, X. Jin, Y. Yu, M. Sun, Selective TRAIL-induced cytotoxicity to lung cancer cells mediated by miRNA response elements, *Cell biochemistry and function*, (2014).
- [95] M.C. Gao, X.D. Jia, Q.F. Wu, Y. Cheng, F.R. Chen, J. Zhang, Silencing Prx1 and/or Prx5 sensitizes human esophageal cancer cells to ionizing radiation and increases apoptosis via intracellular ROS accumulation, *Acta pharmacologica Sinica*, 32 (2011) 528-536.
- [96] Z. Wang, Y. Cheng, N. Wang, D.M. Wang, Y.W. Li, F. Han, J.G. Shen, P. Yang de, X.Y. Guan, J.P. Chen, Dioscin induces cancer cell apoptosis through elevated oxidative stress mediated by downregulation of peroxiredoxins, *Cancer biology & therapy*, 13 (2012) 138-147.
- [97] B. Ha, E.K. Kim, J.H. Kim, H.N. Lee, K.O. Lee, S.Y. Lee, H.H. Jang, Human peroxiredoxin 1 modulates TGF-beta1-induced epithelial-mesenchymal transition through its peroxidase activity, *Biochemical and biophysical research communications*, 421 (2012) 33-37.
- [98] K.H. Zhang, H.Y. Tian, X. Gao, W.W. Lei, Y. Hu, D.M. Wang, X.C. Pan, M.L. Yu, G.J. Xu, F.K. Zhao, J.G. Song, Ferritin heavy chain-mediated iron homeostasis and subsequent increased reactive oxygen species production are essential for epithelial-mesenchymal transition, *Cancer research*, 69 (2009) 5340-5348.
- [99] M.C. Sobotta, W. Liou, S. Stocker, D. Talwar, M. Oehler, T. Ruppert, A.N. Scharf, T.P. Dick, Peroxiredoxin-2 and STAT3 form a redox relay for HO signaling, *Nature chemical biology*, (2014).
- [100] J.S. O'Neill, A.B. Reddy, Circadian clocks in human red blood cells, *Nature*, 469 (2011) 498-503.
- [101] C.S. Cho, H.J. Yoon, J.Y. Kim, H.A. Woo, S.G. Rhee, Circadian rhythm of hyperoxidized peroxiredoxin II is determined by hemoglobin autoxidation and the 20S proteasome in red blood cells, *Proceedings of the National Academy of Sciences of the United States of America*, 111 (2014) 12043-12048.
- [102] J. Furuta, Y. Nobeyama, Y. Umebayashi, F. Otsuka, K. Kikuchi, T. Ushijima, Silencing of Peroxiredoxin 2 and aberrant methylation of 33 CpG islands in putative promoter regions in human malignant melanomas, *Cancer research*, 66 (2006) 6080-6086.
- [103] A.C. Barbosa, N. Funato, S. Chapman, M.D. McKee, J.A. Richardson, E.N. Olson, H. Yanagisawa, Hand transcription factors cooperatively regulate

- development of the distal midline mesenchyme, *Developmental biology*, 310 (2007) 154-168.
- [104] Y. Qi, J.F. Chiu, L. Wang, D.L. Kwong, Q.Y. He, Comparative proteomic analysis of esophageal squamous cell carcinoma, *Proteomics*, 5 (2005) 2960-2971.
- [105] J. Shen, M.D. Person, J. Zhu, J.L. Abbruzzese, D. Li, Protein expression profiles in pancreatic adenocarcinoma compared with normal pancreatic tissue and tissue affected by pancreatitis as detected by two-dimensional gel electrophoresis and mass spectrometry, *Cancer research*, 64 (2004) 9018-9026.
- [106] L.M. Randall, B. Manta, M. Hugo, M. Gil, C. Batthyany, M. Trujillo, L.B. Poole, A. Denicola, Nitration Transforms a Sensitive Peroxiredoxin 2 into a More Active and Robust Peroxidase, *The Journal of biological chemistry*, 289 (2014) 15536-15543.
- [107] S. Salzano, P. Checconi, E.M. Hanschmann, C.H. Lillig, L.D. Bowler, P. Chan, D. Vaudry, M. Mengozzi, L. Coppo, S. Sacre, K.R. Atkuri, B. Sahaf, L.A. Herzenberg, L.A. Herzenberg, L. Mullen, P. Ghezzi, Linkage of inflammation and oxidative stress via release of glutathionylated peroxiredoxin-2, which acts as a danger signal, *Proceedings of the National Academy of Sciences of the United States of America*, 111 (2014) 12157-12162.
- [108] D. Ji, M. Li, T. Zhan, Y. Yao, J. Shen, H. Tian, Z. Zhang, J. Gu, Prognostic role of serum AZGP1, PEDF and PRDX2 in colorectal cancer patients, *Carcinogenesis*, 34 (2013) 1265-1272.
- [109] K.A. Lee, J.W. Kang, J.H. Shim, C.W. Kho, S.G. Park, H.G. Lee, S.G. Paik, J.S. Lim, D.Y. Yoon, Protein profiling and identification of modulators regulated by human papillomavirus 16 E7 oncogene in HaCaT keratinocytes by proteomics, *Gynecologic oncology*, 99 (2005) 142-152.
- [110] M.I. Lomnytska, S. Becker, I. Bodin, A. Olsson, K. Hellman, A.C. Hellstrom, M. Mints, U. Hellman, G. Auer, S. Andersson, Differential expression of ANXA6, HSP27, PRDX2, NCF2, and TPM4 during uterine cervix carcinogenesis: diagnostic and prognostic value, *British journal of cancer*, 104 (2011) 110-119.
- [111] V. Stresing, E. Baltziskueta, N. Rubio, J. Blanco, M.C. Arriba, J. Valls, M. Janier, P. Clezardin, R. Sanz-Pamplona, C. Nieva, M. Marro, D. Petrov, A. Sierra, Peroxiredoxin 2 specifically regulates the oxidative and metabolic stress response of human metastatic breast cancer cells in lungs, *Oncogene*, 32 (2013) 724-735.
- [112] D.J. Lee, D.H. Kang, M. Choi, Y.J. Choi, J.Y. Lee, J.H. Park, Y.J. Park, K.W. Lee, S.W. Kang, Peroxiredoxin-2 represses melanoma metastasis by increasing E-Cadherin/beta-Catenin complexes in adherens junctions, *Cancer research*, 73 (2013) 4744-4757.
- [113] J. Feng, Z. Fu, J. Guo, W. Lu, K. Wen, W. Chen, H. Wang, J. Wei, S. Zhang, Overexpression of peroxiredoxin 2 inhibits TGF-beta1-induced epithelial-mesenchymal transition and cell migration in colorectal cancer, *Molecular medicine reports*, 10 (2014) 867-873.
- [114] Y. Olmos, F.J. Sanchez-Gomez, B. Wild, N. Garcia-Quintans, S. Cabezudo, S. Lamas, M. Monsalve, SirT1 regulation of antioxidant genes is

dependent on the formation of a FoxO3a/PGC-1alpha complex, *Antioxidants & redox signaling*, 19 (2013) 1507-1521.

[115] C.A. Wood-Allum, S.C. Barber, J. Kirby, P. Heath, H. Holden, R. Mead, A. Higginbottom, S. Allen, T. Beaujeux, S.E. Alexson, P.G. Ince, P.J. Shaw, Impairment of mitochondrial anti-oxidant defence in SOD1-related motor neuron injury and amelioration by ebselen, *Brain : a journal of neurology*, 129 (2006) 1693-1709.

[116] D.R. Wonsey, K.I. Zeller, C.V. Dang, The c-Myc target gene PRDX3 is required for mitochondrial homeostasis and neoplastic transformation, *Proceedings of the National Academy of Sciences of the United States of America*, 99 (2002) 6649-6654.

[117] K.K. Li, J.C. Pang, K.M. Lau, L. Zhou, Y. Mao, Y. Wang, W.S. Poon, H.K. Ng, MiR-383 is downregulated in medulloblastoma and targets peroxiredoxin 3 (PRDX3), *Brain pathology*, 23 (2013) 413-425.

[118] J.X. Hu, Q. Gao, L. Li, Peroxiredoxin 3 is a novel marker for cell proliferation in cervical cancer, *Biomedical reports*, 1 (2013) 228-230.

[119] M. Safaeian, A. Hildesheim, P. Gonzalez, K. Yu, C. Porras, Q. Li, A.C. Rodriguez, M.E. Sherman, M. Schiffman, S. Wacholder, R. Burk, R. Herrero, L. Burdette, S.J. Chanock, S.S. Wang, Single nucleotide polymorphisms in the PRDX3 and RPS19 and risk of HPV persistence and cervical precancer/cancer, *PloS one*, 7 (2012) e33619.

[120] H. Roumes, A. Pires-Alves, L. Gonthier-Maurin, E. Dargelos, P. Cottin, Investigation of peroxiredoxin IV as a calpain-regulated pathway in cancer, *Anticancer research*, 30 (2010) 5085-5089.

[121] L. Zhu, K. Yang, X. Wang, X. Wang, C.C. Wang, A novel reaction of peroxiredoxin 4 towards substrates in oxidative protein folding, *PloS one*, 9 (2014) e105529.

[122] I. Mehmeti, S. Lortz, M. Elsner, S. Lenzen, Peroxiredoxin 4 improves insulin biosynthesis and glucose-induced insulin secretion in insulin-secreting INS-1E cells, *The Journal of biological chemistry*, 289 (2014) 26904-26913.

[123] C. Pritchard, B. Mecham, R. Dumpit, I. Coleman, M. Bhattacharjee, Q. Chen, R.A. Sikes, P.S. Nelson, Conserved gene expression programs integrate mammalian prostate development and tumorigenesis, *Cancer research*, 69 (2009) 1739-1747.

[124] K.P. Chang, J.S. Yu, K.Y. Chien, C.W. Lee, Y. Liang, C.T. Liao, T.C. Yen, L.Y. Lee, L.L. Huang, S.C. Liu, Y.S. Chang, L.M. Chi, Identification of PRDX4 and P4HA2 as metastasis-associated proteins in oral cavity squamous cell carcinoma by comparative tissue proteomics of microdissected specimens using iTRAQ technology, *Journal of proteome research*, 10 (2011) 4935-4947.

[125] N. Yi, M.B. Xiao, W.K. Ni, F. Jiang, C.H. Lu, R.Z. Ni, High expression of peroxiredoxin 4 affects the survival time of colorectal cancer patients, but is not an independent unfavorable prognostic factor, *Molecular and clinical oncology*, 2 (2014) 767-772.

[126] W.T. Lowther, A.C. Haynes, Reduction of cysteine sulfinic acid in eukaryotic, typical 2-Cys peroxiredoxins by sulfiredoxin, *Antioxidants & redox signaling*, 15 (2011) 99-109.



- [127] H. Jiang, L. Wu, J. Chen, M. Mishra, H.A. Chawsheen, H. Zhu, Q. Wei, Sulfiredoxin Promotes Colorectal Cancer Cell Invasion and Metastasis through a Novel Mechanism of Enhancing EGFR Signaling, *Mol Cancer Res*, (2015).
- [128] L.A. Torre, F. Bray, R.L. Siegel, J. Ferlay, J. Lortet-Tieulent, A. Jemal, Global cancer statistics, 2012, *CA: a cancer journal for clinicians*, 65 (2015) 87-108.
- [129] R.L. Siegel, K.D. Miller, A. Jemal, Cancer statistics, 2016, *CA: a cancer journal for clinicians*, 66 (2016) 7-30.
- [130] R. Talhout, T. Schulz, E. Florek, J. van Benthem, P. Wester, A. Opperhuizen, Hazardous compounds in tobacco smoke, *Int J Environ Res Public Health*, 8 (2011) 613-628.
- [131] T. Gordon, M. Bosland, Strain-dependent differences in susceptibility to lung cancer in inbred mice exposed to mainstream cigarette smoke, *Cancer letters*, 275 (2009) 213-220.
- [132] X. Ma, J. Deng, N. Cao, Z. Guo, Y. Zheng, S. Geng, M. Meng, H. Lin, Y. Duan, G. Du, Lasting glycolytic stress governs susceptibility to urethane-induced lung carcinogenesis in vivo and in vitro, *Toxicol Lett*, 240 (2016) 130-139.
- [133] D.W. Lachenmeier, Rapid screening for ethyl carbamate in stone-fruit spirits using FTIR spectroscopy and chemometrics, *Anal Bioanal Chem*, 382 (2005) 1407-1412.
- [134] H. Satoh, T. Moriguchi, J. Takai, M. Ebina, M. Yamamoto, Nrf2 prevents initiation but accelerates progression through the Kras signaling pathway during lung carcinogenesis, *Cancer research*, 73 (2013) 4158-4168.
- [135] H.M. Yun, M.H. Park, D.H. Kim, Y.J. Ahn, K.R. Park, T.M. Kim, N.Y. Yun, Y.S. Jung, D.Y. Hwang, D.Y. Yoon, S.B. Han, J.T. Hong, Loss of presenilin 2 is associated with increased iPLA2 activity and lung tumor development, *Oncogene*, 33 (2014) 5193-5200.
- [136] A.G. Planson, G. Palais, K. Abbas, M. Gerard, L. Couvelard, A. Delaunay, S. Baulande, J.C. Drapier, M.B. Toledano, Sulfiredoxin protects mice from lipopolysaccharide-induced endotoxic shock, *Antioxidants & redox signaling*, 14 (2011) 2071-2080.
- [137] H.M. Yun, K.R. Park, M.H. Park, D.H. Kim, M.R. Jo, J.Y. Kim, E.C. Kim, Y. Yoon do, S.B. Han, J.T. Hong, PRDX6 promotes tumor development via the JAK2/STAT3 pathway in a urethane-induced lung tumor model, *Free radical biology & medicine*, 80 (2015) 136-144.
- [138] P.M. Westcott, K.D. Halliwill, M.D. To, M. Rashid, A.G. Rust, T.M. Keane, R. Delrosario, K.Y. Jen, K.E. Gurley, C.J. Kemp, E. Fredlund, D.A. Quigley, D.J. Adams, A. Balmain, The mutational landscapes of genetic and chemical models of Kras-driven lung cancer, *Nature*, 517 (2015) 489-492.
- [139] S. Henery, T. George, B. Hall, D. Basiji, W. Ortyrn, P. Morrissey, Quantitative image based apoptotic index measurement using multispectral imaging flow cytometry: a comparison with standard photometric methods, *Apoptosis*, 13 (2008) 1054-1063.
- [140] J. Wu, X.H. Chen, X.Q. Wang, Y. Yu, J.M. Ren, Y. Xiao, T. Zhou, P. Li, C.D. Xu, ERp19 contributes to tumorigenicity in human gastric cancer by

- promoting cell growth, migration and invasion, *Oncotarget*, 6 (2015) 11794-11805.
- [141] R. Ummanni, D. Duscharla, C. Barrett, S. Venz, T. Schlomm, H. Heinzer, R. Walther, C. Bokemeyer, T.H. Brummendorf, P.V. Murthy, S. Balabanov, Prostate cancer-associated autoantibodies in serum against tumor-associated antigens as potential new biomarkers, *J Proteomics*, 119 (2015) 218-229.
- [142] D.A. Henry, H.L. Corcoran, T.D. Lewis, G.R. Barnhart, S. Szentpetery, R.R. Lower, Orthotopic cardiac transplantation: evaluation with CT, *Radiology*, 170 (1989) 343-350.
- [143] L.G. Hernandez, P.G. Forkert, Inhibition of vinyl carbamate-induced mutagenicity and clastogenicity by the garlic constituent diallyl sulfone in F1 (Big Blue x A/J) transgenic mice, *Carcinogenesis*, 28 (2007) 1824-1830.
- [144] P.C. Chan, NTP technical report on toxicity studies of urethane in drinking water and urethane in 5% ethanol administered to F344/N rats and B6C3F1 mice, *Toxic Rep Ser*, (1996) 1-91, A91-99, B91-99 passim.
- [145] J.M. Schattenberg, M.J. Czaja, Regulation of the effects of CYP2E1-induced oxidative stress by JNK signaling, *Redox Biol*, 3 (2014) 7-15.
- [146] U. Hoffler, H.A. El-Masri, B.I. Ghanayem, Cytochrome P450 2E1 (CYP2E1) is the principal enzyme responsible for urethane metabolism: comparative studies using CYP2E1-null and wild-type mice, *J Pharmacol Exp Ther*, 305 (2003) 557-564.
- [147] M.J. Krauss, P.A. Cavazos-Rehg, A.D. Plunk, L.J. Bierut, R.A. Grucza, Effects of state cigarette excise taxes and smoke-free air policies on state per capita alcohol consumption in the United States, 1980 to 2009, *Alcohol Clin Exp Res*, 38 (2014) 2630-2638.
- [148] G.I. Somers, N. Lindsay, B.M. Lowdon, A.E. Jones, C. Freathy, S. Ho, A.J. Woodroffe, M.K. Bayliss, G.R. Manchee, A comparison of the expression and metabolizing activities of phase I and II enzymes in freshly isolated human lung parenchymal cells and cryopreserved human hepatocytes, *Drug Metab Dispos*, 35 (2007) 1797-1805.
- [149] P.L. Sheets, G.S. Yost, G.P. Carlson, Benzene metabolism in human lung cell lines BEAS-2B and A549 and cells overexpressing CYP2F1, *J Biochem Mol Toxicol*, 18 (2004) 92-99.
- [150] C.S. Ring, F.E. Cohen, Modeling protein structures: construction and their applications, *FASEB journal : official publication of the Federation of American Societies for Experimental Biology*, 7 (1993) 783-790.
- [151] K. Trujillo, S. Paoletta, E. Kiselev, K.A. Jacobson, Molecular modeling of the human P2Y14 receptor: A template for structure-based design of selective agonist ligands, *Bioorg Med Chem*, 23 (2015) 4056-4064.
- [152] P. Kirubakaran, M. Karthikeyan, D. Singh Kh, S. Nagamani, K. Premkumar, In silico structural and functional analysis of the human TOPK protein by structure modeling and molecular dynamics studies, *J Mol Model*, 19 (2013) 407-419.
- [153] H. Park, H. Lee, C. Seok, High-resolution protein-protein docking by global optimization: recent advances and future challenges, *Curr Opin Struct Biol*, 35 (2015) 24-31.

- [154] A. Roy, A. Kucukural, Y. Zhang, I-TASSER: a unified platform for automated protein structure and function prediction, *Nature protocols*, 5 (2010) 725-738.
- [155] Y. Zhang, I-TASSER server for protein 3D structure prediction, *BMC bioinformatics*, 9 (2008) 40.
- [156] L.A. Kelley, M.J. Sternberg, Protein structure prediction on the Web: a case study using the Phyre server, *Nature protocols*, 4 (2009) 363-371.
- [157] K. Arnold, L. Bordoli, J. Kopp, T. Schwede, The SWISS-MODEL workspace: a web-based environment for protein structure homology modelling, *Bioinformatics*, 22 (2006) 195-201.
- [158] B. Pierce, W. Tong, Z. Weng, M-ZDOCK: a grid-based approach for Cn symmetric multimer docking, *Bioinformatics*, 21 (2005) 1472-1478.
- [159] B.G. Pierce, Y. Hourai, Z. Weng, Accelerating protein docking in ZDOCK using an advanced 3D convolution library, *PLoS one*, 6 (2011) e24657.
- [160] F.I. Khan, D.Q. Wei, K.R. Gu, M.I. Hassan, S. Tabrez, Current updates on computer aided protein modeling and designing, *Int J Biol Macromol*, 85 (2015) 48-62.
- [161] L.C. Xue, D. Dobbs, A.M. Bonvin, V. Honavar, Computational prediction of protein interfaces: A review of data driven methods, *FEBS letters*, 589 (2015) 3516-3526.
- [162] W. Huber, F. Mueller, Biomolecular interaction analysis in drug discovery using surface plasmon resonance technology, *Curr Pharm Des*, 12 (2006) 3999-4021.
- [163] T.J. Jonsson, L.C. Johnson, W.T. Lowther, Structure of the sulphiredoxin-peroxiredoxin complex reveals an essential repair embrace, *Nature*, 451 (2008) 98-101.
- [164] Y.M. Go, D.P. Jones, The redox proteome, *The Journal of biological chemistry*, 288 (2013) 26512-26520.
- [165] J.A. Wells, C.L. McClendon, Reaching for high-hanging fruit in drug discovery at protein-protein interfaces, *Nature*, 450 (2007) 1001-1009.
- [166] J. Chen, X. Ma, Y. Yuan, J. Pei, L. Lai, Protein-protein interface analysis and hot spots identification for chemical ligand design, *Curr Pharm Des*, 20 (2014) 1192-1200.
- [167] N.M. Cerqueira, D. Gesto, E.F. Oliveira, D. Santos-Martins, N.F. Bras, S.F. Sousa, P.A. Fernandes, M.J. Ramos, Receptor-based virtual screening protocol for drug discovery, *Arch Biochem Biophys*, 582 (2015) 56-67.
- [168] J.A. Capra, R.A. Laskowski, J.M. Thornton, M. Singh, T.A. Funkhouser, Predicting protein ligand binding sites by combining evolutionary sequence conservation and 3D structure, *PLoS Comput Biol*, 5 (2009) e1000585.
- [169] Z. Zhang, Y. Li, B. Lin, M. Schroeder, B. Huang, Identification of cavities on protein surface using multiple computational approaches for drug binding site prediction, *Bioinformatics*, 27 (2011) 2083-2088.
- [170] J.J. Irwin, B.K. Shoichet, ZINC--a free database of commercially available compounds for virtual screening, *Journal of chemical information and modeling*, 45 (2005) 177-182.

- [171] J.J. Irwin, B.K. Shoichet, M.M. Mysinger, N. Huang, F. Colizzi, P. Wassam, Y. Cao, Automated docking screens: a feasibility study, *Journal of medicinal chemistry*, 52 (2009) 5712-5720.
- [172] K.C. Hsu, Y.F. Chen, S.R. Lin, J.M. Yang, iGEMDOCK: a graphical environment of enhancing GEMDOCK using pharmacological interactions and post-screening analysis, *BMC bioinformatics*, 12 Suppl 1 (2011) S33.
- [173] P. Piechota, M.T. Cronin, M. Hewitt, J.C. Madden, Pragmatic approaches to using computational methods to predict xenobiotic metabolism, *Journal of chemical information and modeling*, 53 (2013) 1282-1293.

## VITA

Murli Mishra

### Education

- 2008-2010 M.S. (Pharm.) Regulatory Toxicology  
National Institute of Pharmaceutical Education and Research  
(NIPER), S.A.S. Nagar, Punjab, India
- 2004-2008 Bachelor of Pharmacy  
Poona College of Pharmacy, Bharati Vidyapeeth University,  
Pune, Maharashtra, India

### Awards and Fellowships

- Society of Toxicology 2014 YouTox Video Challenge 3rd Prize Winner  
(Shared with Shohana Tawrin)
- Society of Toxicology 2012 ASIO-SIG Dr. Harihara Mehendale Graduate  
Student Best Abstract Award
- Availed GATE fellowship as an MS student for 2 years (2008-2010) on  
qualifying GATE 2007 as well as 2008

### Publications

- **Mishra M**, Jiang H, Wu L, Chawsheen HA, Wei Q\*. The Sulfiredoxin-  
Peroxiredoxin (Srx-Prx) Axis in Cell Signal Transduction and Cancer  
Development. Cancer Lett, 2015; 366 (2):150-59
- Jiang H, Wu L, Chen J, **Mishra M**, Chawsheen HA, Zhu H, Wei Q\*.  
Sulfiredoxin Promotes Colorectal Cancer Cell Invasion and Metastasis

- through a Novel Mechanism of Enhancing EGFR Signaling. *Mol Cancer Res*, 2015; 13(12): 1554-66
- Kwatra M\*, Kumar V, Ghosh P, Jangra A, **Mishra M**, Vohora D, Khanam R\*. Ameliorative Effect of Naringin against Doxorubicin-Induced Acute Cardiac Toxicity in Rats. *Pharm Biol*, 2016; 54(4):637-47
  - Jangra A\*, Kasbe P, Pandey SN, Dwivedi S, Gurjar SS, Kwatra M, **Mishra M**, Venu AK, Sulakhiya K, Gogoi R, Sarma N, Bezbaruah BK, Lahkar M. Hesperidin and Silibinin Ameliorate Aluminum-Induced Neurotoxicity: Modulation of Antioxidants and Inflammatory Cytokines Level in Mice Hippocampus. *Biol Trace Elem Res*, 2015;168(2): 462-71
  - Jiang H, Wu L, **Mishra M**, Chawsheen HA, Wei Q\*. Expression of Peroxiredoxin 1 and 4 Promotes Human Lung Cancer Malignancy. *Am J Cancer Res*, 2014; 4(5): 445-60
  - Wu L, Jiang H, Chawsheen HA, **Mishra M**, Young MR, Gerard M, Toledano MB, Colburn NH, Wei Q\*. Tumor Promoter-Induced Sulfiredoxin Is Required for Mouse Skin Tumorigenesis. *Carcinogenesis*, 2014; 35 (5): 1177-84
  - Hensley P, **Mishra M**, and Kyprianou N\*. Targeting Caspases in Cancer Therapeutics. *Biol Chem*, 2013; 394 (7): 831-43
  - **Mishra M**, Chawsheen HA, Wu L, Jiang H, Wei Q\*. PRDX4 (Peroxiredoxin 4). *Atlas Genet Cytogenet Oncol Haematol*, April 2013 URL: <http://atlasonline.critt-informatique.fr/Genes/PRDX4ID50280chXp22.html>

### **Abstracts and Presentations**

- **Mishra M**, Chawsheen H, Wu L, Jiang H, Wei Q. The Biology of Srx-Prx1 Interaction: Structure to Molecular Insights. Abstract presented at Society of Toxicology Annual Meeting 2014 held in Phoenix, Arizona
- **Mishra M**, Poduri R, Jena G, Mohan CG, Parikh N, Chakraborti AK. *In Silico* Methods of Genotoxicity Prediction: Can It Be Used Reliably for Prediction of *In Vitro* / *In Vivo* Genotoxicity? Abstract presented at Society of Toxicology Annual Meeting 2012 held in San Francisco, California
- Freeman SJ, Rowland JL, **Mishra M**, Goebel C, Schellauf F, Scheel J. Meta-Analysis of the Application of Weight of Evidence (WoE) and Read-Across for the Assessment of Repeat Dose Systemic Toxicity Abstract presented at the 8th World Congress on Alternatives and Animal Use in the Life Sciences 2011 held in Montreal, Canada

### **Work Experience**

- Regulatory Toxicologist (July 2010-Aug 2011), GlaxoSmithKline Consumer Healthcare Research and Development